UNIVERSITÉ DE
SHERBROOKE

Faculté de génie
Département de génie civil

MODIFICATION ET VALIDATION DE LA TECHNIQUE DE L'ANNEAU PIÉZOÉLECTRIQUE POUR MESURER LA PRISE ET LE DURCISSEMENT DES MATÉRIAUX À BASE DE CIMENT

MODIFICATION AND VALIDATION OF PIEZOELECTRIC RING ACTUATOR TECHNIQUE TO MONITOR SETTING AND HARDENING OF CEMENT-BASED MATERIALS

Thèse de maîtrise es sciences appliquées

Spécialité : génie civil

Supervisé par:

Prof. Mourad Karray, directeur de thèse

Prof. Kamal Khayat, co-directeur

Nancy Ahmed SOLIMAN

Sherbrooke (Québec), Canada **Octobre 2010**

Your file Votre référence
ISBN: 978-0-494-79747-1
Our file Notre référence
ISBN: 978-0-494-79747-1

ABSTRACT

A period of cement hydration is one of critical in the life span of concrete structures. One of the reasons of collapse of concrete structural elements during and after construction is the error in determining the concrete characteristics at early age. Recently, non-destructive test emerged as a popular way to evaluate the properties of cement-based materials. This test offers continuous measurements of concrete properties as well as ability to monitor any changes in the current state of structural materials. In the existing research, some of these methods fail to capture well properties of the materials in the plastics stage.

A new piezoelectric pulse testing device (Piezoelectric Ring Actuators Technique), *(P-RAT)* was initially developed at the University of Sherbrook as a non-destructive test (*NDT*) for soil. This technique is considered a completely new, versatile, advanced and accurate. The development of the new technique (*P-RAT*) was done on two main bases: the first was the development of piezoelectric ring actuators set-up and the second is the development of the interpretation method. The setup is composed of two main units; emitter and receiver, and is capable of measuring shear and compression wave velocities in specimens. With this technique, many problems of pulse tests, which make interpretation of results difficult and ambiguous, were solved in soil. The *P-RAT* overcomes wave reflections at boundaries (end-caps and sides), sample disturbance, weak shear coupling between soil and device (interaction) as well as the fixation problems, low resonant frequency and limited input voltage of the existing device.

The previous method is exploited forward to measure the hydration properties of cement-based material. To apply this test method, it is necessary to determine how the evolution of shear wave velocity can be related and sensitive to the hydration of cement-based materials. Validation of the *P-RAT* with four conventional test setups that can be used to monitor early setting and hydration of cement-based materials is carried out. These tests include penetration resistance to monitor initial and final setting respectively, calorimetric to monitor heat of hydration, electrical conductivity to monitor change in continuity of the pore structure and compressive strength at 24 hours.

The phase one of this investigation included trial tests to investigate the possibility of employing the original setup used for soil *(P-RAT)* to determine setting and hardening properties of cement-based material. Based on the results of the preliminary test, two modifications were

conducted to the previous test device to fit with cement based material and to obtain adequate resonant frequency for cement-based materials. These modifications are the design of the container and changing the dimensions of the rings. The resultant version of *P-RAT* after the modification was referred to be as *P-RAT2*.

Calibration of the *P-RAT2* with water specimen was undertaken using the compression wave velocity and resulted in 99.33% accuracy. One paste mixture was tested three times to determine the experimental error of the *P-RAT2*. The repeatability carried out on the *P-ART2* proved the ability of this setup to capture accurate results of the shear wave velocity. This relative error is limited to 9 %.

A number of series of validation was performed on cement paste and mortar mixtures proportioned with various water cement ratios (*w/cm)* as well as chemical admixtures. The *w/cm* ratio ranged between (0.35 and 0.50). The investigated chemical admixtures comprise of high-range water-reducing agent, viscosity-modifying agent, set-accelerating agent, and set-retarding agent. The presented validations examine the ability of a *P-RAT2* to monitor the hydration of the cement-based materials. The hydration is characterized by setting time, heat of hydration, electrical conductivity, and compressive strength at 24 hours. The results obtained using the *P-RAT2* was correlated to those obtained using the conventional tests and strength measurement.

The results enable to validate the ability of *P-RAT2* to accurately detect variations in the hydration of cement-based materials. In addition, the initial and final time of setting can be determined from the derivation of velocity vs. time curve. The results show that conductivity, resistivity, has a bilinear relationship to shear wave velocity. The compressive strength at 24 hours was correlated to both the shear wave velocity and shear modulus obtained using the *P-RAT2*. Furthermore, analytical model was derived to estimate the *w/cm* in mortar mixture by measuring the shear wave velocity (V_s) and the corresponding time (t).

Keywords: cement-based materials, hydration, non-destructive test, piezoelectric ring actuator technique, and shear wave velocity

RÉSUMÉ

La période d'hydratation du ciment est l'une des périodes clé du cycle de vie des structures en béton. L'une des raisons de l'effondrement d'éléments structuraux en béton pendant et après la construction peut être attribuée à une détermination des caractéristiques au jeune âge erronée. Depuis quelques années, l'auscultation des structures est devenue une méthode très populaire pour évaluer les propriétés des matériaux cimentaires. Cette méthode permet d'obtenir les propriétés du béton en continue et possibilité un suivi de changements dans l'état des matériaux structuraux. Dans l'état actuel de la recherche dans ce domaine, certaines méthodes ne sont pas adéquates pour bien mesurer les propriétés des matériaux à l'état plastique.

Un nouvel appareil d'essai à impulsions piézoélectriques (Piezoelectric Ring Actuators technique), *(P-RAT)* a initialement été développé à l'Université de Sherbrooke comme technique d'auscultation des sols. Cette technique est considérée complètement nouvelle, polyvalente, évoluée et précise. Le développement de cette nouvelle technique (*P-RAT*) a été effectué en deux volets : la première sole est le développement du dispositif de vérin de commande annulaire piézoélectrique et le deuxième est le développement d'une méthode d'interprétation. Le dispositif d'essai est composé de deux unités principales, un émetteur et un récepteur. Et permet de mesurer la vitesse de propagation des ondes de cisaillement et de compression. Grâce à cette technique, plusieurs des problèmes associés aux dispositifs d'essais par impulsion des ondes, qui rendent les résultats ambigus et difficiles à interpréter, ont été résolu pour les sols. Le dispositif *P-RAT* surmonte les problèmes de réflexion des ondes aux limites (embouts et côtés), la perturbation de l'échantillon, le couplage de cisaillement faible entre le sol et l'appareil (interaction) ainsi que les problèmes de fixation, la faible résonnance des fréquences et le voltage d'entrée limité du dispositif.

La méthode décrite a été utilisée pour mesurer les propriétés d'hydratation des matériaux cimentaires. Pour pouvoir appliquer cette méthode, il faut déterminer comment l'évolution de la propagation des ondes de cisaillement peut être reliée à l'hydratation des matériaux cimentaires et être sensible à ces dernières. La validation de la méthode *P-RAT* est réalisée, à l'aide de quatre configurations conventionnelles que l'on peut utiliser pour faire le suivi de la prise et de l'hydratation des matériaux cimentaires. Ces essais consistent à la résistance à la pénétration afin

de pouvoir déterminer la prise initiale et finale, la calorimétrie pour suivre l'évolution de la chaleur d'hydratation, la conductivité électrique pour effectuer le suivi de la structure des pores et la résistance à la compression à 24 heures.

La phase 1 de l'étude comprend des essais pour évaluer la possibilité d'utiliser la configuration originale utilisée pour les sols (*P-RAT)* pour déterminer les propriétés de prise et de durcissement des matériaux cimentaires. Selon les résultats des l'essai préliminaires, deux modifications ont été effectuées à l'appareil original pour permettre son utilisation avec des matériaux cimentaires et pour obtenir une fréquence de résonnance raisonnable sur les matériaux cimentaires. Les modifications effectuées sont la conception du contenant et un changement de la dimension des anneaux. La version modifiée du *P-RAT* est désignée *P-RAT2.*

La calibration du *P-RAT2* à l'aide d'échantillon liquide sous propagation d'ondes de compression a été menée, avec des résultats d'une précision de 99,33 %. Un mélange a été testé trois fois pour déterminer l'erreur expérimentale du *P-RAT2.* La répétitivité des essais sur le *P-ART2* a démontré la capacité de cet appareil à produire des résultats de cisaillement de propagation des ondes de cisaillement très précis. L'erreur relative se limite à 9 %.

Une série d'essais de validation a été menée sur des mélanges de pâte de ciment et de mortier de rapport eau/ciment variés (*e/c*) ainsi qu'avec des adjuvants. Le rapport *e/c* variait entre 0,35 et 0,50. Les adjuvants utilisés étaient des supers plastifiants (réducteur d'eau), des agents de viscosité, des agents accélérateurs de prise et des agents retardateurs de prise. Les validations présentées ont pour but de valider la capacité du *P-RAT2* à suivre l'hydratation des matériaux cimentaires. L'hydratation est caractérisée par le temps de prise, la chaleur d'hydratation, la conductivité électrique et la résistance à la compression à 24 heures. Les résultats obtenus à l'aide du *P-RAT2* ont été comparés à ceux obtenus à l'aide d'essais de mesure des caractéristiques physiques et de résistance traditionnels.

Ces résultats permettent de valider la capacité du *P-RAT2* à détecter avec précision les variations dans l'hydratation des matériaux cimentaires. De plus, le dispositif *P-RAT2* peut avoir une correction avec mesure obteniez avec les appareils traditionnels. Il est aussi possible de déterminer le temps de prise initial et final à l'aide d'une courbe de propagation vs le temps. Les résultats montrent que la conductivité et la résistivité ont une relation bilinéaire à la propagation des ondes de cisaillement. La résistance à la compression à 24 heures a été comparée à la fois à la propagation des ondes de cisaillement et au module de cisaillement obtenus avec le *P-RAT2.*

De plus, un modèle analytique a été établi pour estimer le rapport *e/c* dans le mélange de mortier en mesurant la propagation des ondes de cisaillement (V) correspondant au temps (t).

Mots-clés : matériaux cimentaires, hydratation, auscultation, technique d'essai à impulsions piézoélectriques et vitesse de propagation des ondes de cisaillement.

DEDICATION

To the researchers and engineers who appreciate the value of science and knowledge.

To my beloved parents who favoured me over themselves and have given me all what they could? "My Mighty GOD! Bestow on them Your Mercy as they did bring me up when I was young."

To my husband supports me and understands my challenging and demanding circumstances as a researcher.

To my son Mustafa and my daughter Merriam came to life and have made a big difference in my life.

ACKNOWLEDGEMENT

First and foremost, praise and thanks go to my Creator and Provider (**The Mighty God**) for his uncounted grace undeservingly bestowed upon me. "Glory is to you, we have no knowledge except what you have taught us. Verily, it is you, the All-Knower, the All-Wise."

The author would like to express his greatest appreciation and thanks to her supervisor, **Prof. Mourad Karray**, for his guidance, helpful advice, and encouragement during this research. The author had a lot of freedom in her work, which she has learned a lot from his thorough knowledge and experience as well as from his nice and decent personality. The author wishes to express her sincere gratitude to him for his patience and understanding during the course of this research. The author is proud to have worked with him and counts her lucky to be one of his master students.

The author is greatly indebted to, **Prof. Kamal Khayat**, for his cooperation, monitoring, guidance, helpful advice, and encouragement during this research project. His unfailing guidance and continuous consulting efforts were valuable to this research. The Author can hardly find the right words to express the extent of his gratitude and thanks.

Appreciations are expressed to **Prof. Yannic Ethier** and **Dr. Deyab Gamal El Dean**, have development the piezoelectric ring actuator technique under supervision of Prof. Guy Lefebvre and Prof. Mourad Karray. The author also thanks **Dr. Ahmed Omran**, her colleague **Fahima Rousis and Dr. Ahmed Godat** for their co-operations, assistances and for the fun we had during some difficult times of her studies. The Author is greatly thanks to **Dr. Trimbak Pavate, Mrs. Ghislaine Luc** and all technicians for their cooperation during the research. The author cannot forget to acknowledge many friends whom she has gained during her study; them stay here at Sherbrooke was made enjoyable.

The Author also thanks the professors of Civil Engineering Department and all the faculty staff he has interacted with. Special thanks to **Mrs. Christine Couture** and **Mrs. Marielle Beaudry** the secretary of the civil engineering department.

The Author is thankful to the members of the dissertation committee; Prof. **Yannic Ethier**, Prof. **Kamal Khayat**, Prof. **Mourad Karray**, , and Prof. **Ammar Yahia**, for their valuable comments and advices.

Finally, the author wishes to express her greatest and profound gratitude to her parents, brothers and sisters, for their support and encouragement. The author wishes to thank her husband **Ahmed Omran** for his love and the happiness he brought to her. The life here at Sherbrook would not have been so full without her husband and her two kids (**Mustafa and Mariam**).

The author,

Nancy Soliman

TABLE OF CONTENTS

LIST OF FIGURES

Chapter 5:

Chapter 6:

Chapter 7:

LIST OF TABLE

SYMBOLS AND NOTATIONS

G_{max} , G_o	small-strain shear modulus
V_p	compression wave velocity
V_{ph}	phase velocity
V_R	Rayleigh wave velocity
V_s	shear wave velocity
θ	The phase angle ($2\pi N$)
φ	friction angle
ω	angular frequency
CM	Conventional Mortar
HRWRA	High-range water-reducing agent
SE	Standard error
SRA	Set-retarding agent
VMA	Viscosity-modifying agent
SAA	Set- Accelerating agent
w/cm	Water-to-cement material
ρ	Density of material (kg/m^3)
f_c	Compressive strength
P-RAT	Piezoelectric ring actuator technique
P-RAT2	Modified Piezoelectric ring actuator technique
SEM	scanning electronic microscope
XRD	X-ray diffraction
t	time
t_i	time of initial set corresponding to penetration and Vicate needle apparatus
t_f	time of final set corresponding to penetration and Vicate needle apparatus
t_1	time of initial set corresponding to P-RAT2
t_2	time of final set corresponding to P-RAT2
C-S-H	calcium silicate hydrate
E	Young's modulus
ν	Poisson's ratio

CHAPTER 1
INTRODUCTION

1.1 Importance of early-age properties of cement-based materials

One of the reasons of collapse of concrete structural elements during and after construction is the error in determining the concrete characteristics at early age. Thus the investigation of early-age properties is vital to produce a concrete satisfying the requirements of strength and durability in the final structural element. During the early period of concrete life, numerous operations are performed, such as mixing, transport to the job site, placement in the formworks, consolidation, finishing, curing, and formwork removal. These operations are mainly affected by characteristics of fresh concrete properties; including workability, segregation, bleeding, settlement, rheology, and setting time. Consequently, the control of properties and operations of fresh concrete are essential to ensure that the finished concrete product is structurally adequate for the purpose for which it was designed [Mehta 2003].

Among the most important properties of cement-based material is determination of strength gain at early age. The strength development is highly important property since the concrete has not to carry on its own weight, but also it has to gain sufficient minimum strength to remove the formworks. This minimum strength is beneficial to reduce the construction time, increase safety, and avoid the probability of occurring accidents due to unforeseen conditions.

The hydration development is a fundamental property of concrete and is controlled by cement hydration. There are well established test methods to evaluate hydration development of cement-based materials, includes the penetration resistant test, heat rise or calorimetry, and electrical conductivity tests. These tests enable the determinations of the initial setting, end of workability, and final setting which corresponds to the begging of hardening. The determination of setting is vital as it is responsible for the strength gain and stiffness development.

The physical setting, strength gain and lifetime of cements are accompanied by a series of chemical and microstructural changes during the hydration. The significant of hydration process has attracted a considerable attention and has been studied by many methods, like the commonly used Vicat needle, universal testing machine, scanning electronic microscope (SEM), X-ray diffraction (XRD), etc... However, measured setting time and strength parameters cannot directly

show the materials and the microstructural changes in hydration process. For example, the setting time defined by penetration values of Vicat needles (ASTM C191) correspond to two particular practical points, which are loosely defined as the limit of handling and the beginning of mechanical strength development, respectively. Also the test's accuracy depends largely on the skill and experience of the person performing it, [Mehta 1993]. Therefore, alternative techniques, which are accurate and non-destructive, are highly needed to monitor the hydration process of cement-based material.

1.2 The requirement for non-destructive testing

The non-destructive tests are considered as alternatives to monitor the early-age properties of cement-based materials. The main advantages obtained from the non-destructive tests are their ability to monitor any changes in the current state of structural materials, and they provide continuous following up for the skeleton built up of structural materials. Currently, little research of the non-destructive tests existed that have proven relative successfulness for monitoring the development of the early-age properties of cement-based materials. The available test methods suffer from fundamental and accuracy of interpretative methods.

The target test should be designed to produce high precision. The aimed test method should provide monitoring of the hydration process and hardening of cement-based materials on a continuous basis. The foreseen test method to monitor the early-age properties of concrete should not be expensive and should be compatible with the field applications.

Currently, efforts have been exerted towards developing of an accurate way to measure the early-age properties of cement-based materials based on the shear wave propagation. Piezoelectric ring actuator setup (*P-RAT*), which has been developed at University of Sherbrook by El-Dean [2007] for granular soil and Ethier [2009] for clay soil, is considered as new non-destructive setup based on shear wave. This technique is considered a completely new, versatile, advanced and accurate. The development of the new technique (*P-RAT*) was done on two main bases: the first was the development of piezoelectric ring actuators set-up and the second is the development of the interpretation technique used in the results analysis by Karray [2008]. The setup is composed of two main units; emitter and receiver, and is capable of measuring shear and compression wave velocities in specimens. With this technique, many problems of pulse tests, which make interpretation of results difficult and ambiguous, were solved in soil. The *P-RAT*

overcomes wave reflections at boundaries (end-caps and sides), sample disturbance, weak shear coupling between soil and device (interaction) as well as the fixation problems, low resonant frequency and limited input voltage of the existing device.

A proposed configuration for the *P-RAT* that can be applicable with the cement-based materials and a trend for the expected correlation between the results of *P-RAT* and traditional test method are given in Fig. 1.1.

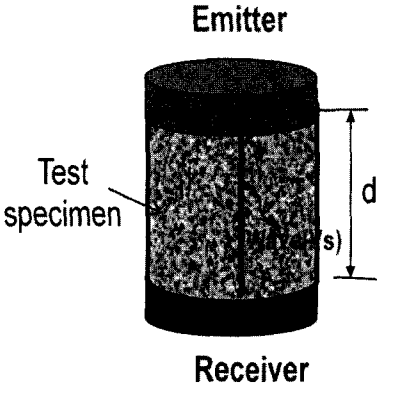

Fig. 1.1 A proposed configuration for the *P-RAT* with the cement-based materials

1.3 Scope and objectives

The main goal of the research undertaken in this master's thesis is to adapt the new piezoelectric device (*P-RAT*) to monitor the early-age properties of cement-based materials. The objectives can be summarized as follows:

1. Evaluate the possibility of using the exists piezoelectric ring actuators technique, (*P-RAT*) to monitor setting and hardening of cement based-materials; and
2. Determine how the variation in shear wave velocity can be related to the evolution of hydration, changes of electrical conductivity, penetration resistance and compressive strength at 24 hours in cement based-material.

1.4 Thesis outlines

The thesis is divided into seven chapters. This section introduces in brief the contents of each chapter.

Chapter 1 gives an introduction about the importance of the early-age period in the concrete life. Description of the undesirable advantages accompanied with the existing mechanical and non-destructive test methods employed to estimate the early age properties of concrete is highlighted. The necessity for new non-destructive test method is also discussed. The objectives and the thesis outline are also presented.

Chapter 2 gives an overview about the properties of cement-based materials at early-age, including the setting time, kinetic heat of hydration, conductivity, resistivity, and compressive strength. This chapter provides also an overview about the wave propagation. Theory of wave propagation (wave speed, characterization of wave reflection and wave refraction). The existing non-destructive methods used to monitor the early-age properties of cementitious materials are presented in this chapter. Overviews for the following techniques used on non-destructive test methods are given based on acoustics wave, ultrasonic pulse velocity, impact-echo method, ultrasonic wave reflection method, and guided wave method.

Chapter 3 presents the experimental program proposed to evaluate possibility of using the version of piezoelectric ring actuators techniques (*P-RAT*) on cement-based materials. Descriptions of materials, mix designs, and mixing sequence used in the experimental tests are given in this chapter. The testing sequences and methods used to examine the fresh properties of the cement-based materials including Vicat needle apparatus, penetration resistance test, calorimetric test, electrical conductivity test, and compressive strength test are also detailed in this chapter.

Chapter 4 introduces historical backgrounds about the use of piezoelectric devices used in soil applications in this chapter. The description of *P-RAT* is also detailed. A strategy for using the *P-RAT* to estimate fresh properties of cement-based materials is described. Test results for the first implementation of *P-RAT* in concrete mixtures are discussed in terms of signal analysis and configurations of the moulds. Modifications to the *P-RAT* to be adapted with the cement-based materials are highlighted. Calibration and repeatability determination of a modified version of the piezoelectric ring actuators setup *P-RAT2* to evaluate accurate responses are also discussed in this chapter.

Chapter 5 describes the validation of *P-RAT2* with conventional methods. The results of heat of hydration, setting time, electrical conductivity, and compressive strength obtained using the traditional test methods recommended by the ASTM Standards and the shear wave behaviour obtained using *P-RAT2* were analyzed.

Chapter 6 gives mutual correlation between conventional methods. In addition fundamental relationships between the results obtained using the *P-RAT2* and those obtained using the traditional test methods are presented in this chapter. A derivation of analytical model to predict the *w/cm* in a mortar mixture by knowing the shear wave velocity (V_s) and a specific time (t) is presented alsoin this chapter.

Chapter 7 gives summary and major conclusions of the study.

CHAPTER 2
LITERATURE REVIEW

2.1 Introduction

The purpose of this chapter is to provide a brief overview of cement-based materials properties at early- age (setting time, kinetic heat of hydration, conductivity, resistivity and compressive strength), and provide an overview of wave propagation theory, including the most important type of (acoustics) waves (longitudinal and shear wave) is reviewed. An overview of wave speed, characterization of wave reflection and wave refraction are also presented. Finally, the propagation of shear wave velocity in cement-based materials during hydration is introduced in this chapter. Also the purpose of this chapter gives an over view of some common for non-destructive methods used for monitoring early age properties of cementitious materials.

2.2 Concrete at early age

2.2.1 Setting time

The initial and final setting times of concrete are defined as the onset of solidification of fresh concrete mixture, and the transition from a fluid to rigid state, respectively, [Mehta 2006]. Setting time is effectively many factors including, material characteristics (cement, admixture type, etc.), mixture composition (water to cement ratio *(w/cm),* binder composition, etc. and medium temperature.

The phenomena of setting and hardening are the physical manifestation of progressive hydration of cement with time. In order to setting time to occur, solid hydration products must be created. Primarily calcium silicate hydrate (C-S-H) and to a lesser degree, ettringite are formed. These components are created by the hydration of C_3S and C_3A, respectively, at early age. The hydration products fill in some of space between cement grains and increase the rigidity of the skeletal structure, [Mehta 2006].

The initial and final setting times of concrete are specific moments during the life of concrete. Unfortunately, initial and final setting times are widely considered to be arbitrary and depending on the particular test method being applied [Struble et al., 2001]. According to,

ASTM C-403, [1985] the initial set represents approximately the time at which concrete can no longer be properly mixed, placed, and compacted. In addition, the final set represents approximately the time of start of mechanical strength gain. So the initial and final set times are essential to know the changes in concrete characteristics. Figure 2.1 illustrates the progress of initial and final setting of concrete measured by Mindess and Young [1981].

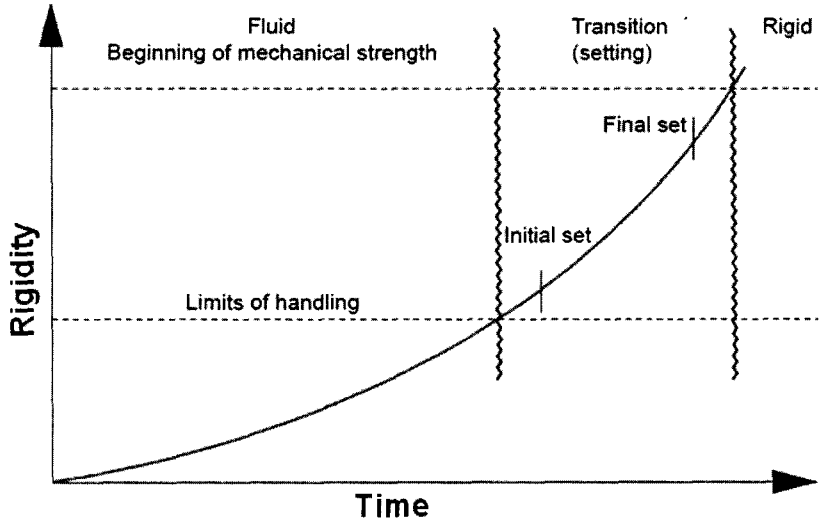

Fig. 2.1 Progress of setting and hardening of concrete [Mindess and Young, 1981]

2.2.2 Hydration and development of microstructure

The heat of hydration is the heat generated when water and cement react. Strength development of concrete depends on the rate and hydration of cement. The primary cause of the hydration phenomena is the reactions between cement and water hydration resulting reduction in capillary porosity. Composition and fineness of cement, water to cement ratio (*w/cm)*, type and contents of supplementary materials (fly ash, slag and silica fume), type and content ratio of chemical admixtures (superplasticizer, set accelerator, set retarder, etc.), and medium temperature have significant influence on cement hydration.

Typical Composition of Portland cement is shown in Table 2.1. Tricalcium silicate (C_3S) hydrates and hardens rapidly and is largely responsible for initial set and early strength. Dicalcium silicate (C_2S) hydrates and hardens slowly and is largely responsible for strength

increases (beyond one week). Tricalcium aluminate (C_3A) is highly reactive with water. The C_3A necessitates the addition of calcium sulfate dehydrate (CSH or gypsum) to prevent flash set. Tetracalcium aluminoferrite (C_4AF) hydrates rapidly but contributes little to strength development [Mindess and Young, 2002].

Table 2.1 Main constituents of a typical Portland cement [Mindess and Young, 2002]

Chemical Name	Chemical Formula	abbreviation	Percent by weight
Tricalcium Silicate	$3CaO{\cdot}SiO_2$	C_3S	55
Dicalcium Silicate	$2CaO{\cdot}SiO_2$	C_2S	18
Tricalcium Aluminate	$3CaO{\cdot}Al_2O_3$	C_3A	10
Tetracalcium Aluminoferrite	$4CaO{\cdot}Al_2O_3{\cdot}Fe_2O_3$	C_4AF	8
Calcium sulphate dehydrate	$CaSO_4{\cdot}H_2O$	CSH_2	6

Because cement consists of several components, the hydration is a complex sequence of overlapping chemical reactions between clinker components. Mindess et al., [2003] and Neville [2002] have divided the hydration processes in five stages. Schematic represents heat evolution during hydration of cement and water is shown in Fig. 2.2, [Gartner et al., 2002].

In Stage I and when the C_3S in the cement contact with water, the reactions starts releasing calcium and hydroxyl ions into the solution and generating an explosion of heat. The reaction in this stage can be expressed as follows:

$$2C_3S + 11H \rightarrow C_3S_2H_8 + 3CH \tag{2.1}$$

$$2C_2S + 9H \rightarrow C_3S_2H_8 + CH \tag{2.2}$$

where; H is water, $C_3S_2H_8$ is calcium silicate, and CH is calcium hydroxide.

The principal product of hydration process is the calcium silicate hydrate (C-S-H) (or cement gel). The cement gel is considered the most important part of the hardening of concrete because it constitutes more than half of the hydrated paste volume and is the primary source of strength. Two sequential reactions of less importance can be expressed as follows:

$$C_3S + C\bar{S}H_2 + 26H \rightarrow C_6A\bar{S}_3H_{32} \tag{2.3}$$

$$2C_3A + C_6A\bar{S}_3H_{32} + 4H \rightarrow 3C_4A\bar{S}H_{12} \quad (2.4)$$

where; $C_6A\bar{S}_3H_{32}$ is ettringite and $C_4A\bar{S}H_{12}$ is monosulfoalumonate.

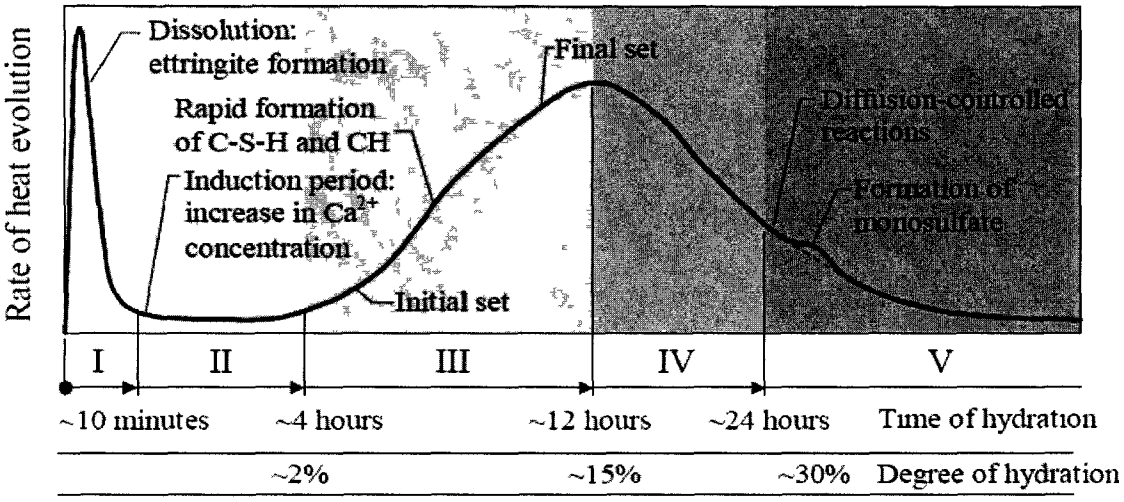

Fig. 2.2 Schematic representation of heat evolution during hydration of cement and water [Gartner et al., 2002]

After Stage I, an induction period (or dormant period) is entered (Stage II). In stage II, the dissolution continues and pH reaches a high value (~12.5). During this induction period less hydration takes place. After critical values of calcium and hydroxide ions are reached, a rapid crystallization followed by a rapid reaction of CH (calcium hydroxide) and calcium silicate hydrate (C-S-H) is formed (Stage III). In this acceleration stage there is an onset of transformation to rigidity. In Stage IV and Stage V, there are continuous formations of hydration products, yet the rate of reaction is slowing down. In the final stage (Stage V) there is only a slow formation of products and the reaction is diffusion-controlled. The initial set occurs somewhat after the transition from Stage II while the final set occurs just before the peak between Stage III and Stage IV. The setting process is the consequence of a change from a concentrated suspension of flocculated particles to a viscoelastic skeletal solid capable of supporting an applied stress. Figure 2.3 shows schematic representation of the early microstructural development [Mindess et al., 2003] and [Neville, 2002].

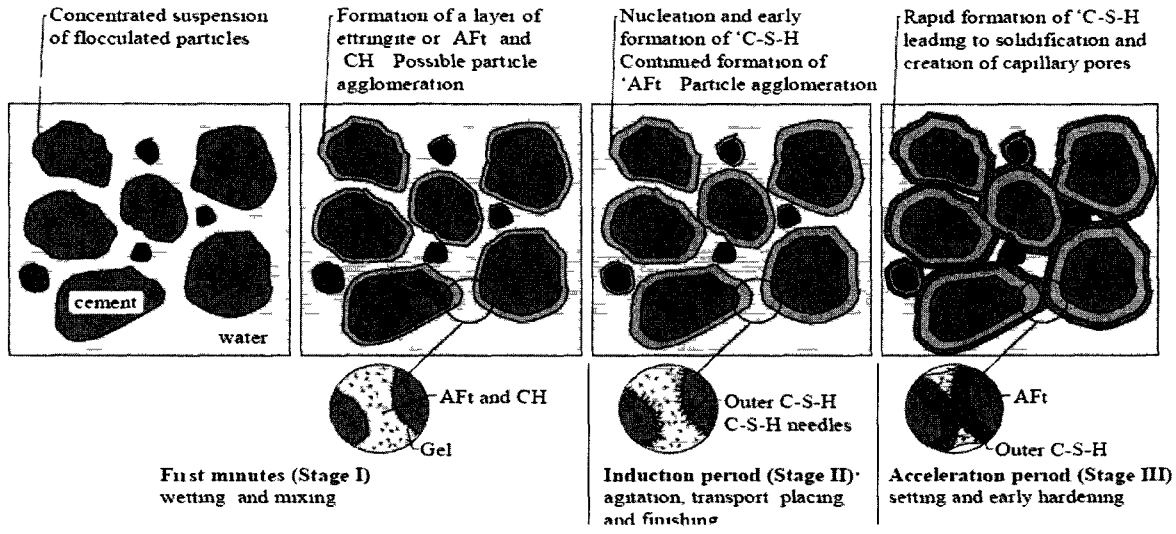

Fig. 2.3 Schematic representation of early microstructure development

Sandberg et al. [2007] reported two alternate methods, the derivatives method and the fractions method, for estimating thermal setting times from semi-adiabatic temperature profiles. The first method defines the time of the maximum slope (maximum first derivative) of the hydration peak as final set, and the time of maximum 2nd derivative as initial set. The fractions methods defines a baseline and a maximum temperature, and then calculate initial and final set as the time when the measured temperature has risen a certain percentage from the baseline towards the maximum temperature measured. Figure 2.4 represented Calculation of Thermal set using the derivatives method in the left and the Fractions method in the right. The results data presented from semi-adiabatic temperature curves correlated well with manual setting times measured according to ASTM C403, and presented a good correlations.

2.2.3 Electrical conductivity

The electrical conductivity test method was used for quantitative evaluation of fresh cementitious systems towards bleeding and segregation based on monitoring changes in electrical conductivity in the plastic material. Such changes reflect variations in homogeneity of the fresh sample as a function of time [Khayat et al., 2003].

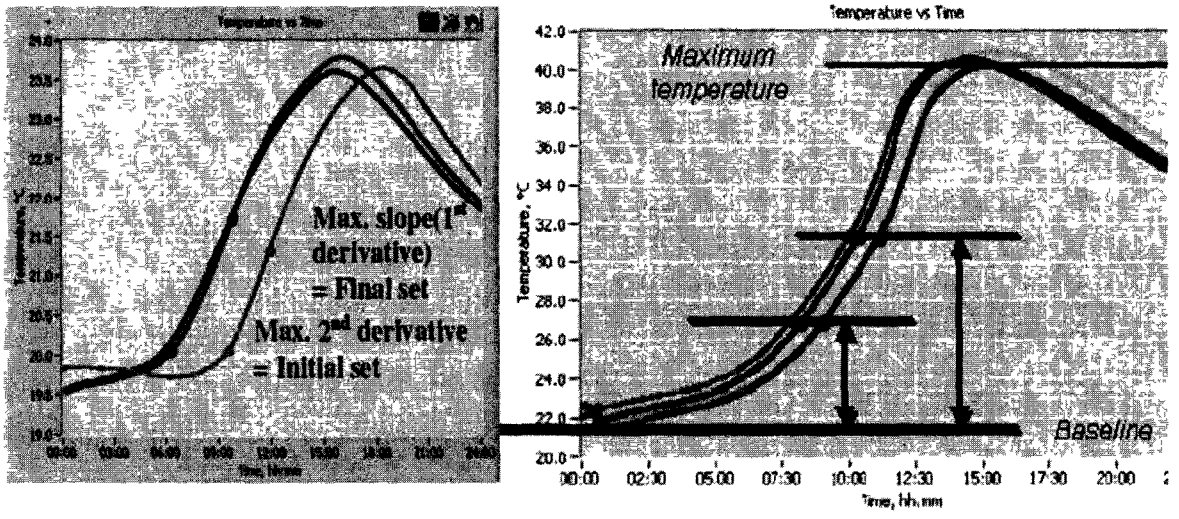

Fig. 2.4 Calculation of thermal set using the derivatives method in the left and the Fractions method in the right

In general, the evolution of conductivity with time can sharply increase in the first instants following mixing of cement and water (point B in Fig. 2.5) given by the rapid dissolution of alkali sulfates. These results in an increase of Na^+, K^+, and SO_4^{2-} ions and early surface hydration of the most reactive phases in the cement, generating Ca^{2+} and OH^- ions. During the period (B to C), the conductivity increases slowly as the hydration reactions proceed, further increasing the concentration of Ca^+ and OH^- ions in the solution reaching a super saturation level (point C). As the conditions for $Ca(OH)_2$ precipitation become favourable, sharp decrease in Ca^{2+} and OH^- ions concentration takes place, initiating a rapid decrease in conductivity which signals the onset of setting (C to D and thereafter) [Khayat et al., 2003].

Typical conductivity curves for M4 mortar (made with polycarbonate sulphate, PC1 and *w/cm* of 0.8) and M6 mortar (prepared with PC2 cement and 0.5 *w/cm*) tests is illustrated in Figs. 2.6 and 2.7, respectively. Different changes in conductivity over the height of the test jar as well as over the elapsed measurement time can clearly be observed at the different electrode pairs. In the case of the M4 mortar, sharp downward slopes of conductivity curves at all four levels of the electrode pairs along the tested column are shown, indicating segregation during the first few minutes from testing. The upward migration of free water can thereby result by high conductivity leading to high risk of bleeding, particularly at the top pair of electrodes. This is indicated by the

rise in slopes after 30 minutes and continuing up to approximately 60 minutes. This mortar being very fluid and unstable yielded 300 mm slump spread and 244 ml of external bleeding. Conversely, the M6 mortar exhibited better stability with uniform segregation at the bottom, 3rd, 2nd, and top pairs of electrodes. The downward slopes of conductivity curves for the lower three levels of electrode pairs were flatter than those for the M4 mortar. The bleeding reflected by the upward migration of free water was also uniform at all levels of electrode pairs. The M6 was being more uniform and stable yielded 145 mm of slump spread and 71 ml of external bleeding [Khayat et al., 2003].

Electrical resistivity is a measure of how strongly a material opposes the flow of electric current. A low resistivity indicates a material that readily allows the movement of electrical charge. The SI unit of electrical resistivity is the ohm metre (Ω m). Electrical resistivity is also defined as the inverse of the conductivity σ (sigma), of the material, or

$$\rho = \frac{1}{\sigma} \tag{2.5}$$

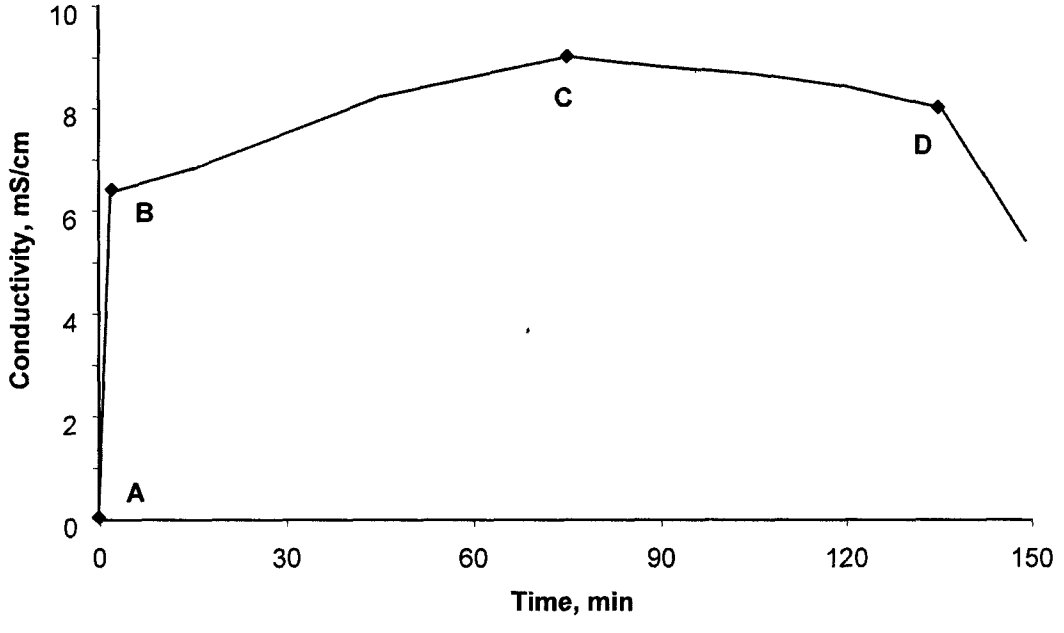

Fig. 2.5 Typical conductivity curve for cementitious materials; A: dry material, B: at contact with water, B-C: increase of ionic strength with dissolution of ions in pore solution, C-D: precipitation of portlandite, etc. [Khayat et al., 2003]

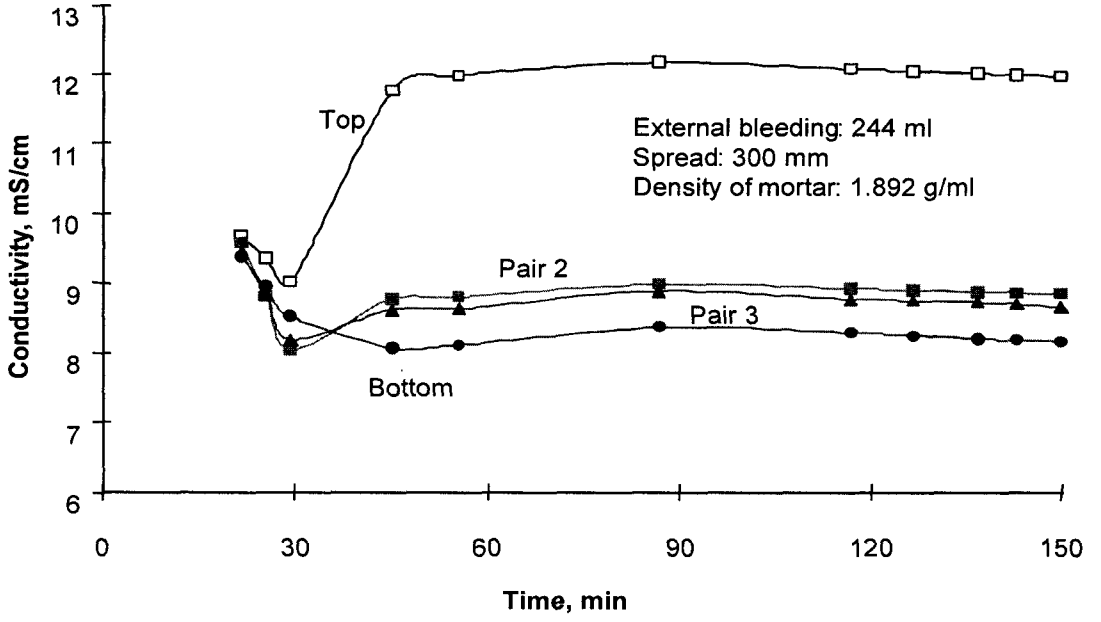

Fig. 2-6 Typical variations in conductivity for the M4 mortar made with PC1 and W/B of 0.8 exhibiting high degree of bleeding and segregation [Khayat et al., 2003]

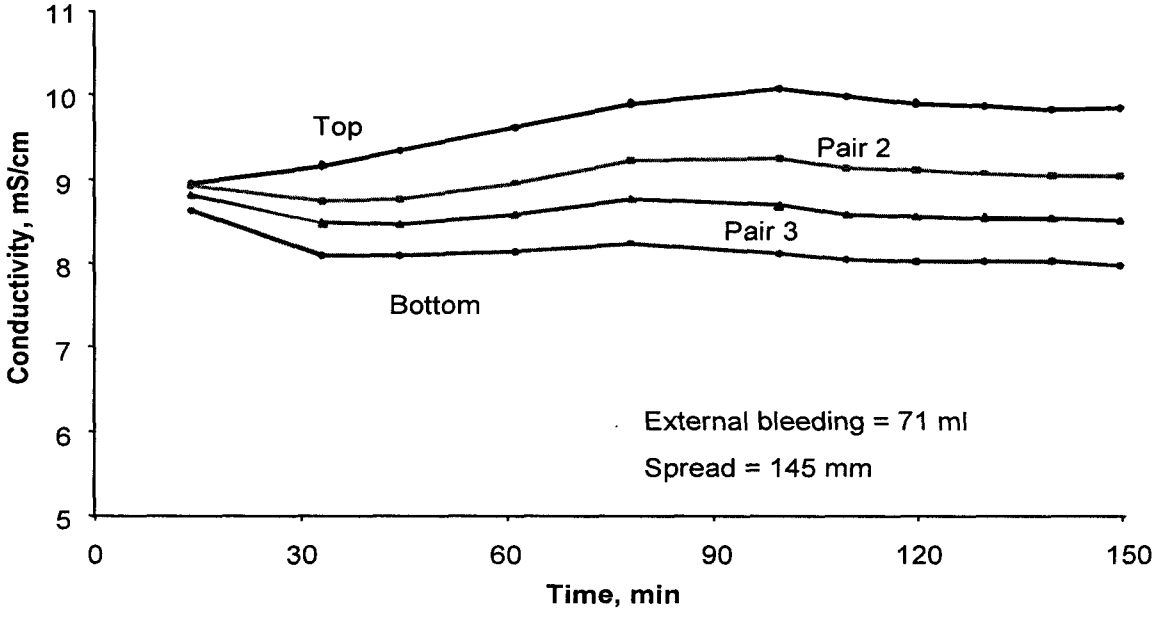

Fig. 2.7 Typical variations in conductivity for the M6 mortar made with PC2 and W/B of 0.5 exhibiting homogeneity [Khayat et al., 2003]

2.2.4 Compressive strength

Compressive strength of a material is that value of an axial compressive stress reached when the material fails completely. The compressive strength is usually obtained experimentally by means of a compressive test. The apparatus used for this experiment is the same as that used in a tensile test. However, rather than applying an axial tensile load, an axial compressive load is applied. As can be imagined, the specimen (usually cylindrical) is shortened as well as spread laterally.

2.3 Wave propagation theory

2.3.1 Theory of wave propagation

There are three types for propagating stress waves in a solid. These waves are created when the surface of a large solid elastic medium is disturbed by dynamic or vibratory load. Starting from the point of excitation, the waves propagate uniformly, but with different velocities through the medium. Figure 2.8 represents a schematic showing generation of different wave types by a mechanical impact [Sansalone and Streett, 1997].

The three wave types comprise of:

Two types of volume waves (or body wave):

- Compression wave (longitudinal or P-wave).
- Shear wave (transverse or S-wave).

One type of surface waves:

- Rayleigh wave (or R-wave)

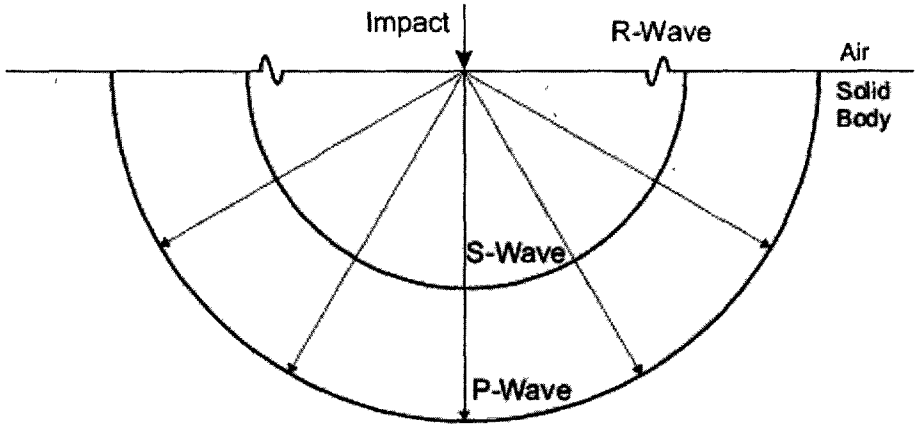

Fig. 2.8 Generation of different wave types by a mechanical impact [Sansalone and Streett, 1997]

The compression wave can be named primary wave (P-wave) as it is the fastest wave. In the compression wave, the movement is parallel to the direction of travel so it can be defined as longitudinal wave. The compression wave can travel through gasses, elastic solid and liquid.

Because the speed of the shear wave is less than the P-wave, the former is named secondary wave (S-wave). The velocity of the S-wave is typically 60% of the velocity of P-wave for cement- based material [Hills, 1998]. In the S-wave, the movement is perpendicular to the direction of travel, which is why it is called as transverse wave. S-wave travels only through solids and does not travel through liquids or gasses.

The Rayleigh wave travels in both directions; direction parallel and perpendicular to the propagation. The motion of the Rayleigh wave is generally as elliptical shape. The velocity of Rayleigh wave is typically 55% of velocity of the P-wave [Hills, 1998].

Propagation and direction of P-wave, S-wave, and R-wave are shown in Fig. 2.9. The relationships between different wave velocities are governed by Poisson's ratio (ν) of the considered material. For normal concrete of $\nu = 0.18$, the ratio between P-wave and S-wave velocities is 62% and between P-wave and R-wave is 57% [Sansalone and Streett, 1997].

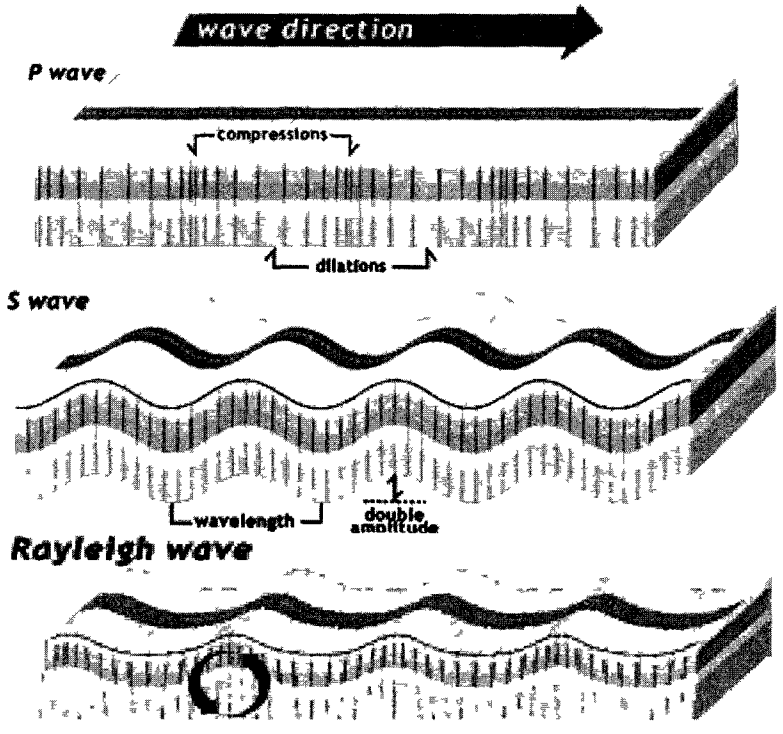

Fig. 2.9 Propagation and direction of P-wave, S-wave, and R-wave

2.3.2 Wave speed

The relationship between the wave speed and the physical properties of a material can be acknowledged from the theory of wave propagation through infinite, isotropic, and elastic media [Timoshenko et al., 1970]. The velocity of P-wave in an infinite elastic solid is related to density (ρ), Young's modulus (E), shear modulus (G), and Poisson's ratio (ν) as in Eq. (2.6). Also the velocity of the S-wave can be calculated according to Eq. (2.7). Finally, the velocity of the R-wave is approximately estimated from Eq. (2.8) [Viktorov et al., 1967].

Speed of P-wave $$V_P = \sqrt{\frac{E(1-\nu)}{\rho(1+\nu)(1-2\nu)}} \tag{2.6}$$

Speed of S-wave $$V_S = \sqrt{\frac{G}{\rho}} \tag{2.7}$$

Speed of R-wave $$V_R = V_s \times \frac{0.87+1.12\nu}{1+\nu} \tag{2.8}$$

where:

E: modulus of elasticity

ρ: density of material

ν: Poisson's ratio

G: shear modulus of elasticity = E/2(1-ν)

2.3.3 Reflection and refraction

When a P-wave or S-wave is incident on a boundary between different media, reflection and refracted are occurs. At the boundary between two dissimilar media, only portion of stress waves is reflected while the remaining waves are passed into the under laying medium (refracted wave) as shown in Fig. 2.10 (a) [Carino, 2004]. The angle of reflection (θ_1) is equal to the angle of incidence (θ_1). The relationship between θ_1 and refracted angle (θ_2) is given by Snell's law as follows:

$$\frac{\sin\theta_1}{\sin\theta_2} = \frac{V_1}{V_2} \tag{2.9}$$

where; V_1 and V_2 are wave velocities in material 1 and 2, respectively.

Stress wave can change their mode of propagation when striking boundary at an oblique angle. Depending on the angle of incidence, the P-wave can be partially reflected as both P-wave and S-wave and can be refracted as P-wave and S-wave. As the S-wave travels at lower speed than P-wave, the angle of reflected S-wave (Φ_1) and the angle of refracted S-wave (Φ_2) are less than the angles of reflection and refraction for P-wave as shown in Fig. 2.10 (b). The angels of incidence, reflected, and transmitted rays are related according to Snell's law as follows [Carino, 2004].

$$\frac{\sin\theta_1}{V_{p1}} = \frac{\sin\theta_2}{V_{p2}} = \frac{\sin\Phi_1}{V_{s1}} = \frac{\sin\Phi_2}{V_{s2}} \tag{2.10}$$

where; V_p and V_s are compression and shear wave velocities, respectively.

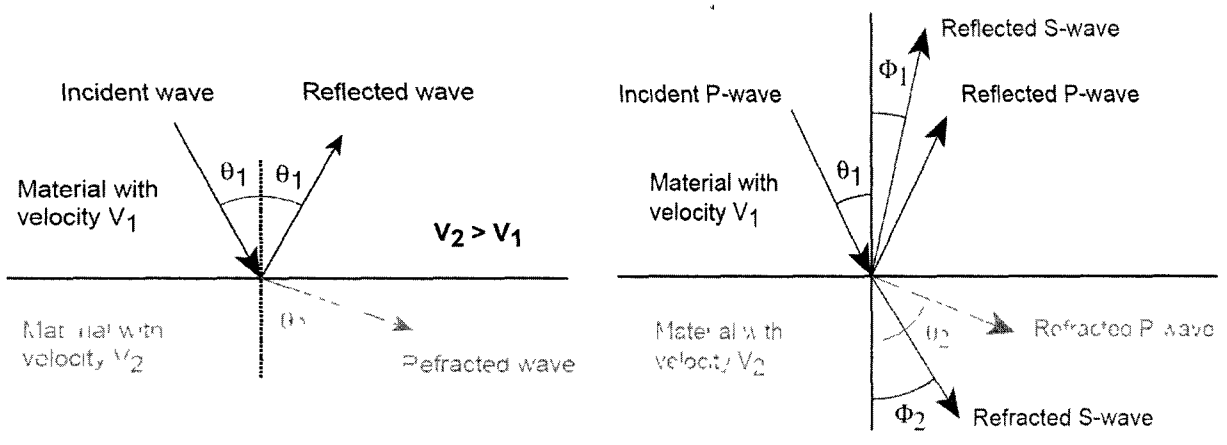

(a) Reflection and refraction (b) Mode conversion

Fig. 2-10 Behavior of P-wave incident on an interface between two dissimilar media [Carino, 2004]

2.3.4 Elastic wave velocity

From the basis of the elasticity and acoustics, two elastic moduli can directly be derived from density and wave velocity. The two elastic moduli are the longitudinal modulus (L) and shear modulus (G). Knowing the velocity of P-wave (V_p) and S-wave (V_s) in a material of (ρ) density, L and G can be calculated from Eqs. (2.11) and (2.12).

$$L = \rho v^2_p \tag{2.11}$$

$$G = \rho v^2_s \tag{2.12}$$

The L and G elastic moduli are related to the direction of particle motion caused by P-wave and S-wave. The L modulus relates strain to longitudinally applied stress, while G modulus describes the elastic behavior of a material when the strain perpendicular to the direction of the applied stress is zero. The L and G moduli are interrelated through the Lame's constant (λ) as given in Eq. (2.13) [Schreiber et al., 1973].

$$L = \lambda = 2G \tag{2.13}$$

2.4 Historical background about the non-destructive testing of early-age cementitiousa materials

2.4.1 The Maturity method

Carino, [2004b] reported that the maturity method was conceived by McIntosh, Nurse and Saul between [1949 and 1951],. Since then, the maturity method has been treated by numerous researchers and was finally standardized by ASTM C1074 [1998]. The method makes use of the combined effects of time and temperature on the strength gain of concrete. By knowing the age and the temperature history of the concrete an equivalent age value can be calculated which is related to the concrete compressive strength. The equivalent age can be understood as the length of the curing period at a certain reference temperature that would result in the same maturity as the curing period at a given (variable) temperatures that is currently observed and therefore these two factors can indicate the strength gain of concrete at early age, [Carino, 2004b] has provided an excellent reference about the principle and the application of the maturity method.

The method requires the recording of the concrete temperature as a function of time, which then used to determine the maturity of concrete. There are two functions that can be used when estimating the maturity index. One of the functions that are needed for applying the maturity method is the temperature-time factor can be calculated from Eq. (2.14), [Saul, 1951].

$$M(t) = \sum (T_\alpha - T_0)\Delta t \tag{2.14}$$

where; $M(t)$ is the temperature-time factor at age t, Δt is the time intervals, T_a is the average concrete temperature during the time interval, and t_0 is the datum temperature. The second one is equivalent age at specified temperature can be estimated from Eq. (2.15), [Hansen and Pedersen, 1977].

$$t_e = \sum e^{-Q\left(\frac{1}{T_a}-\frac{1}{T_s}\right)}\Delta t \tag{2.15}$$

where; t_e is the equivalent age at specified temperature, Q is the activation energy divided by gas constant, T_a is the average concrete temperature during the time interval, T_s is the specified temperature, and Δt is the time intervals.

There are two steps process to apply the maturity methods; the first one is the strength maturity relationship and second measure the maturity on side. The first procedure can be developed by casting compression specimens in parallel with specimens that have temperature sensors embedded. The concrete temperature data is recorded as a function of time, which then used to determine the maturity of concrete. At regular time intervals, the compressive strength specimens are tested. The compressive strength and maturity index is recorded. In specified time period, compressive strength is plotted as a function of maturity, predetermined strength-equivalent age relationship.

The application of the maturity for strength prediction on site requires only the measurement of the in-situ temperature of the concrete member to be tested. This temperature is used to determine the equivalent age which in turn allows the calculation of the strength by using the predetermined strength-equivalent age relationship. Figure 2.11 shown the application of the maturity method requires laboratory testing and field measurement of temperature history, [Carino and Lew, 2001]. This requires that the field concrete has the same properties as the concrete that was used for the laboratory testing. Furthermore, the field concrete must be cured properly, that is moisture must be available to allow sufficient hydration.

The maturity method is one of the more popular methods for monitoring the strength developments in concrete. However, the method has identified an influence of the early-age temperature history on the final strength of a given concrete mixture. Since the final strength is a parameter of the strength-equivalent age relationship, this dependency cannot be considered to be unique. In other words, if the early-age temperature history of the laboratory concrete significantly differs from that of the field concrete, the maturity method produces erroneous strength predictions. Consequently, requires the application of additional techniques to estimate the absolute strength level of the concrete, which is most often of interest, [Carino, 2004b].

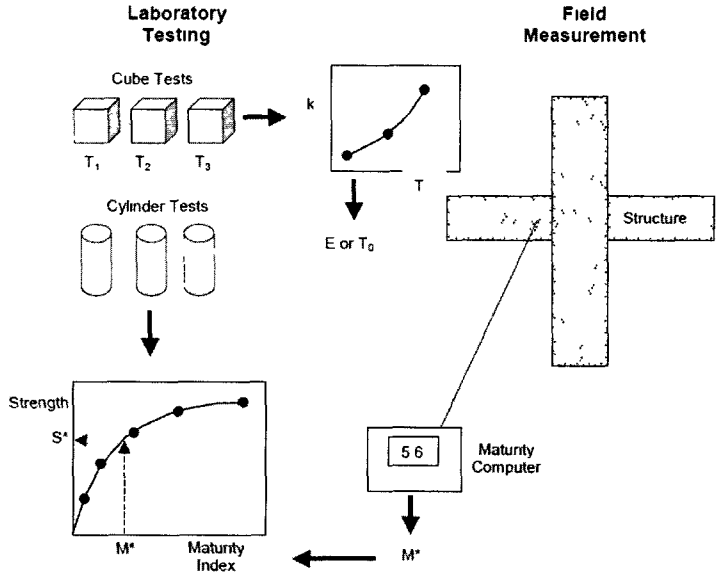

Fig. 2.11 Application of the maturity method requires laboratory testing and field measurement of temperature history, [Carino and Lew, 2001]

2.4.2 Ultrasonic pulse velocity method

The development of the pulse velocity methods began in Canada and England at the same time after World War II [Carino, 2004 c]. An ultrasonic pulse velocity method is a technique that uses tow transducers to measure velocity of a compression wave. One transducer will transmit the wave through the concrete and other receives the wave. By measuring the velocity of the wave, the properties of concrete can then be estimated. Like strength, durability of concrete, homogeneity of concrete, hydration of cement, and measurement of surface crack depth, [Carino, 2004].

Cheesman [1949], Jones [1949], and Whitehurst [1951] were the first who have conducted ultrasonic wave transmission experiments on concrete during setting. Jones [1949] observed that the P-wave velocity, measured on concrete during final setting, increases rapidly and that its rate of increase reduces considerably after one day of curing. Whitehurst [1951] investigated the quantitative relationship between P-wave velocity and final setting time of concrete containing different types of cement. The wave transmission measurements were conducted as early as two hours after casting the specimens. It was noted that P-wave velocity increase very rapidly in the beginning. However, a sudden decrease of the rate of change was reported before ten hours, with only little increase of the P-wave velocity after that. As a result of the investigations it was

shown that the marked change in the growth rate of the P-wave velocity coincides with the experimentally determined final setting time of the tested concrete.

The use of P-waves and S-waves in transmission mode to monitor concrete in the first hours and days after casting was reported by Pimenov et al. [1972]. It was shown that both wave types have the ability to detect internal changes of concrete when it is in fresh state or subjected to heat curing. The comparison of P- and S-wave velocity measurements to the appropriate compressive strength data showed that especially the S-wave velocity reproduced the trend of the strength data in a very good qualitative manner.

Neisecke [1974] has also reported the application of combined measurements with P-waves and S-waves. Development of P- and S-wave velocity and Poisson's ratio of cement paste hydration during first 24 hours after mixing was studied in Fig. 2.12. One of the findings was that the S-wave velocity develops after a clearly different trend than the P-wave velocity. Immediately after mixing, S-wave velocity remains at a value of zero before increasing gradually after approximately two hours. This phenomenon was interpreted with the absence of a continuous skeleton of solid particles that would allow the shear waves to propagate. The availability of P- and S-wave measurements allowed also the direct determination of the Poisson's ratio in a completely non-destructive manner. The development of this elastic constant from a value of 0.5 (fluid state) to approximately 0.25 (hardened state) is a very effective measure of the phase transition occurring to the cement paste.

Elvery and Ibrahim [1976] made a significant contribution to the understanding of the relationship between P-wave velocity and compressive strength of concrete by Experiments are reported that examine both parameters on concretes with different water/cement-ratios (0.4–0.7), aggregate/cement-ratios (1.0–5.9) and cement types at curing temperatures ranging from 1°C to 60°C. The tests were conducted with the main emphasis on the early age of the concretes (2 hours to 4 days). Figure 2.13 shows the compressive strength and P-wave velocity of early-age concrete. One of the most important conclusions was that for a concrete with a given cement type and aggregate content, the relationship between compressive strength and P-wave velocity is independent from w/c-ratio and curing temperature. When the logarithm of compressive strength is plotted against the P-wave velocity then this relationship was found to exhibit a clear bilinear characteristic.

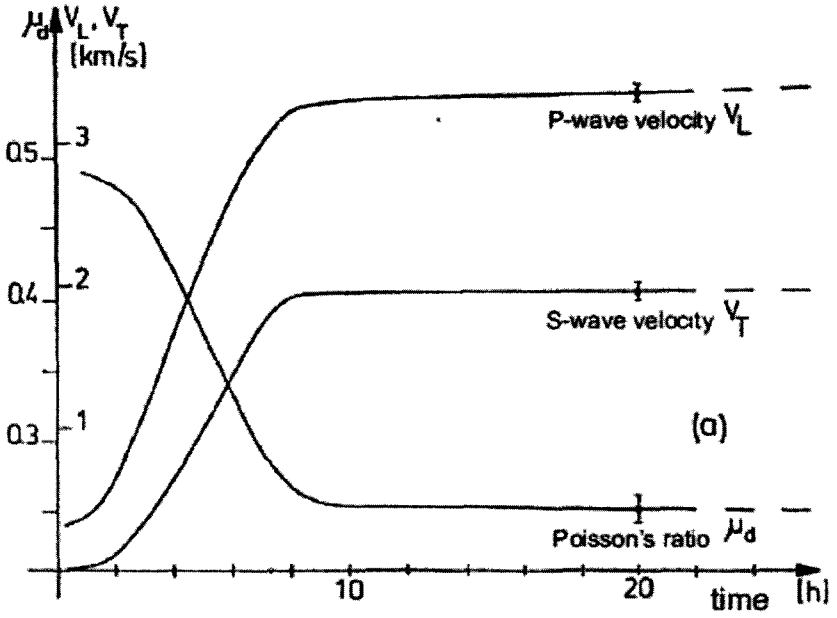

Fig. 2.12 Development of P- and S-wave velocity and Poisson's ratio of cement paste [Neisecke, 1974]

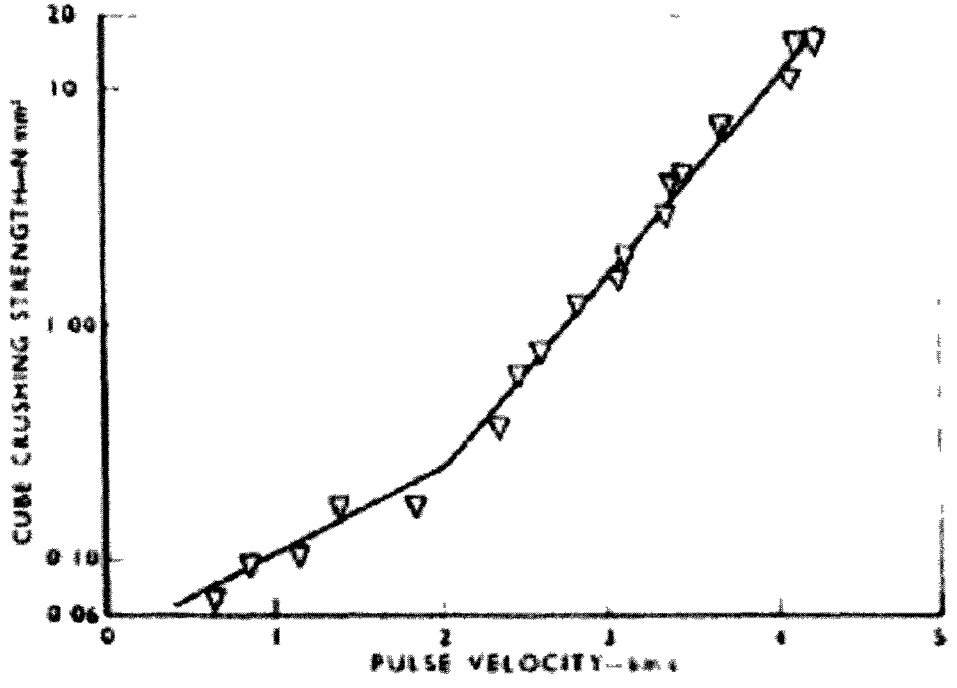

Fig. 2.13 Compressive strength vs. P-wave velocity of early-age concrete [Elvery and Ibrahim, 1976]

Kruml [1990] and Domone and Thurairatnam [1990] investigated the setting behaviour of concrete with the P-wave velocity method and compared the obtained results to those of other suitable methods, such as pin penetration, calorimetry and viscometer tests. The P-wave velocity was found to be indicative of the examined setting process and comparable to the other methods used. Popovics et al. [1994] analyzed the propagation of P-waves in fresh and hardened concrete. The experiments showed that at very early ages the P-wave velocity is influenced by the cement paste portion of the concrete. Consequently, appropriate changes in the P-wave velocity can be observed, when the cement paste builds up solid structure. These changes were found to be especially rapid immediately after the initial setting time as shown in Fig. 2.14. The attenuation of the transmitted pulses also appeared to be very sensitive to changes in the internal structure of the hydrating cement paste. The same technique was compared to other methods in its ability to determine the w/c-ratio of concrete by Popovics [1998]. Although the method gave the most reliable results, general dependencies could not be derived.

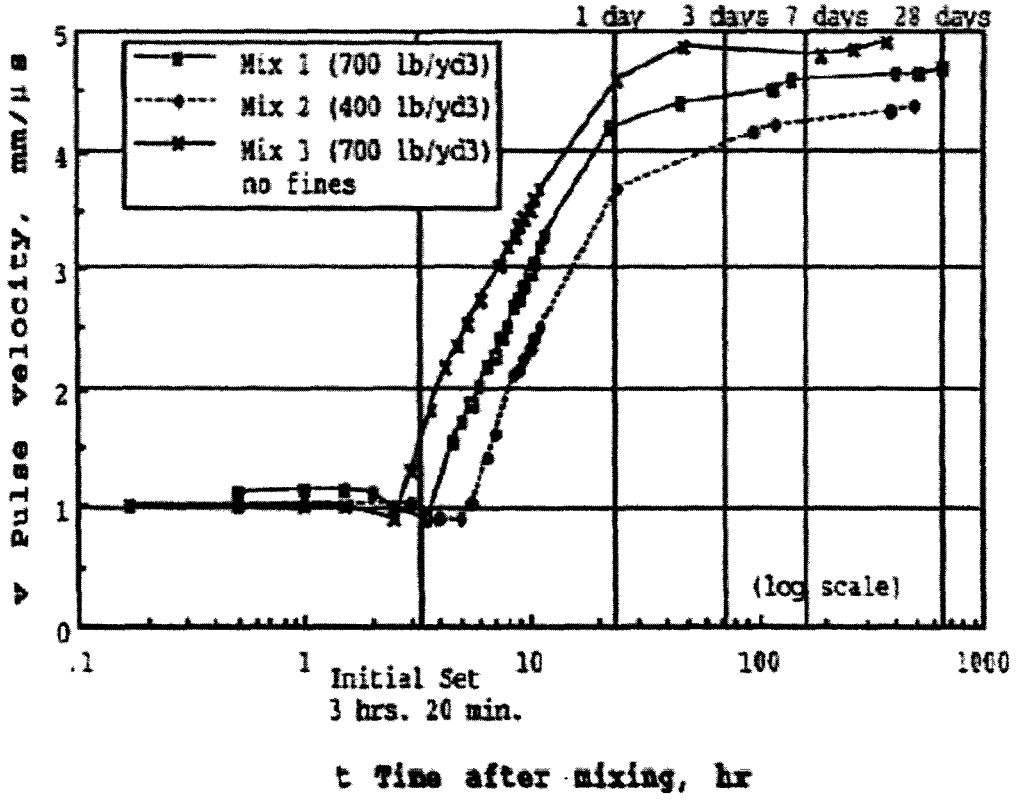

Fig. 2.14 Effect of cement content on P-wave velocity at early age [Popovics et al., 1994]

Reinhardt et al. [1998] reported the parameters P-wave velocity, relative energy as well as the frequency spectrum can indicate the setting and hardening behaviour of concrete influenced by cement type, w/c-ratio, aggregate size and chemical admixtures, such as retarder (in different contents), air entrained, and super plasticizer. The authors also suggest modelling the development of the P-wave velocity with the Boltzmann equation. It is shown how the different parameters of this equation can be varied to model the influence of, for example, the w/c-ratio on the shape of the P-wave velocity curves.

Newly developed equipment combined with the appropriate computer software for the continuous measurement of the P-wave velocity in setting mortar and concrete were presented by Reinhardt et al. [2000]. The method uses a PMMA container with attached ultrasonic transducers to hold the fresh materials to be tested as shown in Fig 2.15. The measurements are fully automated and analyzed by special software, which results in the immediate availability of the test parameters P-wave velocity, relative energy and frequency spectrum. Further details about this test setup and its application are also given in [Grosse, 2000] and [Reinhardt and Grosse, 2004].

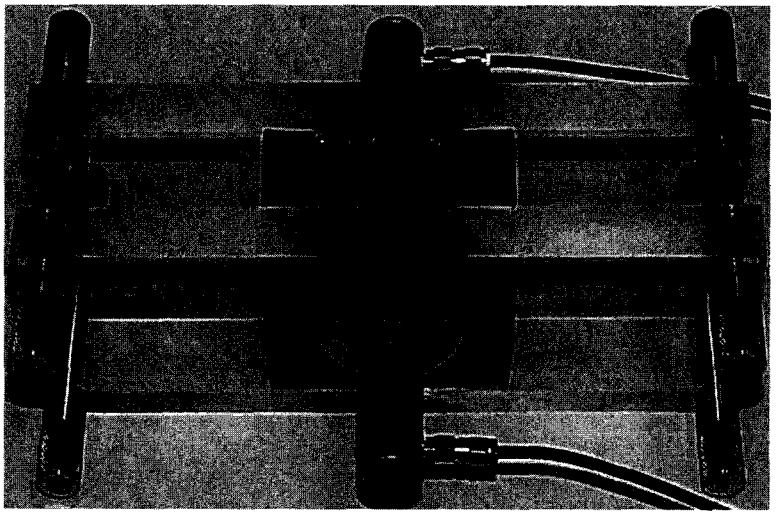

Fig. 2.15 Container for pulse velocity measurements of fresh and hardened mortar developed at Stuttgart University, Germany [Grosse, 2004]

Lee et al. [2004] analyzed how P-wave transmission experiments using a technique identical to that developed by Reinhardt et al. [2000]. The focus of the investigations was to develop relationships between the setting behaviour and the P-wave velocity measured on

mortars and concretes in four different water/cement-ratios with and without fly ash. It was found that a certain range of P-wave velocity can be taken as an indicator of the occurrence of the initial setting time of the tested mortars. However, this range was found to influenced by the presence of fly ash in the mixture (without fly ash: 800–980 m/s; with fly ash: 920–1070m/s).

J. Zhang et al. [2008] detected the setting and hardening behaviours of cement paste during the first 7 days of hydration using two techniques, the electrical resistivity and ultrasonic techniques. In the electrical resistivity method, a non-contacting device was used. In the ultrasonic method, a wave was transmitted and measured by the embedded piezoelectric ultrasonic transducers, which had good coupling with the surrounding materials. The results illustrated that both electrical resistivity and ultrasonic techniques were effective to accurately monitor the hydration of cement pastes. The resistivity method was able to study both the chemical reaction and physical change during hydration, while ultrasonic method was sensitive to physical change of cement only.

The pulse velocity method is an excellent test. It can be used to evaluate the development of the mechanical properties of early age of cementitious materials. The pulse velocity method has been applied to monitor the setting time, compressive strength, uniformity, and elastic moduli of cementitious materials. The testing procedure is simple and the equipment is easy to use in the situ as well as in the laboratory. The test methods has few disadvantages; difficulty penetrating large specimens due to the high attenuation of concrete, and the speed of sound is dependent on many factors in concrete, which effects the velocity of the wave, [Borgerson, 2007].

2.4.3 Impact-echo method

The impact-echo method was developed by researchers of the National Institute of Standards and Technology (NIST), which was formerly known as the National Bureau of Standards (NBS), of the United States of America. The main application field of the impact-echo method is the detection of internal features of concrete structures, such as cracks, [Carino 2004].

Pessiki and Carino [1988] reported how the impact-echo method can also be used for monitoring the setting and hardening of early-age concrete. The authors conducted impact-echo measurements on freshly cast mortar and concrete. Figure 2.16 shows the schematic of experimental apparatus of impact-echo method. The obtained P-wave velocity data were analyzed in regard to the initial and final setting time measured with the pin penetration method

as well as compressive strength of cylinders. The results indicated the general suitability of the impact-echo method to measure the P-wave velocity of concrete and mortar during setting. Furthermore, the value of the P-wave velocity that was found to correlate to the time of initial set was 670 m/s.

A continuance of the efforts to apply the impact-echo method for measurements of fresh concrete was presented by Grosse et al. [2004]. To perform the measurements, a glass plate was placed on the surface of a fresh concrete slab and used to induce the mechanical impact. The measurements were conducted on slabs with a thickness of 5 to 20 cm during the first 22 hours of hydration. The authors compared the resonant frequency measured on the slab with that theoretically derived from the P-wave velocity in through transmission and found that both parameters agreed reasonably well. Based on these results, it is concluded that the impact-echo has the potential to evaluate early-age concrete properties with good accuracy. Newly developed impact-echo equipment allowing the application of the method for field testing is also presented.

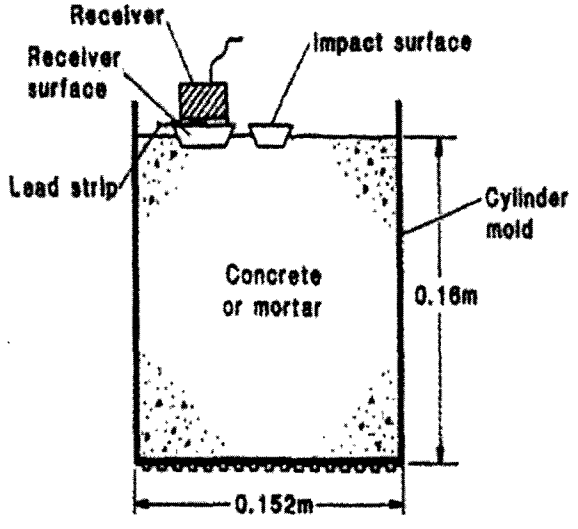

Fig. 2.16 Schematic of experimental apparatus impact-echo method [Pessiki and Carino, 1988]

The impact-echo method has shown it can be effectively monitor the development of set and strength, of early age. While this approach has proven to be successful, it has difficulty to identify the correct peak which causes by multiple reflections.

2.4.4 Ultrasonic wave reflection method

The first application of the wave reflection method for testing cementitious materials was reported by Stepisnik et al. [1981] and Lasic and Stepisnik [1984]. The extensive research has been undertaken to investigate the applicability of the wave reflection method to monitor the setting and hardening of cement-based materials. The method evaluates the development of the cementitious materials by evaluating the loss of bulk waves to specimen from a buffer material, usually steel. Waves are transmitted and received through a buffer material which is placed in contact with a sample of concrete. The reflection of the wave is related to properties of cementitious materials: as the skeleton of the concrete change, consequently wave reflected will be change.

Ozt¨urk et al. [1999] investigated the ability of the wave reflection method to monitor the setting and hardening of concrete when influenced by several admixtures. Besides a plain concrete mixture for reference, concretes containing accelerator, retarder, superplasticizer, and silica fume were tested. The ultrasonic measurements were complimented by heat of hydration measurements and the determination of the initial and final setting time. Compression and shear waves were used for the wave reflection measurements. The results have shown that the development of the shear wave reflection coefficient indicates very well the influence of the different admixtures on the hydration behaviour of the tested materials. It was also observed that the initial setting time and the time of the decrease in the reflection coefficient are influenced to the same degree by the different admixtures.

The previous study was extended by Rapoport et al. [2000] studied the relation between the wave reflections and the development of shear modulus. The method has shown to be able to monitor strength gains in large slab.

Shah and his associates have developed an application of the wave reflection technique that uses a steel plate as the buffer material. Figure 2.17 shows schematic of experimental apparatus for WR-measurements. In several studies the applicability of the method for fundamental laboratory investigations of hydrating cement, mortar and concrete was investigated. Furthermore, the possibility of the practical application of the method was addressed by designing experiments to extract potentials and limitations. A general overview about the method used by this group is given by Shah et al. [2000], Voigt and Shah [2002-2003] and Voigt et al. [2004].

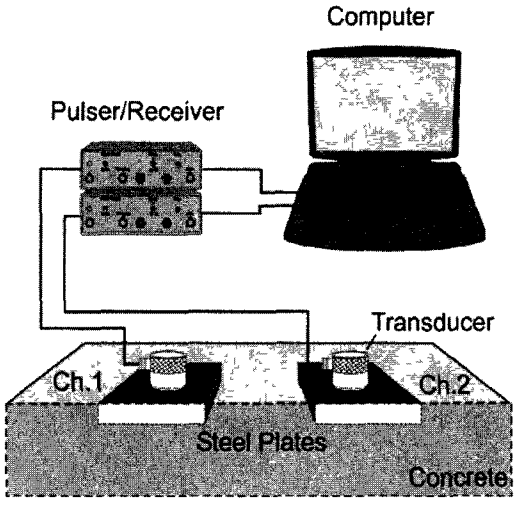

Fig. 2.17 Schematic of experimental apparatus for WR-measurements [Voigt et al., 2005]

In order to increase the sensitivity of the ultrasonic measurement, steel was replaced by a material with lower acoustic impedance for the buffer material. [Ozt¨urk et al., 2004] improved the wave reflection test setup that was developed earlier [Ozt¨urk et al., 1999]. A correlation between the setting and hardening of cement-based materials and the development of the reflection coefficient was done. The initial set and final set were correlated to the inflection point and the increase of the wave reflection curve after having reached its minimum, respectively. The dynamic Young's modulus, the compressive strength and the degree of hydration were reflected in the development of the wave reflection curve. The sensitivity of the technique to the influence of the ambient temperature on the hydration process of early-age concrete was also investigated.

The wave reflection method has shown it can be effectively monitor the development of set, strength, shear modulus, and microstructure of early age cementitiouse materials. The primary advantage of the reflection method is its ability to operate from one side of the specimen. While this approach has proven to be successful, it only gives information at or near the surface of the concrete, and properties of concrete will often vary with depth in addition the transducer and steel plate was coupling [Borgerson, 2007].

2.4.5 Ultrasonic guided wave

The guided wave approach monitors the development of the concrete properties by evaluating the loss of bulk waves to concrete from another material, usually steel. However, using the guided wave technique transmits and receives waves through a cylindrical wire or rode, [Borgerson, 2007].

Pu et al., [2004] investigated the use of a longitudinal mode to get shear wave velocity of a concrete mixture by monitoring the attenuation of guided wave. The results were shown that guided wave can be used to monitor the hydration of mortar and concrete.

Borgerson [2007] analyzed tow ultrasonic guided wave methods for monitoring early age cementitious materials: a through –transmission system and a pulse- echo system. Both approaches utilize the fundamental tensional wave mode at low frequency-radius products.

The through-transmission system transmits the torsional wave mode on one end of a steal rod embedded in mortar and then receives the signal on the opposite end of the rod. The attenuation due to energy leakage from the waveguide into surrounding material is measured over time. Several different mixtures with varying water-cement ratios and admixture (mineral and chemical) were tested. Figure 2.18 shows the schematic of experimental apparatus wave guided testing system in system in a through-transmission arrangement [Borgerson , 2007].

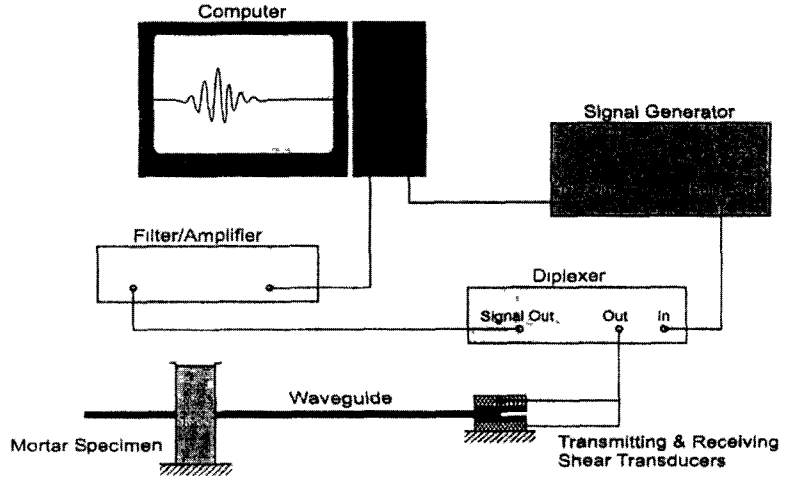

Figure 2.18 Schematic of experimental apparatus wave guided testing system in a through-transmission arrangement [Borgerson, 2007]

The other technique is pulse-echo ultrasonic guided wave approach. This method transmits the torsional wave mode on the free end of a steal rode partially embedded in mortar and monitors reflected signals. Both the reflection from the end of the rod and the reflection from the point where the waveguide enters the mortar are monitored. The development of the mortar's mechanical properties is related to both the energy leaked into the surrounding mortar and the energy reflected at the entry point. As the embedding develops, the end –reflection will attenuate due to the leakage of bulk shear wave while the entry- reflection will increase in magnitude due to the increase in rigidity of the mortar. Figure 2.19 shows the schematic of experimental apparatus wave guided testing system in alternative a pulse-echo [Borgerson, 2007].

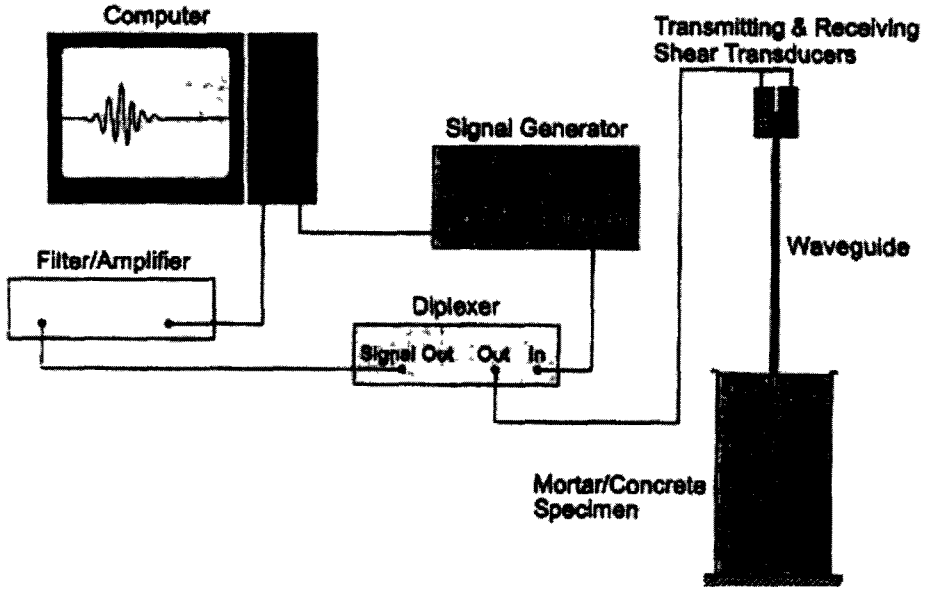

Fig. 2.19 Schematic of experimental apparatus wave guided testing system in alternative a pulse-echo [Borgerson, 2007]

The wave guided method has shown it can be effectively monitored the development of set and strength of early age cementitious materials. While this approach has proven to be successful, but little research has been conducted on this method.

2.5 Summary

In this chapter a brief overview of cement-based materials properties at early- age (setting time, kinetic heat of hydration, Conductivity, Resistivity and Compressive strength) were given. Furthrmore , a reiview of wave propgation fundamentals was given. The different tybe of wave motion were discriebed. Tow tybe of waves exist in finite elastic soild media; compresison and shear wave. Longitudial waves travel fasrer and the partical motion is in the direction of propgation. However shear wave velosity travel slower and the partical in prependicular to the direction of propgation.

The shear-wave velocity (V_s) and compresion wave (V_p) are fundamental parameter that correlates well to cement-based materials properties, and is important in many applications. Hence, there is an increasing interest in using these wave velocities to define cement-based materials properties at early ages (setting time, heat of hydration, compressive, etc).

Previous nondistructive test methods to evaluate development of early age cementitious materials were presented. Each method has strengths and weaknesses. At currently there are two standardized methods that can characterize the properties of early age cement-based materials, ultrasonic pulse velocity and maturity method. The ultrasonic pulse velocity has been applied to monitor the setting time, compressive strength, uniformity, and elastic moduli of cementitious materials. The testing procedure is simple and the equipment is easy to use in the situ as well as in the laboratory. The test possess has few disadvantages; difficulty penetrating large specimens due to the high attenuation of concrete, and the speed of sound is dependent on many factors in concrete, which effects the velocity of the wave. The maturity method has achieved moderate success for monitoring the strength gain development. The method relates early age strength to a chemical reaction, its temperature over time. The large variation in the environmental condition can cause inaccurate estimation of strength. Ultrasonic shear wave reflection methods has shown it can be effectively monitor the development hydration cement-based materials at early age while this approach has proven to be successful, it only gives information at or near the surface of the concrete, and properties of concrete will often vary with depth. Ultrasonic guided wave, this approach has proven to be successful to evaluate hydration of early age properties, unfortunately little research connected and also there is no application on the field at the current time.

CHAPTER 3
EXPERIMENTAL PROGRAM

3.1 Introduction

Development of simple and accurate device to evaluate properties of cement-based material at early age is important to replace the existing empirical test methods to evaluate the kinetics of cement hydrations. The possibility of using pulse velocity test (Piezoelectric ring actuator technique, *P-RAT*) developed at the University of Sherbrooke to evaluate soil properties are explored in this research. This chapter presents the experimental program proposed to evaluate possibility of using the version of *P-RAT*, to be employed to estimate the hydration properties of the cement-based materials. Descriptions of materials, mixture preparation, and mixing sequence used in the experimental tests are given in this chapter. The traditional test methods used to examine the fresh properties of cement–based materials including Vicat needle apparatus, penetration resistance test, calorimetry test, electrical conductivity test, and compressive strength test are also detailed in this chapter.

3.2 Testing proposal

A summary of the overall testing program presented in this study is given in Fig. 3.1. The investigation carried out through five main parts. The first part includes trial tests to investigate the possibility of employing the *P-RAT* to determine the fresh properties of cement-based materials. The main issue here is to obtain adequate accuracy of signal processing and satisfactory measurement of fresh properties of the cement-based materials. The first trial tests were carried out on two mortar mixtures proportioned with different *w/cm*.

Based on the results of the trial tests, two probabilities can be raised. The *P-RAT* may offer adequate or inadequate evaluation of hydration for cement-based materials properties. In the latter case; not obtaining adequate accuracy of signal processing or satisfactory measurement of fresh properties of the cement-based materials, adaptation to the *P-RAT* conducted. The resulted version of *P-RAT* after the modification was referred to as *P-RAT2*.

Repeatability of *P-RAT2* carried out in the third part of the study. Typical paste mixture with *w/cm* of 0.42 was prepared and tested three times to determine the relative error corresponding to 95% confidence interval for the values of shear wave velocity obtained using the new version of *P-RAT*.

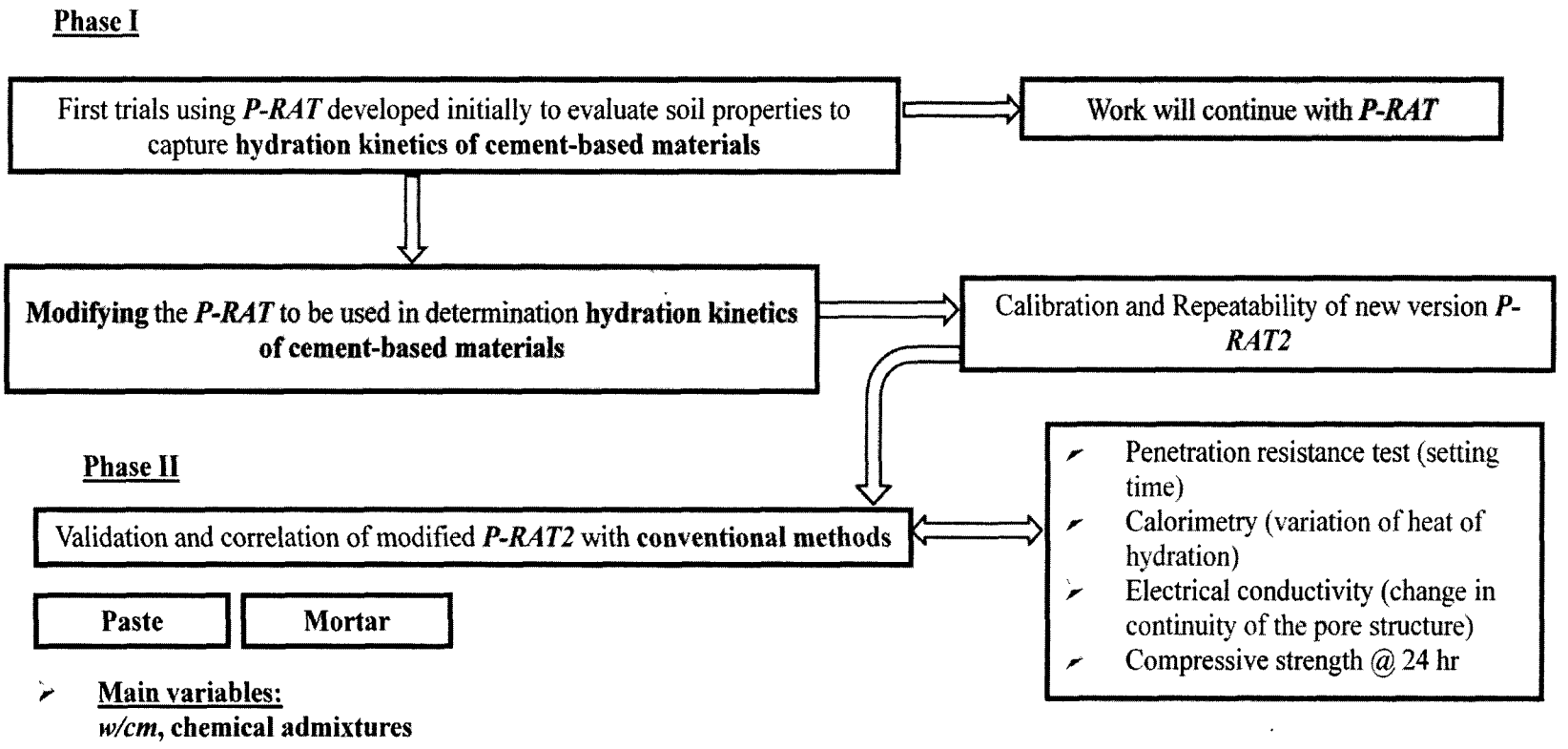

Fig. 3.1 Schematic for testing program

In the fourth part of the study, an extensive validation for recommended *P-RAT2* was tested. The validation was achieved through comparing the hydration properties (heat of hydration, setting time, and electrical conductivity) and compressive strength obtained using the conventional test methods to the shear wave behaviour obtained using recommended *P-RAT2*. The previous properties were obtained for various cement-based materials including paste and mortar mixtures.

Finally, correlating results obtained using the recommended *P-RAT2* to those obtained using the traditional test methods. The correlations improve the capability of *P-RAT2* to interact with different apparatus used to evaluate fresh properties of cement-materials at early ages.

3.3 Materials

A wide variety of materials was used in this research. A focus on the material characteristics used in the laboratory investigations for the evaluated mixtures are elaborated in the following sections. In order to avoid contamination with external agents and moisture, sufficient quantities of the used materials for the entire investigation were prepared and stored in air-tight barrels.

3.3.1 Cement

General use cement (Type GU) from St-Laurent cement was used. The particle-size distribution for the cement is presented in Fig. 3.2. Its physico-chemical properties and mineralogical compositions are given in Table 3.1.

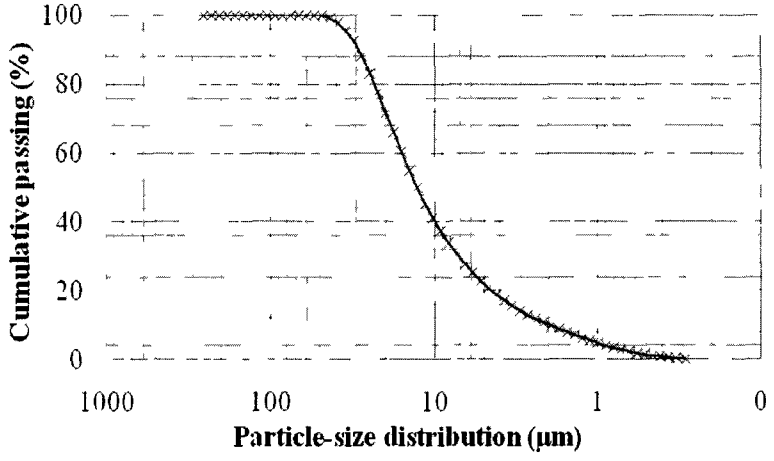

Fig. 3.2 Grain-size distribution of Type-GU cement

Table 3.1 Characteristics of GU cement

Identification	Type GU cement
Silicium (SiO_2), %	19.9
Alumina (Al_2O_3), %	4.7
Iron oxide (Fe_2O_3), %	3
Total calcium oxide (CaO), %	62.7
Magnesium oxide (MgO), %	2.1
Sulfur trioxide (SO_3), %	3.4
Equivalent alkali (Na_2O_{eq}), %	0.89
Loss on ignition (LOI), %	2.4
C_3S, %	58.2
C_2S, %	13.1
C_3A, %	7.4
C_4AF, %	9.3
Blaine surface, m^2/kg	384
Specific gravity	3.15
Autoclave expansion, %	0.03
Percentage passing 45 μm, %	94
Air content, %	6.4
Compressive strength at 3 days, MPa	27.8
Compressive strength at 7 days, MPa	31.9
Compressive strength at 28 days, MPa	39
Initial setting time (Vicat), min	125
Final setting time (Vicat), min	210

3.3.2 Sand

Well-graded natural siliceous sand was used. The sand was provided by Bétons Aimé Côté Inc. It has saturated-surface dry (SSD) specific gravity of 2.70, absorption of 1.12%, and fineness modulus of 2.4. The particle-size distribution of the sand lies within CSA A23.2-5A recommended limits given in Fig. 3.3.

3.3.3 Chemical admixtures

Several chemical admixtures were used in this study to introduce some variation in cement hydration. Poly-naphthalene sulfonate (PNS) high-range water-reducing agent (HRWRA) under the commercially Disal from Handy Chimical was used. The HRWRA was present with the mixing water in order to homogenize the solution. The water in the HRWRA was taken into account in the mixture proportioning to maintain a fixed *w/cm*. Na-Glucorate set-retarding agent (SRA) was employed. $CaCl_2$ set-accelerating agent (SRA) was also used in some mixtures. Welan gum from was used for the viscosity-modifying agent (VMA). In some mixtures the SRA, SRA, and VMA were mixed with part of the mixing water in the mixer prior usage. The values for specific gravity, and solid contents, are given in Table 3.2.

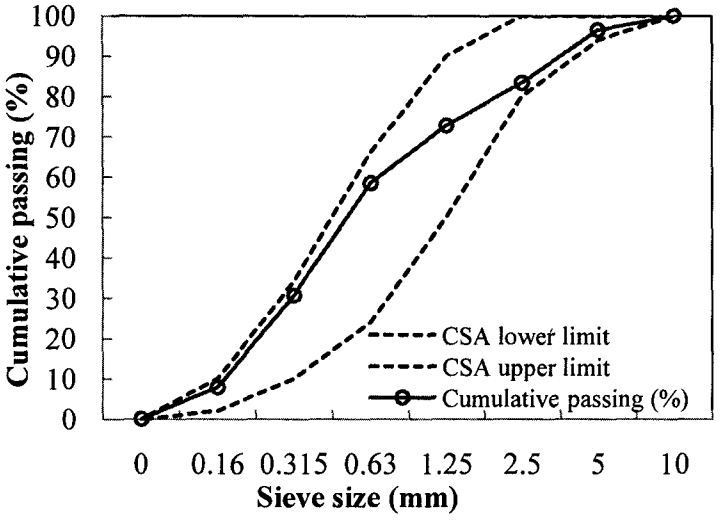

Fig. 3.3 Grain-size distribution of sand

Table 3.2 Characteristics of chemical admixtures used

Admixture	Identification	Company	Specific gravity	% Solid content
HRWRA	Disal	Handy Chemicals	1.2	42
VMA	Welan gum	CP-Kelco	-	Solid powder
SRA	Na-Glucorate	-	-	Solid powder
SAA	$CaCl_2$	-	-	Solid powder

3.4 Mixture composition

In total, 12 mixtures were prepared for this investigation, including three paste mixtures and nine mortar mixtures. The mixture proportions of the 12 mixtures are given in Table 3.3. In term of cement content the mixture compositions are listed in Tables 3.4 and 3.5 for the paste and mortar mixtures, respectively. Both paste and mortar mixtures were designed with *w/cm* varied between 0.35 and 0.5. The paste mixture proportioned with *w/cm* of 0.42 (Mix-2) was prepared and tested three times to determined the repeatability of the *P-RAT*. As will as Mix-6 mortar mixture that proportioned with w/cm of 0.42 and contained only HRWRA without any other chemical admixtures was selected as a reference for Mix-7, Mix-8 and Mix-9 mixtures. In the latter three mortar mixtures SAA, SRA, and VMA were added, respectively. The four mortar mixtures were selected to evaluate the ability of P-RAT2 to examine the effect of chemical admixture on the early properties.

Table 3.3 Mix designs proportioned to cement

Material	Paste			Mortar								
	Mix-1	Mix-2#	Mix-3	Mix-4	Mix-5	Mix-6	Mix-7	Mix-8	Mix-9	Mix-10	Mix-11	Mix-12
Type-GU cement	1.0	1.0	1.0	1.0	1.0	1.0	1.0	1.0	1.0	1.0	1.0	1.0
w/cm	0.5	0.42	0.35	0.5	0.35	0.42*	0.42	0.42	0.42	0.42	0.35	0.39
Sand	--	--	--	2.0	2.0	2.0	2.0	2.0	2.0	2.0	2.0	2.0
HRWRA%	--	0.38	0.61	--	1.6	1.123	1.123	1.123	2.25	--	--	--
Set accelerator %	--	--	--	--	--	--	1.0	--	--	--	--	--
Set retard %	--	--	--	--	--	--	--	0.075	--	--	--	--
VMA%	--	--	--	--	--	--	--	--	0.06	--	--	--

was repeated three times to determine the relative error
* Reference mixture

Table 3.4 Mix design of paste mixtures

Materials	Paste mixtures		
	Mix-1	Mix-2*	Mix-3
Target mini slump flow (mm)	75 ± 5	75 ± 5	75 ± 5
Cement (kg/m^3)	1197	1327	1466
Water (kg/m^3)	599	557	513
w/cm	0.50	0.42	0.35
HRWRA (kg/m^3) (liquid)	--	5.1	9

3.5 Fresh properties

Summary of the fresh properties of the tested paste and mortar mixtures used in this study, including slump flow diameters, are given in Table 3.5. The slump flow values for paste and mortar mixtures were determined according to the ASTM C 230/C 230 M-03. The mini cone test of the paste was used to determine the slump flow for paste mixtures of 20 mm top diameter and 39 mm bottom diameter with 54 mm height. For the mortar mixtures, mini slump cone test (70 mm top diameter, 100 mm bottom diameter, 50 mm height) was conducted to measure the slump spread. The spread of the slumped samples was measured after lifting the sample by 25 blows from the mechanical vibrator. The slump flow values ranged between 72 and 79 mm for the paste mixtures, while these values varied between 210 and 265 mm for the mortar mixtures. The measurements of slump flow are shown in Figs. 3.4 and 3.5 for the paste and mortar mixtures, respectively. The temperatures of the fresh mixtures were controlled at approximately 24 °C. The unit weights of the tested mixtures are given in Table 3.6.

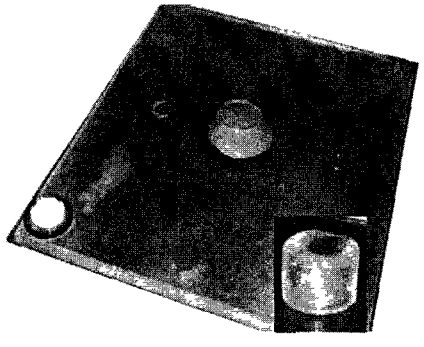

Fig. 3.4 Slump flow for typical paste mixture

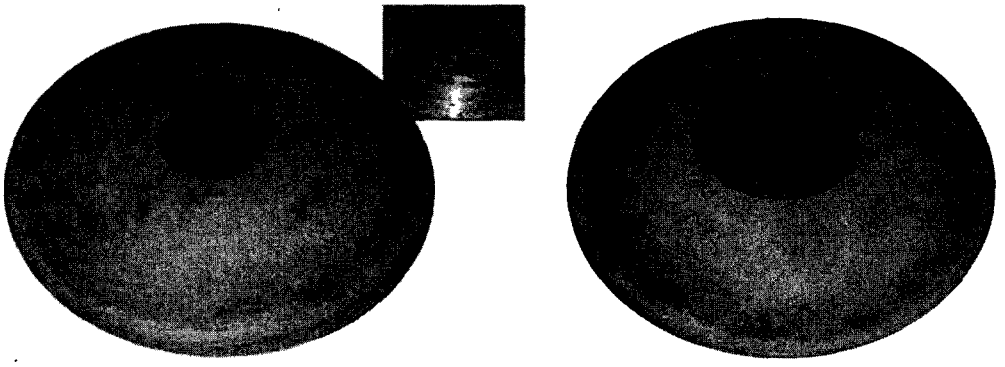

Fig. 3.5 Slump flow for typical mortar mixture before vibration (left) and after vibration (right)

Table 3.5 Mixture proportion for the mortars through this study

Mix design	Mix 4	Mix 5	Mix 6	Mix 7	Mix 8	Mix 9	Mix 10	Mix 11	Mix 12
Target slump flow (mm)	265±5	265±5	265±5	--	--	--	--	--	--
Cement (kg/m^3)	673	751	713	713	713	713	713	751	728
Sand (kg/m^3)	1137	1267	1203	1203	1203	1203	1203	1267	1229
Water (kg/m^3)	337	277	313	313	313	313	313	277	298
w/cm	0.50	0.35	0.42	0.42	0.42	0.42	0.42	0.35	0.39
SAA (kg/m^3)	--	--	--	5.18	--	--	--	--	--
SRA (kg/m^3)	--	--	--	--	1.42	--	--	--	--
VMA (kg/m^3)	--	--	--	--	--	0.4	--	--	--
HRWRA (kg/m^3)	--	12	8	8	16	8	--	--	--

Table 3.6 Fresh properties of the pastes and mortar mixture

Mixture		*w/cm*	Slump flow (mm)	Unit weight (kg/m^3)	Temperature (°C)
Paste	Mix-1	0.50	79	1796	24
	Mix-2	0.42	76	1886	23.5
	Mix-3	0.35	72	1983	24
Mortar	Mix-4	0.50	265	2160	24
	Mix-5	0.35+ HRWRA	263	2232	24
	Mix-6	0.42+ HRWRA	260	2300	24
	Mix-7	0.42+SAA	210	2232	24
	Mix-8	0.42+SRA	285	2263	24
	Mix-9	0.42+VMA	260	2197	24
	Mix-10	0.42	235	2228	24
	Mix-11	0.35	218	2295	24
	Mix-12	0.39	-	-	24

3.6 Mixing procedure

3.6.1 Paste mixing procedure

The paste was mixed according to ASTM C 305-99, as follows;

1. Dry up the paddle and bowel;
2. Add the entire quantity of mixing water with admixture in the bowel (keep the temperature of mixing water at 23 ± 1.7 ° C);
3. Add cement to mixing water and rest them in the bowel for 30 s for full absorption of cement with water;
4. Mix at slow speed for 30 s
5. Stop mixing for 15 s, in which scrape down any patch that may have collected on sides of the bowel

6. Mix at medium speed for 60 s; and
7. Measure slump flow.

3.6.2 Mortar mixing

The batching sequence for the mortar mixtures were carried out according to ASTM C 305-99, as follows:

1. Dry up the paddle and bowel;
2. Add equivalent quantity of sand similar to that used in the batch to the mixer and homogenize for 30 s, then take 500-g sample to determine its humidity;
3. Correct the quantity of mixing water, if any, due to the humidity of sand;
4. Place the chemical admixtures diluted in the mixing water to the bowel (keep the temperature of mixing water at $23 \pm 1.7\,^{\circ}C$);
5. Add the cement to the water and mix at slow speed for 30 s;
6. Add the sand over 30 s of mixing at low speed;
7. Stop the mixer and change to the medium speed for extra 30 s;
8. Pause mixing for 90 s; during the first 15 s of the 90 s, scrape down any patch that may have collected on sides of the bowel, then cover the mortar with a lid for the rest 75 s; and
9. Mix at the medium speed for extra 1min.

3.7 Test methods

The standard test methods was used to characterize the hydration processes of the cement-based materials at early age, including the penetration resistance test, Vicat needle, calorimetric test, conductivity test, and compressive strength test at 24 hr. The measurements obtained using these test methods were used to validate results of *P-RAT*. The measurements of these set up were measured sequent after cement water contact.

3.7.1 Penetration resistance test

The penetration resistance test method (Fig. 3.6) is used to determine the initial and final setting times of mortar or mortar extracted from concrete, by means of penetration resistance measurements according to ASTM C403. The apparatus consists of three containers, needles, and loading apparatus. The containers were used, rigid, watertight, nonabsorptive, free of oil or grease,

and either cylindrical or rectangular in cross section. The surface area of the container was provided for ten undisturbed readings of penetration resistance in accordance with clear distance requirements (25 mm). Penetration needles with bearing areas of 1, 1/2, 1/4, 1/10, 1/20, and 1/40 in.^{2} [645, 323, 161, 65, 32, and 16 mm^2] that was attached to the loading apparatus, were used.

To evaluate setting times of mortar or mortar extracted from concrete, a representative sample is placed in the three containers. Measurements of the force required to develop certain resistance over early hours after cement water contact are conducted. The measurements of penetration resistance were performed in regular-time intervals until the specimen is completely set. The penetration resistance was calculated as the ratio between the applied force and the bearing area of the used needle. The readings of penetration resistance are plotted against the elapsed time as shown in Fig. 3.5. The initial and final setting times correspond to penetration resistances of 3.5 and 27.6 MPa, respectively. The two values of penetration resistance correspond to two particular practical points; (i) limit of handling and (ii) beginning of mechanical strength development, respectively [Mehta,1993].

Fig. 3.6 Experimental equipment for penetration resistance test

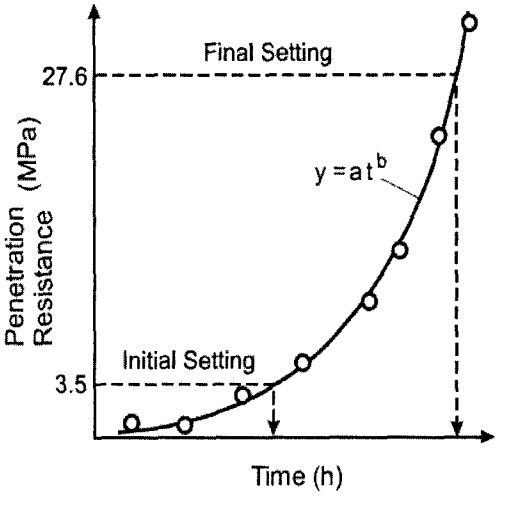

Fig. 3.7 Determination of initial and for penetration resistance test

3.7.2 Vicat needle apparatus

Vicat needle apparatus (Fig. 3.8) is used for determination of the normal consistency and setting times of cement [ASTM C 191–04a]. The apparatus consists of a metallic frame bearing a

sliding rod with a cap at top, one Vicat conical mould, split type and glass base plate, and one set of needles one each initial needle, final needle, and consistency plunger. An adjustable indicator moves over a graduated scale. The needle or plunger is attached to the bottom end of the rod to make up the test weight of 300 g.

According to ASTM C 191–04a.The test was performed form the cement paste into a ball with gloved hands and toss six times from one hand to the other. The ball was pressed, rested in the palm of the hand, held in the other hand. The mould was filled completely with paste. The test specimen was placed immediately after moulding in the moist cabinet. A periodic penetration test was performed on this paste by allowing a 1-mm Vicat needle to settle into this paste.

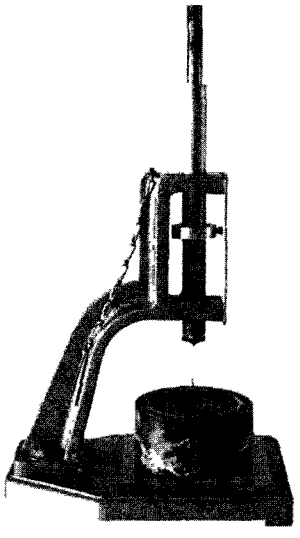

Fig. 3.8 Vicat needle apparatus

The Vicat initial time of setting was calculated as the time elapsed between the initial contact of cement and water and the time when the penetration is at 25 mm. The Vicat final time of setting was calculated as the time elapsed between initial contact of cement and water and the time when the needle does not sink visibly into the paste.

3.7.3 Calorimetry

To evaluate heat of hydration of hydraulic cement, a semi-adiabatic calorimetric was used (Fig. 3.9). The heat of hydration was measured on cement paste or mortar. The calorimeter test

contains cylindrical plastic mould of 51 mm in diameter and 102 mm in height isolated by a curing room. The curing room was filled with 100 mm and 25 mm of water at temperature of 25°C in case of paste and mortar specimens, respectively. The cylindrical mould was filled with a freshly mixed cement paste or mortar. The test specimen should be placed in the cylindrical mould of the calorimeter at 25°C. A temperature sensor is attached to the cylindrical mould to monitor the variations in temperature of the test sample with time.

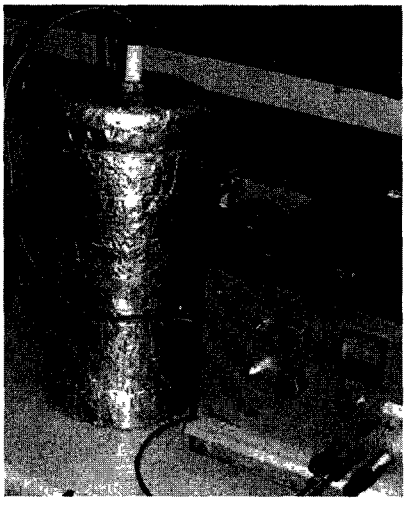

Fig. 3.9 Experimental equipment to evaluate the heat of hydration

The heat transfer from the test specimen to the outer chamber is evaluated by a software program based on the degree of the insulation provided by the calorimetric equipment and the difference between the sample and room temperature. The heat loss was used to calculate the adiabatic heat release of the tested materials during hydration based on the measured semi-adiabatic heat release development. Further details about the used calorimetric equipment are given by Radji and Douglas [1994].

3.7.4 Electrical conductivity

The variations of ionic conductivity are monitored by inserting a conductivity probe into the paste or mortar specimen that used with the calorimetric test (Fig. 3.9). This means that the test sample filled in the calorimeter is used to determine the development of semi-adiabatic heat release as well as the changes of the ionic conductivity with time. The conductivity probe is an

electrode of stainless steel measuring 5 mm in diameter and 30 mm in length. Measurements of electrical conductivity are made by using an excitation voltage of 5 V square-wave operated at a frequency of 1 kHz. The conductivity data are recorded at preselected time interval and downloaded to a computer.

A calibration procedure was used to allow the calculation of an effective 'cell constant' for each electrode pair. This is performed by immersing the probe in a standard solution of NaCl of known conductivity and measuring sequentially the electrical resistivity of the electrode probe. By several repetitions of readings taken at every 20 s with flip-flap and acquisition system, the constants of electrode pairs were calculated. The coefficient of variation (C.O.V.) was calculated for all constants of electrode pairs. The constants were accepted when the C.O.V. was less than 0.5%.

3.7.5 Compressive strength test

The compressive strength measurements of cement paste and mortar were measured on cubical specimens ($50\times50\times50$ mm^3) according to [ASTM C 109/C 109M]. Specific loading rate was adjusted for the paste mixtures and another rate for the mortar mixtures. The load increase was monitored until the failure of specimens. The compressive strength was then calculated as the maximum bearing load by the surface area. The tests were carried out using hydraulic pressure 2*92 KN capacities. The compressive test machine is shown in Fig. 3.10.

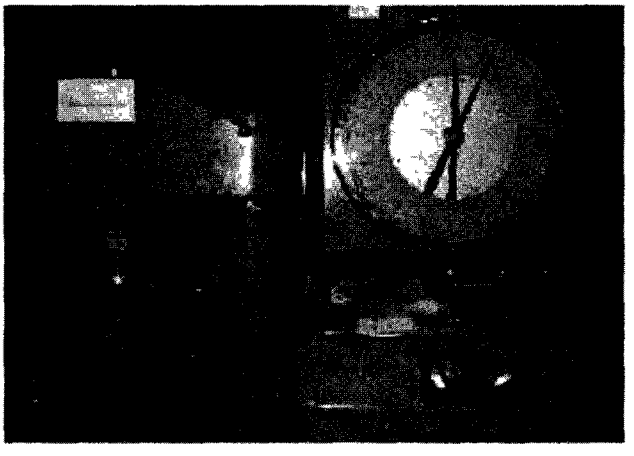

Fig. 3.10 Compressive test machine

CHAPTER 4
ADAPTION OF PIEZOELECTRICRING ACTUATOR TECHNIQUE FOR USAGE WITH CEMENT-BASED MATERIALS

4.1 Introduction

Historical background about the use of piezoelectric devices used in soil applications and their disadvantages are presented in this chapter. Description of a piezoelectric ring actuator setup (*P-RAT*) recently developed to characterize the soil properties are detailed in this chapter. A strategy for using the (*P-RAT*) to estimate hydration properties of cement-based materials is described in this chapter. Test results for the first implementation of *P-RAT* in mortar mixtures are discussed in terms of configurations of the moulds and signal analysis. Two-step modifications to the *P-RAT* to be adapted with the cement-based materials are highlighted. The new version of *P-RAT* after the modification is referred to be as *P-RAT2*. Calibration and repeatability characteristics of *P-RAT2* are also measured and discussed in this chapter.

4.2 Historical background of P-RAT's and their Preference

A piezoelectric material generates electrical output when subjected to mechanical deformation and vice versa, it changes its shape when an electrical field is applied to it. Transducers made of piezoelectric materials have been experimented for measuring the small-strain shear modulus (G_{max}) Lawrence [1963, 1965]. The G_{max} is directly related to shear wave velocity, V_s, through bulk density, ρ, ($G_{max} = \rho V_s^2$). The usual existing piezoelectric devices are:

Shear-plate transducer: The shear-plate transducer is used in testing undisturbed stiff soils and soils with large aggregate since shear-plate transducers do not penetrate into the soil. Based on the work of Brignoli, Gotti, Stokoe II [1996], flat-plate shear transducers showed significant potential for future laboratory use because of their robustness and non-invasive nature. Figure 4.1 presents shear plate (22 mm diameter) and compression (14 mm diameter) transducers [Ismail and Rammah, 2006].

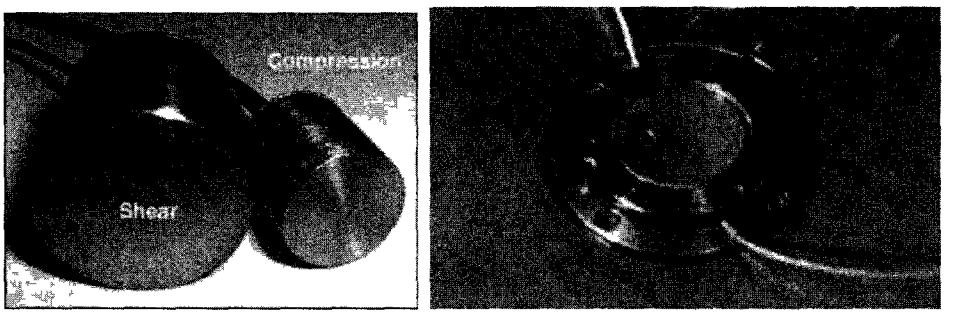

Fig. 4.1 Shear-Plate, Compression Transducers at University of Western Australia (Ismail and Rammah, 2005) and a Commercial Shear Plate Setup.

Bender Transducer: A bender element is an electro-mechanical transducer that either bends as an applied voltage is changed or generates a voltage as it bends. A bender element typically consists of two thin piezoceramic plates rigidly bonded to a central metallic plate.

Two thin conductive layers (electrodes) are applied externally to the bender. When a driving voltage is applied to the electrode, the polarization causes a bending displacement of the whole element. Benders are usually available in two types that differ simply in the electrical connection to the two polarized plates: a series or parallel connection.

Compression Transducer: For the generation of P-waves, ceramic elements are polarized in the thickness direction, and electrodes are placed on the element faces normal to the polarization direction.

Bender/Extender Element: Lings and Greening [2001] introduced a modification to a standard bender element design which resulted in a transducer capable of transmitting and receiving both P-waves and S-waves as shown in Fig. 4.2. A control box has been developed to allow transducers to be quickly converted from bender to extender mode.

Disadvantages of the piezoelectric devices: Ismail and Rammah (2005) reported many physical disadvantages of bender elements as follow:

(i) The bender element should penetrate into the sample to transmit its bending deformation into shear strains in the surrounding soil. This process is invasive for undisturbed and cemented samples. Digging holes into a sample requires more work to refill the holes with a coupling material, usually epoxy or gypsum; further disturbance to the sample is possible during this handling.

(ii) The bender element is affected by the stresses within the sample, most notably in the conical zone adjacent to the rough, conventional platens of the triaxial apparatus.

(iii) The bender element is not suitable for harsh environments, where electrolytes may penetrate through the epoxy, as in the case of electrokinetic treatment in laboratory experiments.

(iv) Because of its relatively small thickness (0.5 - 1.0 mm), the bender element is prone to depolarization at high voltage (maximum working voltage $\cong$ 100 V per 1-mm thickness). However, this depends on the number of working cycles and shape of the input signal. A higher voltage may be required in situations where signal attenuation is of concern, such as in the case of soft soils or stiff soils with a long travel distance.

(v) Two different types of electrical connection are used for the transmitter and receiver for any pair of bender elements, to amplify both the transmitted and received signals: a parallel connection is required for the transmitter and a series connection for the receiver. This requires special care during manufacturing and testing.

(vi) For shear-plate, it needs high voltage to produce enough energy for a readable output signal. Ismail and Rammah [2005]found that the output signal amplitude of bender-elements is 10-times that of shear plates when testing soft clay sample, although the input voltages were 40 V and 200 V, respectively. The authors attributed this fact to the better coupling between the benders and soil. However, the shear plate performed better than bender elements for both a sandy sample and a cemented sand sample giving about 7 and 25 times, respectively, higher amplitude than benders. These findings show the importance of having good coupling between the piezoelectric device and soil. Also, they reflect the preference of shear plates because of their larger contact areas compared to benders.

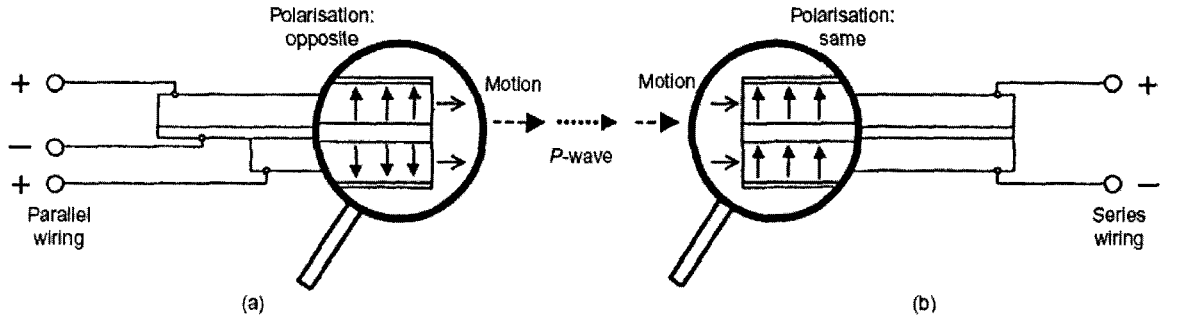

Fig. 4.2 Typical Bender/Extender Elements Wiring, Polarization and Displacement Details: a) Transmitter; b) Receiver [Lings and Greening, 2001]

4.3 The piezoelectric ring-actuator setup (P-RAT)

4.3.1 Development and manufacture of (P-RAT)

The piezoelectric ring actuator technique, *(P-RAT)* has been developed in University of Sherbrook. This technique is considered a completely new, versatile, advanced and accurate. The development of the new technique *(P-RAT)* was done on two main bases: the first was the development of piezoelectric ring actuators set-up by team work, El-Dean [2007] for granular soil and Ethier [2009] for clay. The second is the development of the interpretation method used in the results analysis by Karray [personal communication, 2008]. The setup is composed of two main units; emitter and receiver, and is capable of measuring shear and compression wave velocities in specimens. With this technique, many problems of pulse tests, which make interpretation of results difficult and ambiguous, were solved in soil. The *P-RAT* overcomes wave reflections at boundaries (end-caps and sides), sample disturbance, weak shear coupling between soil and device (interaction) as well as the fixation problems, low resonant frequency and limited input voltage of the existing device. Figure 4.3 shows a new setup.

The developing process of the *P-RAT* that was applied in soil mechanics has been passed through eight steps. The final version resulted from that development (version-8) was employed in the current investigation to determine the hydration properties of the cement-based materials. Table 4.1 summarizes the specifications for the development process of the *P-RAT* followed in the eight steps of devising by [Gamal El-Deen, 2007].

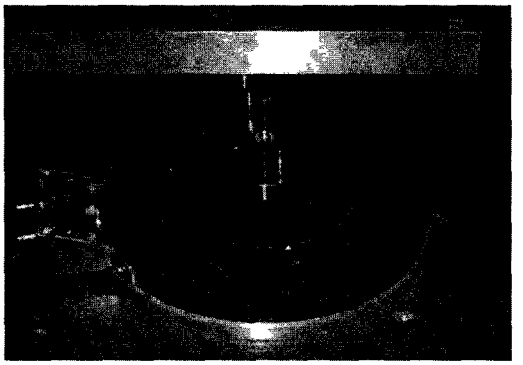

Fig. 4.3 Configuration *P-RAT* in the granular soil [Gamal El-Dean, 2007]

The *P-RAT* was manufactured from a piezoelectric material to generate an electric potential when subjected to an applied mechanical deformation, and vice verse. The type of cylinder of piezoelectric materials was used of this study in ABCI, 42-1021, Table 4.2 summarizes the standard piezoelectric cylinders manufactured by APC international Ltd and constructed from Type II ceramic material (see appendix A). The cylinder divided to 3 mm in thickness. The dimensions of *P-RAT* version-8 were 44 mm in outer diameter, 38 mm in inner diameter, and 3mm in thickness while the inner stone thickness is 6 mm. Thus, the rings are not directly contacting material with the surface of specimen. Only the surface of inner-stone transmits the signal to material and vice versa. The *P-RAT* was designed to eliminate reflected waves coming from the back of rings by introducing a rubber pad behind the rings and inner stone. In addition, the rings were coated by three to four layers of epoxy to have waterproof element to isolate the rings from humidity and prevent short cuts between electrodes. *P-RAT* is built with ground wires connected to the inner-stone expect that the gab behind the inner stone was filled with an epoxy material in order to have a full support at back [El-Deen, 2007].

The resonant frequency of the piezoelectric unit is proportional to the ratio of stiffness and unit weight. Hence, the unit weight and stiffness are the primary factors that control the natural frequency of system. Hence, decreasing the diameter of rings lead to increasing the rigidity of the inner-disc, accordingly, increase the resonant frequency.

Table 4.1 Specifications for the development of *P-RAT* [Gamal El-Deen, 2007]

Setup No.	Date	Ring Dim. (mm)	Inner stone	Outer stone	Base & Cap	Attenuator	Resonant Frequency	Notes
1	April 2003	D_{out} = 16 D_{in} = 11 t = 2.5	3-mm porous brass + 3-mm back porous plastic	6-mm porous plastic	PVC, D = 63 mm t = 19.2 mm	3-mm rubber attenuator	--	Preliminary testing
2	Oct. 2003	D_{out} = 44 D_{in} (E) = 38 D_{in} (R) = 40 t_{ring} = 2.5	3-mm porous brass + 3-mm back porous plastic	6-mm porous plastic	Steel top cap of: D = 105.5 mm & t = 30 mm PVC base of: D = 196.5 mm & t = 30 mm	3-mm rubber attenuator	32 KHz	Chips porous stone
3	Dec. 2003	D_{out} = 44 D_{in} (E) = 38 D_{in} (R) = 40 t_{ring} = 2.5	3-mm porous brass + 3-mm back porous plastic	6-mm porous plastic	Steel top cap of: D = 105.5 mm & t = 30 mm PVC base of: D = 196.5 mm & t = 30 mm	3-mm rubber attenuator	33 KHz	Grounding wires installed + Epoxy is added to the back of the porous stone
4	June 2004	D_{out} = 44 D_{in} (E) = 38 D_{in} (R) = 40 t_{ring} = 2.5	6-mm porous brass	6-mm porous brass	Steel top cap of: D = 105.5 mm & t = 30 mm PVC base of: D = 196.5 mm & t = 30 mm	3-mm rubber attenuator	33 KHz	
5	Dec. 2004	D_{out} = 44 D_{in} (E) = 38 D_{in} (R) = 40 t_{ring} = 3.5	6-mm cemented sand	6-mm porous brass	Steel top cap of: D = 105.5 mm & t = 30 mm PVC base of: D = 196.5 mm & t = 30 mm	Rubber lamina + 3-mm PVC disc	43 KHz	
6	April 2005	D_{out} = 44 D_{in} (E) = 38 D_{in} (R) = 40 t_{ring} = 3.5	6-mm Alumunium	6-mm porous brass	Steel top cap of: D = 105.5 mm & t = 30 mm PVC base of: D = 196.5 mm & t = 30 mm	Rubber lamina + 3-mm PVC disc	112 KHz	Sand grains glued to the Aluminium top surface by conductive epoxy
7	Aug. 2005	D_{out} = 44 D_{in} (E) = 38 D_{in} (R) = 40 t_{ring} = 3.5	6-mm Alumunium cut into 4 pieces and glued by silicon	6-mm porous brass	Steel top cap of: D = 105.5 mm & t = 30 mm PVC base of: D = 196.5 mm & t = 30 mm	Rubber lamina + 3-mm PVC disc	17 KHz	Aluminium surfaces made rough by scratching in two directions
7c	Oct. 2005	D_{out} = 44 D_{in} (E) = 38 D_{in} (R) = 40 t_{ring} = 3.5	6-mm Alumunium cut into 4 pieces and glued by silicon, surfaces roughed by scratching	6-mm porous brass covered by 0.6-mm Aluminium plate	Steel top cap of: D = 105.5 mm & t = 30 mm PVC base of: D = 196.5 mm & t = 30 mm	Rubber lamina + 3-mm PVC disc	17 KHz	Aluminium plates extend over the rings
8	Oct. 2005	D_{out} = 44 D_{in} (E) = 38 D_{in} (R) = 40 t_{ring} = 3.5	6-mm Alumunium cut into 4 pieces and glued by silicon + 0.6-mm sand layer glued by epoxy at soil sides	6-mm porous brass covered by 0.6-mm Aluminium plate	Steel top cap of: D = 105.5 mm & t = 30 mm PVC base of: D = 196.5 mm & t = 30 mm	Rubber lamina + 3-mm PVC disc	17 KHz	Aluminium plates extend over the rings

In order to increase the energy of emitted and received shear wave, the inner-stone was cut into four equal pieces that were connected by an elastic material. This would make the emitter-ring displaces the inner-stone pieces in and out easily without deforming them and thus apply uniform shear deformation to the sample. Also, the p-wave amplitude is presumed to be greatly reduced or eliminated; the p-wave will theoretically be emitted only from the piezoelectric ring as long as the inner-stone continues to be flexible and displaces with deformation of ring. Figure 4.4 represents the dimensions of piezoelectric ring and shear plate transducers as well as Fig 4.5 shows Schematic of the plan view of piezoelectric ring and its 4 pieces split inner stone.

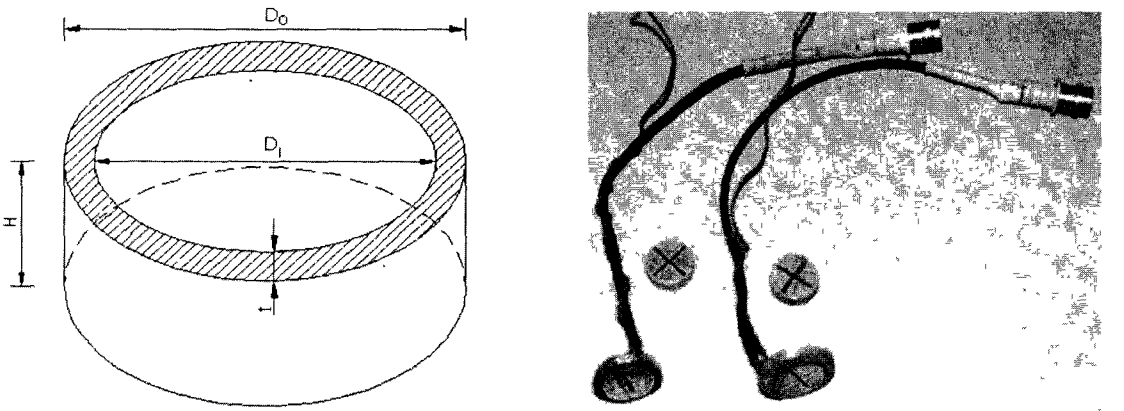

Fig. 4.4 Dimensions of Piezoelectric ring and shear plate transducers

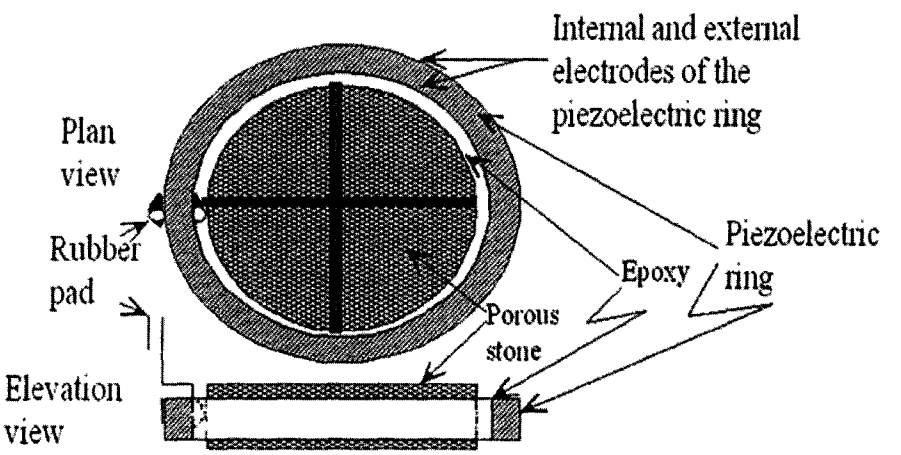

Fig. 4.5 Schematic of the plan view of piezoelectric ring and its 4 pieces split inner stone

4.3.2 Signal analysis of *P-RAT*

It is known that identifying the exact time from the signal in the time domain when the wave arrives can be difficult and subjective. The pervious methods reported that the measurements of the shear wave velocity vary with input frequency. On the other hand the problem of dispersive nature observed by Arulnathan et al.,[1998], Arroyo et al., [2006], Gamal El-Dean [2007], and Ethier [2009] both from laboratory tests and numerical simulations for a given materials characterized by a certain shear wave velocity. Consequently, investigations of pulse tests in previous studies have justified the development of a new method.

The interpretation method for pulse test was recently developed by Karray [2008] and Ethier [2009]. This method analyzes the signals in frequency domain considering the dispersive nature of pulse tests as demonstrated by Ethier [2009]. The new interpretation methods addresses the effect of frequency on the measurements of *Vs*. Indeed, V_s should not vary with input frequency. Ethier, [2009] reported that a systematic error in phase (function of frequency) is introduced in a shear wave velocity test by the emitter-receiver system and by the medium itself. The error produced by the setup (emitter-receiver) can be measured directly by carrying out a calibration test by putting directly the emitter on the receiver. Figure 4.6 shows the response of the *P-RAT* (small diameter, D = 16 mm) setup without material (ring-to-ring). From this test it is possible to evaluate the phase shift error produced by the step as a function of frequency as shown in Fig. 4.7. Figures 4.8 and 4.9 show the calibration test signals and the phase shift error reproduced by the medium diameter ring setup (D = 30 mm), respectively.

As discussed earlier, the dispersion is related to the phase shift that introduced by emitter, receiver and medium. The total phase shift error produced by the setup is usually around zero at low frequency as shown in Figs 4.7 and 4.9. At high frequency this error is as much as 2π as can be calculated theoretically for any dynamic system of one single degree of freedom (SDOF)as shown in the equation (4.1). The error produced by medium vary also between 0 and 2π as demonstrated by Ethier, [2009] leading to a total error varying between 0 and 4π. The principal idea here is that the correct phase shift of the shear wave velocity can be obtained by removing the phase shift produced by the setup and the medium (0-4π). This can lead to a constant phase velocity that corresponds to the shear wave velocity of the medium as shown in the equation (4.2).

$$\theta_{exp}(\omega) = \theta_{corr}(\omega) + \theta_E(\omega) + \theta_R(\omega) + \theta_{medium}(\omega) \quad (4.1)$$

where;

ω is the angular frequency

θ_{exp} is measured total phase shift

θ_E is phase shift error of the emitter

θ_R is phase shift error of the receiver

θ_{medium} is phase shift error produced by the interaction between the medium and the setup

θ_{corr} is corrected phase shift.

$$V_s = V_{ph} = \omega.Distance/(\theta_{exp}(\omega) - \theta_E(\omega) - \theta_R(\omega) - \theta_{medium}(\omega)) \quad (4.2)$$

To carry out this operation, software was developed at the University of Sherbrooke [Karray, 2008]. This program allows not only to calculate the dispersion curve from the experimental signals, emitted and received at the laboratory, but also to take into account the phase shift produced by the sensors and the medium.

Figure 4.10 presents the dispersion curve determined starting from the emitted signals (force applied to the transmitter) and of the received signals (displacement of the receiving ring). This curve (in red) shows a decreasing in the phase velocity with the increasing of frequency. For example, the phase velocity is about 277 m/s at 12 kHz and about 250 m/s at 30 kHz. This variation is related to the phase shift error which is more important at high frequency as demonstrated by the calibration tests. When the phase error produced by the setup and the medium is discarded the phase velocity (blue curve) becomes independent of frequency leading to a constant velocity that corresponds to the shear wave velocity of the medium. Figure 4.11 shows the phase-shift correction obtained by the software to calculate de shear wave velocity.

In the other hand, when different tests are realised for the same sample using the same setup, it is possible to evaluate the shear wave velocity by calculating the relative difference in time from one test to another as shown in Fig 4.12. Thus, a first velocity is evaluated in frequency domain and the then the subsequent velocities are calculated using the following equation:

$$V_{s(n)} = Distance / (Distance / V_{s(n-1)}) - \Delta_{t(n-1)}) \quad (4.3)$$

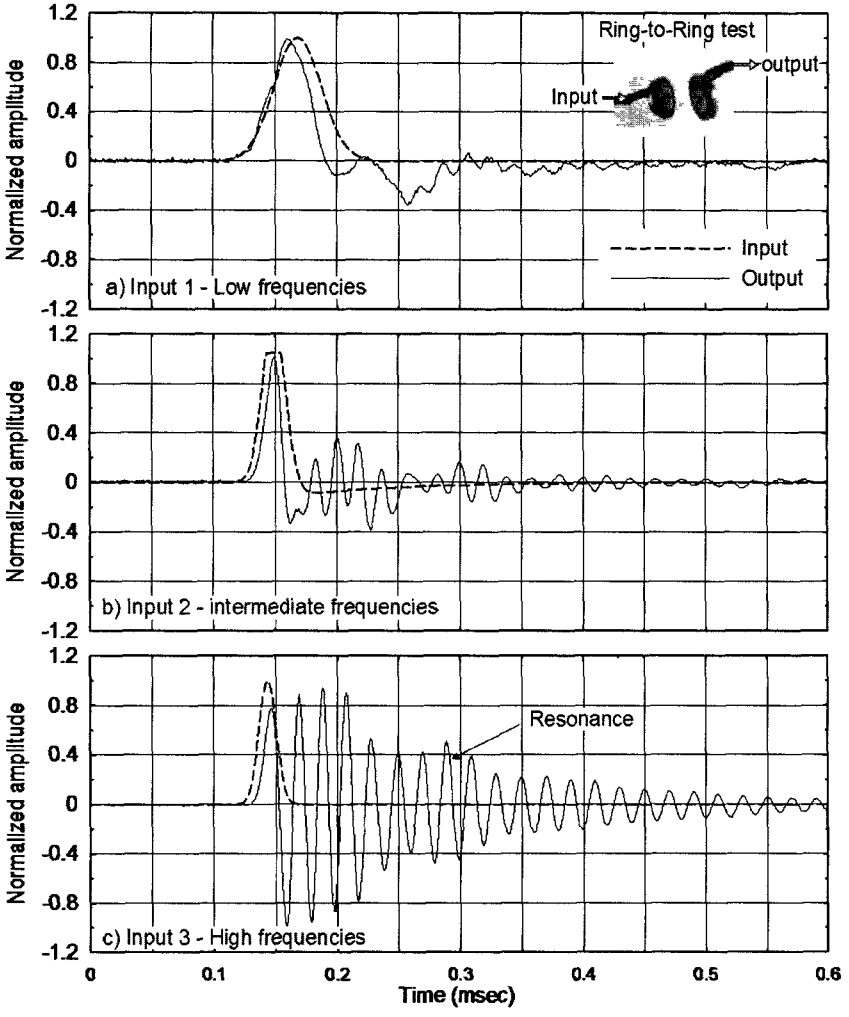

Fig. 4.6 Response of the *P-RAT*$_1$ setup without material (ring-to-ring): small diameter

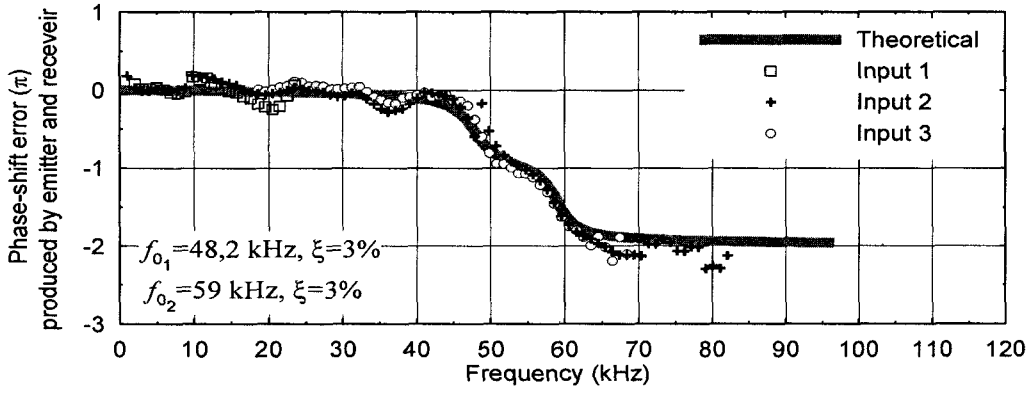

Fig. 4.7 Comparison between experimental and theoretical Phase shift error produced by emitter and receiver (D = 16 mm)

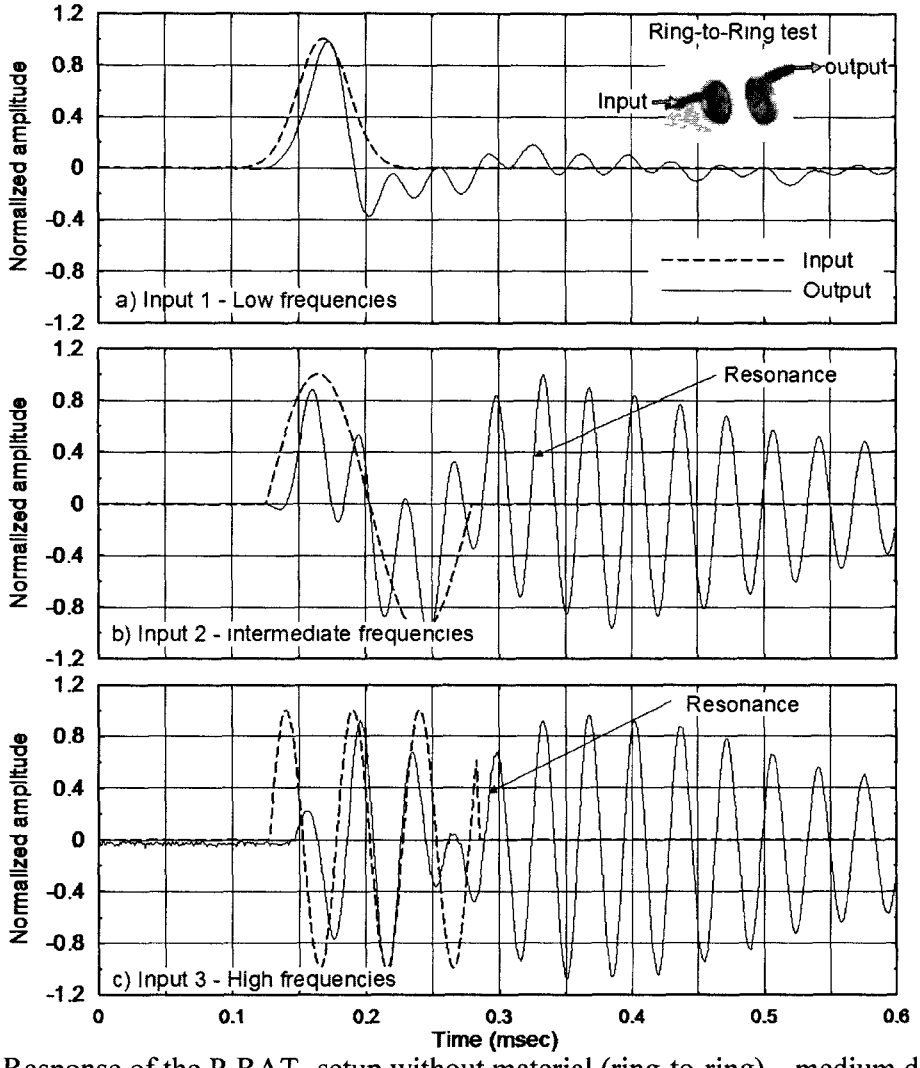

Fig. 4.8 Response of the P-RAT$_2$ setup without material (ring-to-ring) – medium diameter

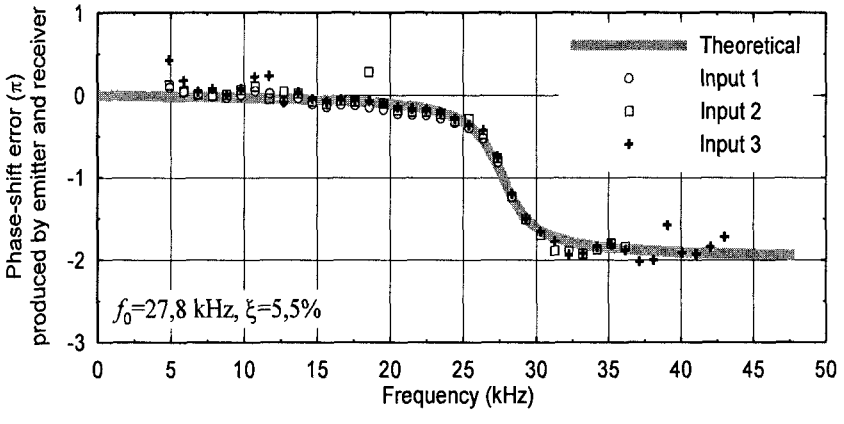

Fig. 4.9 Comparison between experimental and theoretical Phase shift error produced by emitter and receiver (medium ring diameter D = 30 mm)

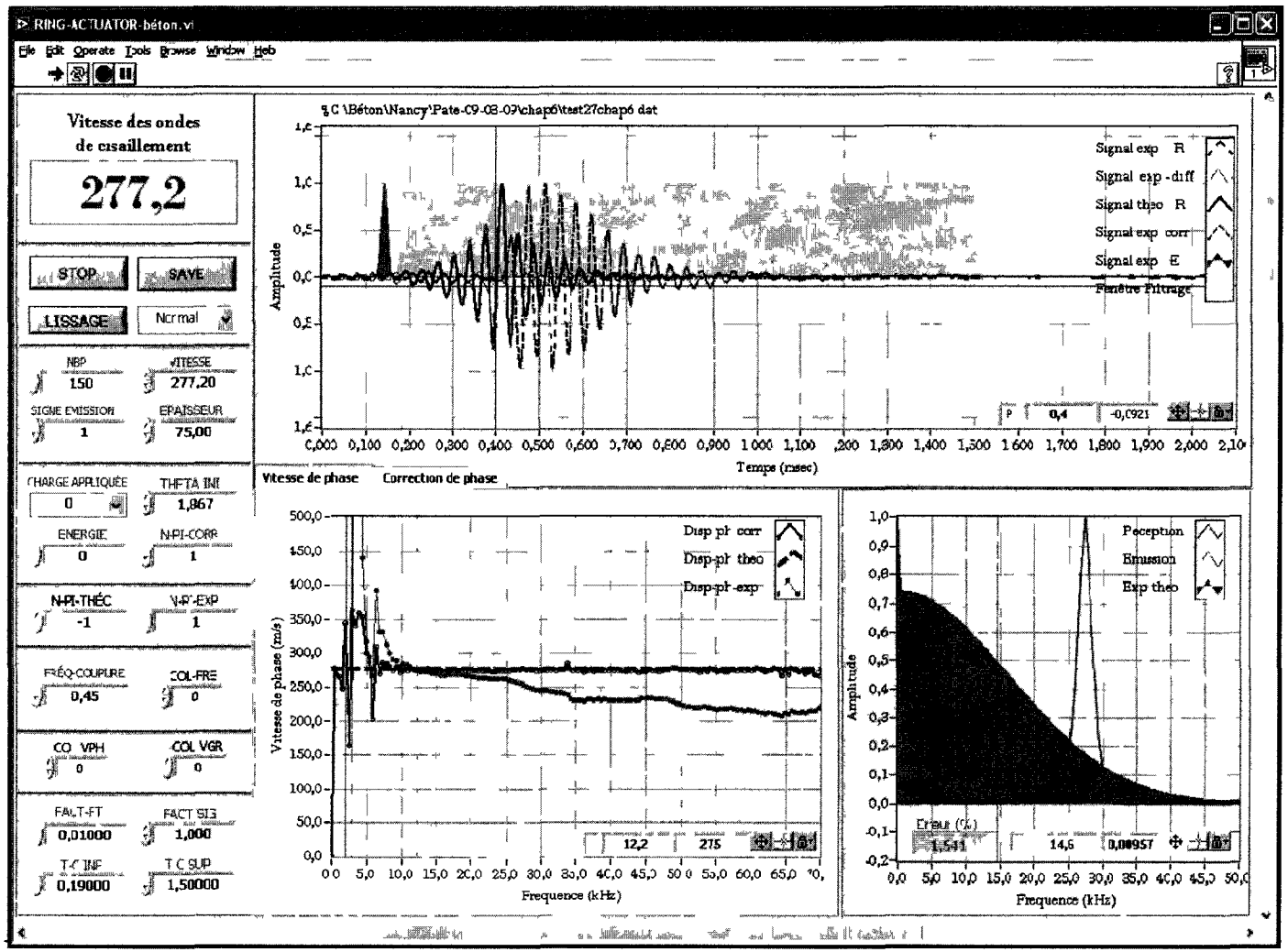

Fig. 4.10 Software for the determination of shear wave velocity by correction of the phase shift errors produced by emitter, receiver and medium

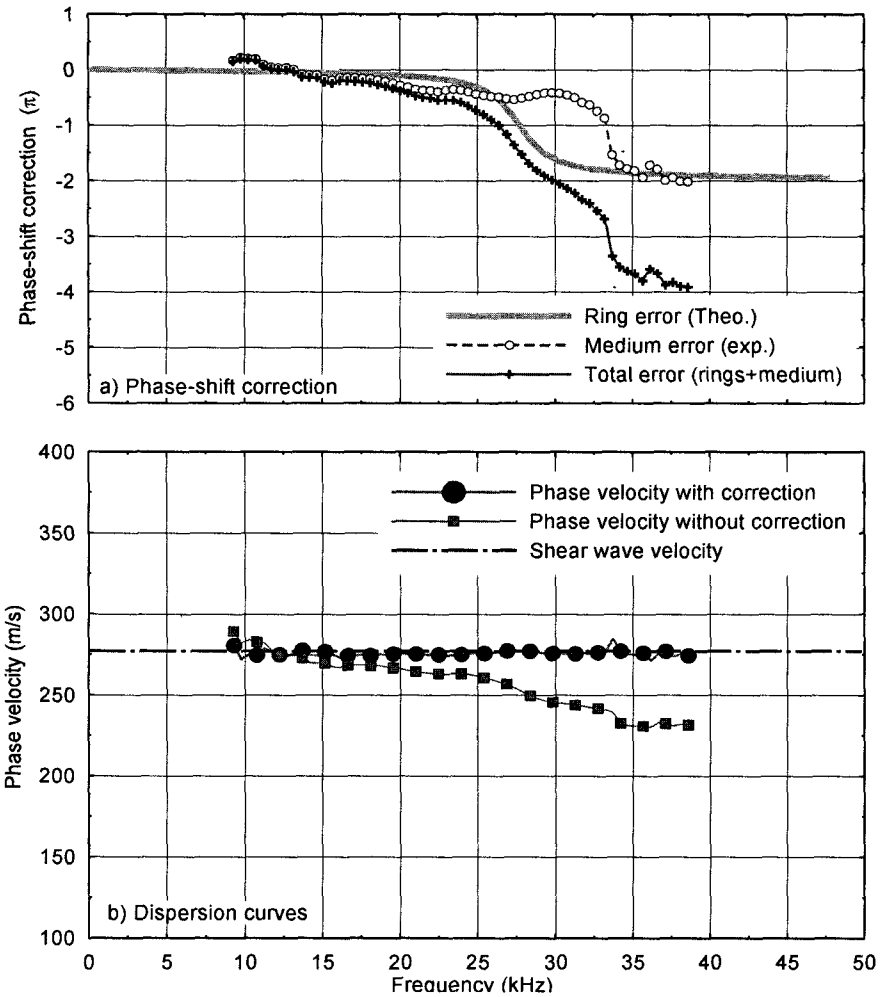

Fig. 4.11 Example of application of phase-shift correction to calculate value of (V_s)

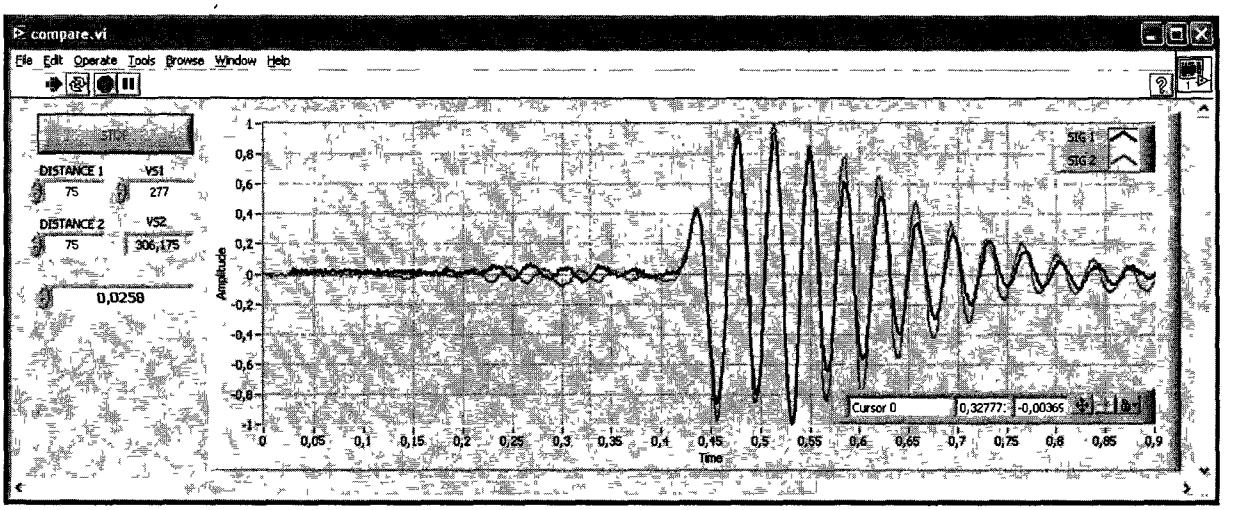

Fig. 4.12 Software for computation of shear wave velocity using to subsequent test signal

4.3.3 Advantages of using *P-RAT*

The *P-RAT* gives the advantage of being able to measure both shear and compression wave velocities even if it is designed to minimize the energy of the compression wave. The P-RAT has been adapted to overcome the wave reflection at top and bottom caps of the testing apparatus that takes place with the old test setups.

The *P-RAT* does not need to penetrate into the sample, which makes it suitable for testing all types of samples without special penetrations. This advantage solved the problems related to the sample disturbance and weak shear coupling between sample and device (interaction). In addition, it facilitated the fixation problems, low resonant frequency and limited input voltage of the existing device and some of interpretation problems associated with previous devices. With this device, many problems of pulse tests, which make interpretation of results difficult and ambiguous, were solved. This setup made a drastic change in the quality of output signals of pulse tests. A clear dominant shear arrival was obtained. The amplitude of the compression wave is much less that of shear wave. Moreover, the Winger-Ville analysis has become much better so that the dispersion of the received signals approached the theoretical trend. This was achieved by trimming the received signal so that the analysis is made only for the shear wave component.

4.4 First application of P-RAT to characterize cement-based material

Schematic for the *P-RAT* system used for the measurement of shear wave velocity is given in Fig. 4.13. The system consists of a computer with an analog-to-digital converter, a signal generator unit, a filter/amplifier unit, as well as an emitter, receiver and mould. The emitter transmits the shear wave velocity through the sample, while the receiver on the opposite side of the sample receives that wave. The used mould is 90 mm in height and 80 mm in diameter. The mould was placed and sealed to the receiver to prevent water leaking from the mould. The top cap including the transmitter was placed on the specimen. Balancing load was then applied on the top cap to ensure fully contact between the ring and the specimen. After that, the total cell was managed through special software using a computer. The frequency of the transmitted shear wave used in this-investigation was 17 kHz. The shear wave velocity is measured by recording the accurate arrival time of the wave for a known propagation distance. The arrival time is determined by an accurate interpretation method [Mourad Karray 2008]. The arrival time can be

relative to contact time of water and cement. The velocity is recorded at a regular time intervals. The velocity (V_s) of the wave can be calculated, as follows:

$$V_s = \frac{d}{t} \tag{4.4}$$

where; t is arrival time of the wave and d is the travelling distance of the wave.

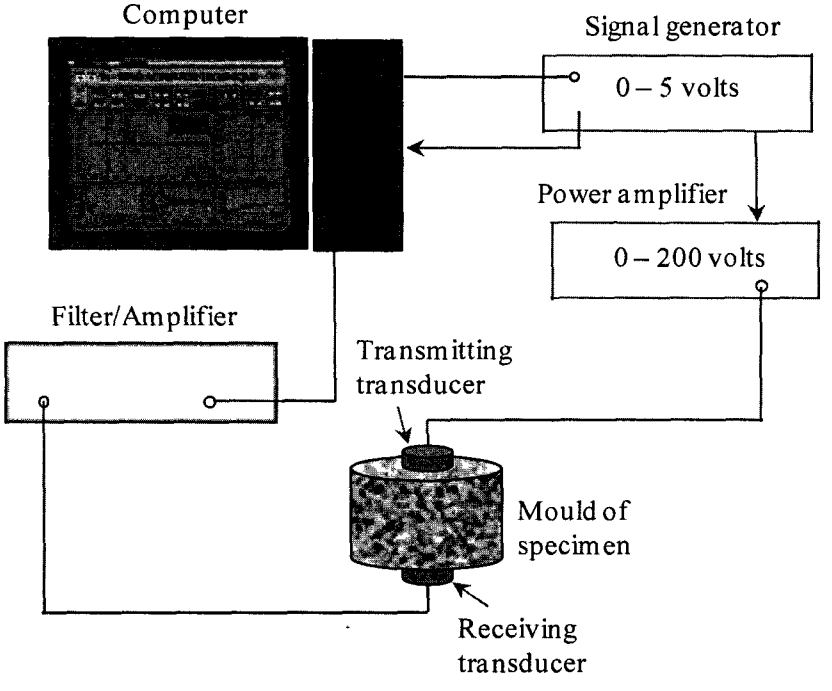

Fig. 4.13 Schematic of an experimental apparatus for *P-RAT* measurements

Two mortar mixtures made with varied *w/cm* of 0.5 and 0.42 (Mix-4, and Mix-10, respectively) were employed in primary tests to investigate the behaviour of *P-RAT* with cement-based materials. When shear waves are used for the measurements and the test material (e.g. cement paste) is in liquid state, the value of shear wave is very small, since shear waves cannot propagate in liquids. This can be seen in Fig. 4.14 at approximately 235 min when the mortar still in its liquid state. With proceeding hydration the cement grains percolate and build up a skeleton, allowing the shear waves to propagate. After a certain time the value of the shear wave velocity start to increase due to increasing in hydration proceeding and changes in the microstructure of the cement based-materials. In addition, the development of the shear wave

velocity with the elapsed time for mixture made with *w/cm* of 0.42 showed early and steep increase of the shear wave velocity (V_s) with the elapsed time. On the other hand, mixture made with *w/cm* of 0.5 exhibited slow rate of shear wave velocity with time as shown Fig. 4.14.

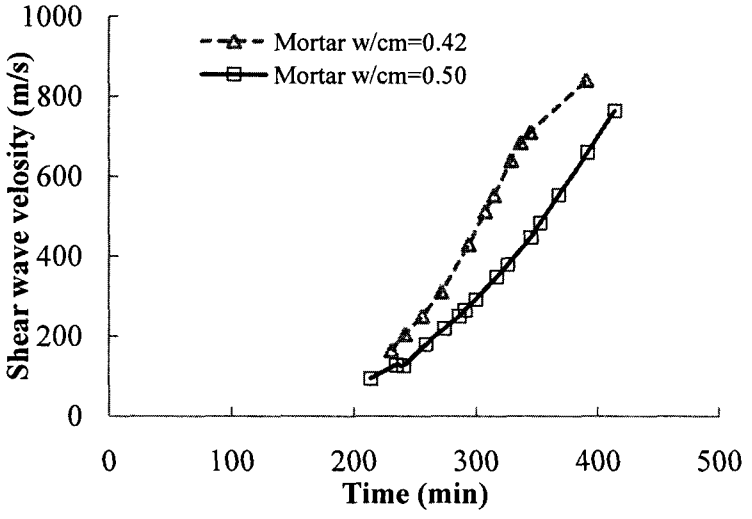

Fig. 4.14 Primary results for *P-RAT* in two mortar mixtures of different *w/cm*

It can clearly be seen that the result of shear wave velocity obtained of the *P-RAT* reproduce very well the characteristics of the hydration behaviour. The *P-RAT* can also be employed to differentiate between the hydration behaviour of the mortar mixtures proportioned with various *w/cm.*

4.5 Drawbacks and modifications of *P-RAT*

4.5.1 Mould configuration

The mould of the *P-RAT* used in the soil application was circular in cross section as shown in Fig. 4.15. Surcharge load was used with the soil sample. Loading is important in the soil sample to insure good contact between the soil and the ring actuator, but this is not the case in the fresh concrete that is almost liquid leading to a good contact with the ring actuator either in the fresh state. The rough surface nature of the ring actuator leads also to a better contact with the concrete sample in the hardened state. On the other hand, applying the surcharge load can lead to force the water to get out from the concrete. This would change the characteristics of the

tested sample because this changes the water cement ratio. The over head load can also lead to a change in the sample length; accordingly, the value of shear wave velocity will be affected. Moreover, concrete sample could have different characteristics in the top surface compared to the bottom layer when it has segregation or bleeding. In that case, the ring actuator in the top cap will contact with a non representative concrete sample at the top due to the bleeding.

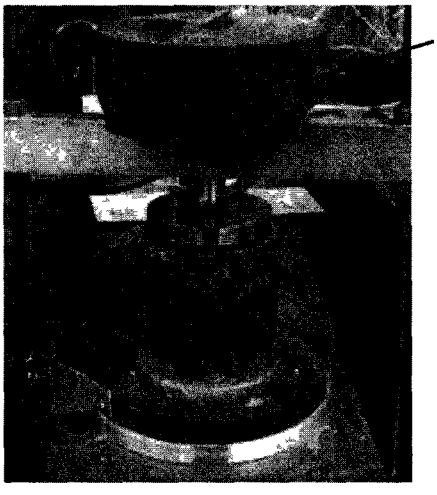

Fig. 4.15 Over head load used in mortar specimen on primary test

Based on the preliminary application, it is appeared to propagate the waves in a horizontal direction. This can result in many advantages. There is no need for applying surcharge load on the top cap. The characteristics of the sample will not be affected. This will avoid the bleeding problems. This also eliminates the need to measure the deformation that could occur near top of samples.

Based on that, it was suggested to change the mould configuration from circular to a rectangular shape. The mould is fabricated from plexifibre material. The mould has 200 mm in length, 75 mm in width, 170 mm in height, and 0.75 mm in wall thickness. In addition, the way of the attachment of the ring actuator was changed. Two holes were drilled in the middle of the opposite sides of the plexifibre mould in order to allow the transducers to be set flush with the tested sample. The edges around the holes were sealed to prevent water leaking from the mould. Figure 4.16 represents the instrumented mould with the rings.

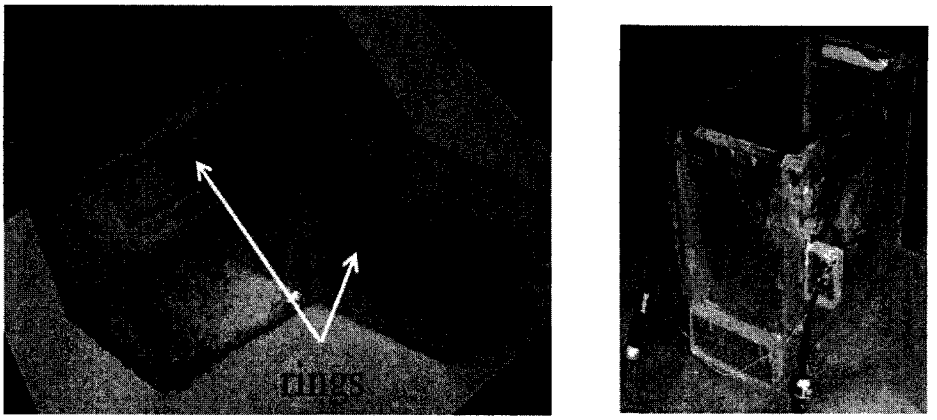

Fig. 4.16 New mould configuration and fixation of rings used in *P-RAT2*

4.5.2 Low resonant frequency

Tow trial tests were suggested to increase the resonant frequency Karray [2009]. Trial-1 (small ring) was proposed to increase the resonant frequency from 17 kHz to 60 kHz. This was achieved by decreasing the ring actuators dimensions. The new dimensions were 22 mm in outer diameter, 16 mm in inner diameter, and 3.5 mm in thickness. The thickness of the inner stone was not changed (6 mm).

Trial-2 (big ring) was proposed also to increase the resonant frequency from 17 to 30 kHz. This was done by using ring actuators dimensions of 30 mm in outer diameter, 26 mm in inner diameter, and 3.5 mm in thickness. The thickness of the inner stone was not change and kept of 6 mm. Figs. 4.17 and 4.18 show output signals of the Lab. view software used with the small and big ring actuator setup, respectively Karray [2009].

Summary of the advantages and disadvantages accompanied with the small and big rings of the *P-RAT2* are indicated in Table 4.2. Figs. 4.17 and 4.18 show output signals of the Lab. view software used with the small and big ring actuator setup, respectively Karray [2009]. The *P-RAT2* made with small ring gave high resonant frequency, small energy, small contact surface with the tested sample, and high noise level as shown in Fig. 4.17. The high noise level affected the interpretation of the shear wave velocity. As well as the obtained curve of shear wave velocity with time was not smooth, as shown from the results indicted in Fig. 4.19. On the other hand, the *P-RAT2* made with big ring gave high energy, large contact surface, low noise level as shown in Fig. 4.18, and good signal quality.

After investigation it was shown that version of *P-RAT2* made with big ring was found more compatible and suitable with the cement-based materials at early age. As well as reproduced good signal quality. As known the damping of cement-based materials at early age is high, consequently, it needs more energy.

Table 4.2 Advantages and disadvantages of the *P-RAT2* made with small and big ring

Advantages of *P-RAT2* (small ring)	Advantages of *P-RAT2* (big ring)
• High resonant frequency (fr = 60 kHz) • Large ring of work frequency	• High energy • Large contact surface • Low noise level • Good signal quality
Disadvantages of *P-RAT2* (small ring)	**Disadvantages of *P-RAT2* (big ring)**
• Small energy • Small contact surface • High noise level	• Lower resonant frequency (fr = 30 kHz)

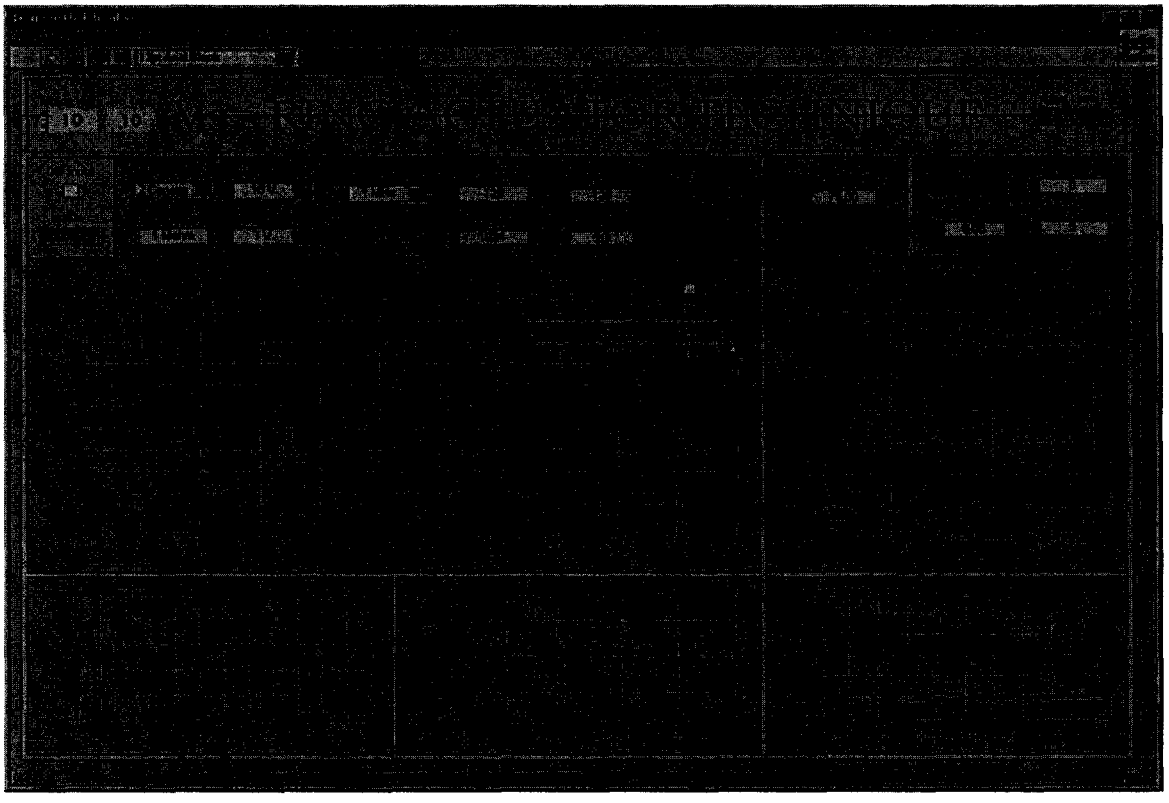

Fig. 4.17 Output signal of the Lab. view software used with the small ring actuator setup

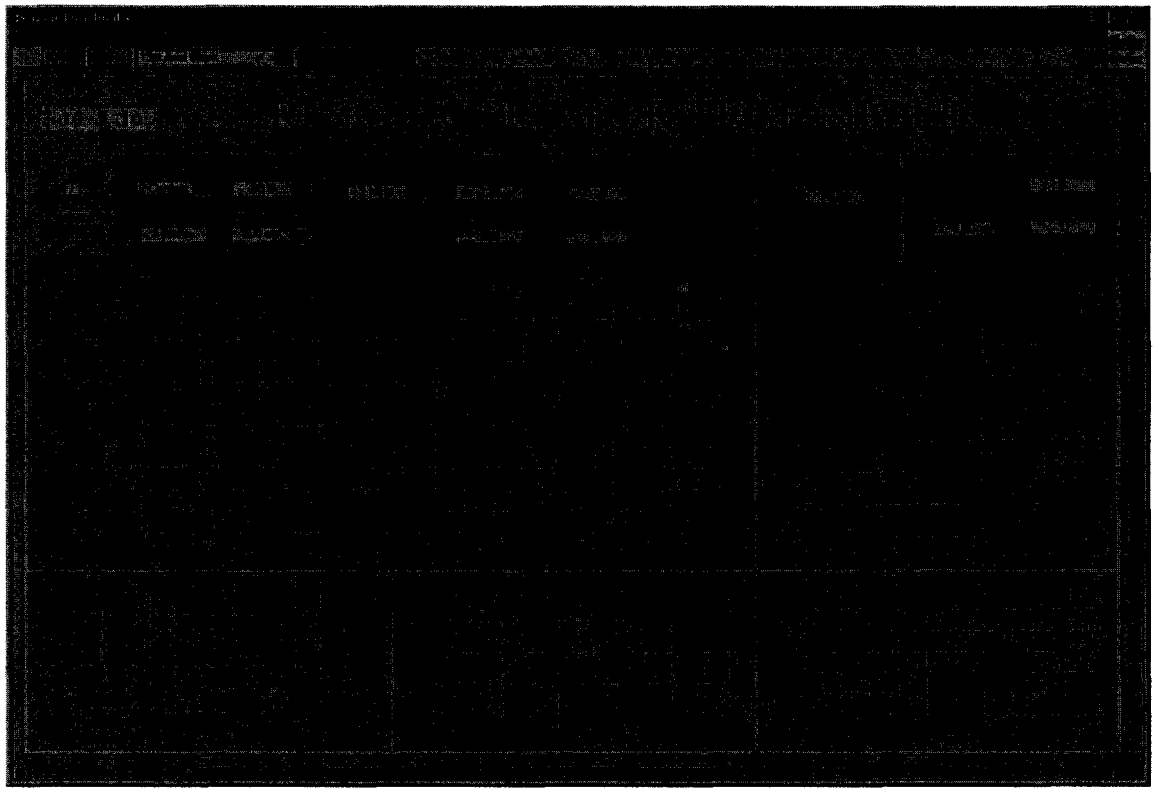

Fig. 4.18 Output signal of the Lab. view software used with the big ring actuator setup

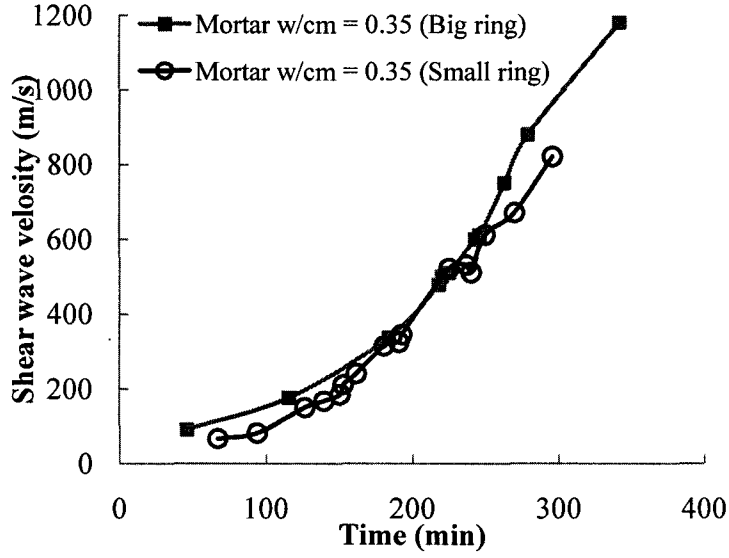

Fig. 4.19 Comparison between evolutions of shear wave velocity with time obtained using *P-RAT2* made with small and big rings

4.6 Calibration of *P-RAT2* with water

The *P-RAT2* was calibrated with water solution. The water was chosen as it has known value of compression wave V_p, approximately ($V_{p\ water}$ = 1482 m/s) [Santamarina, et al, 2001]. The compression wave velocity from the calibration was determined as the distance over the elapsed time to travel from one side to another side of the mould (Δt). The monitoring of the normalized amplitude with the time is shown in Fig. 4.20

The value of the compression wave obtained from the calibration was 1490 m/s. This indicates the adequate precision of the P-RAT2 to capture the precise measurement of compression wave velocity accordingly, accurate measurement of shear wave velocity.

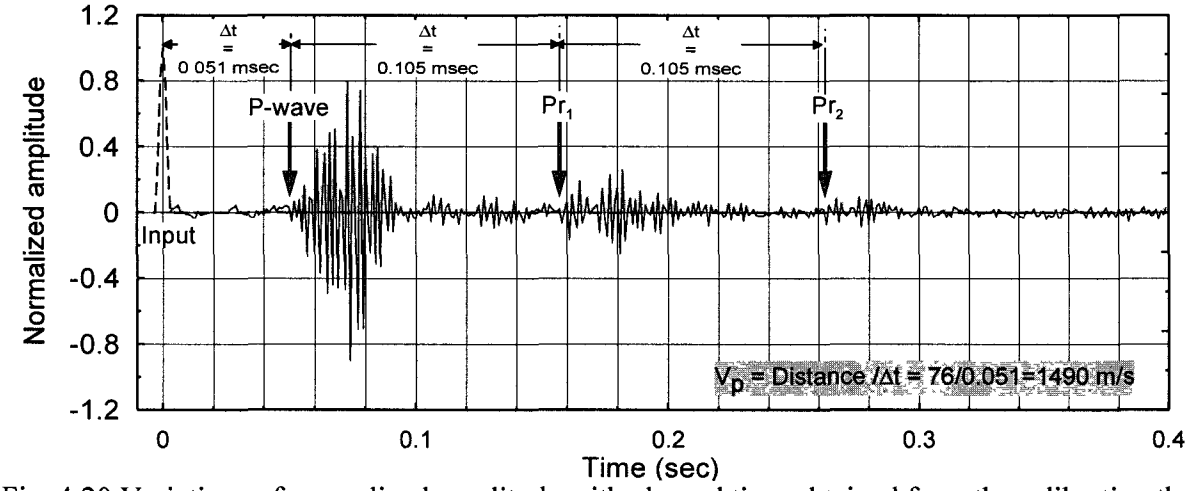

Fig. 4.20 Variations of normalized amplitude with elapsed time obtained from the calibrating the *P-RAT2* with water

4.7 Repeatability responses of *P-RAT2*

To determine the repeatability of the *P-RAT2*, the shear wave velocity exerted by paste with *w/cm* = 0.42 tested three times were determined. The variation of shear wave velocity over time is presented in Fig. 4.21. The repeatability was evaluated statistically by relative error (RE). The RE is calculated according to a 95% confidence interval using the Student's distribution (Eq. 2) and the COV is calculated according to Eq. 4.5, as follows:

$$RE = \frac{SE}{\bar{x}}.100\ (\%) = 4.3027\frac{\sigma}{\bar{x}\sqrt{n}}.100\ (\%) \tag{4.5}$$

where;

4.3027 is the coefficient representing 95% confidence interval for the Student's distribution for n equal to three observations

SE is the standard error representing 95% confidence limit

σ is the standard deviation

n is the number of observations

$\bar{x}$ is the mean value of the observations

The RE estimated for the shear wave velocity readings at various time are indicated in Table 4.3. The RE was limited to ± 9%, this give best indication on the repeatability of the *P-RAT2*.

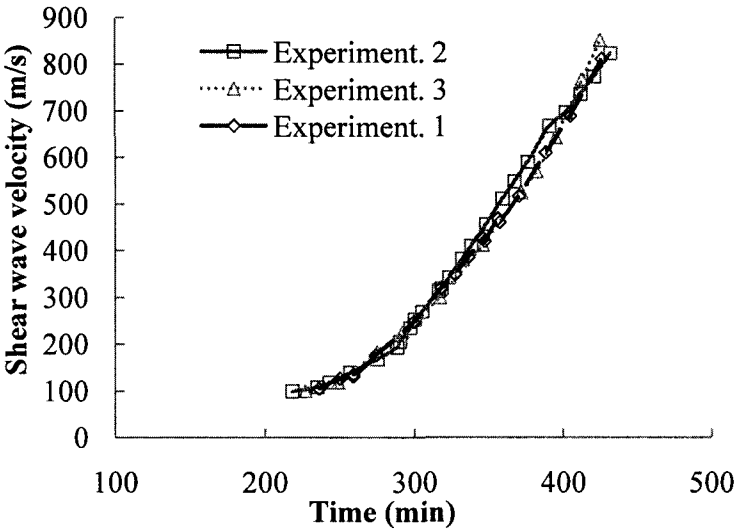

Fig. 4.21 Repeatability responses of *P-RAT2*

Table 4.3 Repeatability of shear wave velocity at various times

Time (min)	Relative error (%)
235	± 4.8
275	± 2.4
318	± 6.6
425	± 8.9

4.8 Summary and conclusions

A historical background about *P-RAT* as a non-destructive test method that was initially developed for determination of soil properties was presented. The development processes, manufacture and signal processing followed with the *P-RAT* was presented in this review. The advantages of using *P-RAT* are also presented. The *P-RAT* was exploited forward to measure the hydration properties of cement-based material. In order to adapt this test method, trial tests were conducted to investigate the possibility of employing the original setup used in the soil application to determine setting and hardening properties of cement-based materials. Based on these trials, two modifications were conducted regarding the mould configuration and size of the rings. The new version of the P-RAT test was calibrated with water specimen. The experimental error of the test setup was carried out using one paste mixture tested three times.

Based on the results presented in this chapter, the following conclusions can be made:

- The primary results demonstrated that the shear wave velocity obtained using the *P-RAT* reproduce approximate estimation of the hydration behavior of mortar mixture. However, some drawbacks were raised concerning the mould configuration and ring dimensions.
- Sealed trapezoidal mould shape and a resonant frequency of 30 kHz were selected to avoid the drawbacks in the initial version of *P-RAT*. These modifications approved success and matching with fresh characteristics of the cement-based materials. The resultant version of *P-RAT* after the modifications is referred to be as *P-RAT2*.
- Calibration of the *P-RAT2* with water specimen was undertaken using the compression wave velocity and resulted in 99.33% accuracy.
- The repeatability carried out on the *P-ART2* proved its the ability to capture accurate results of the shear wave velocity. The relative error is limited to 9%.

CHAPTER 5
VALIDATION OF PIEZOELECTRIC RING ACTUATOR TECHNIQUE WITH CEMENT BASED MATERIALS

5.1 Introduction

This chapter aims at validating the results of the *P-RAT2* using paste and mortar mixtures. The results of *P-RAT2* in terms of shear wave velocity are compared to the results obtained using the conventional test methods including (penetration resistance to monitor initial and final setting respectively, calorimetric to monitor heat of hydration, electrical conductivity to monitor change in continuity of the pore structure and compressive strength at 24 hours).

5.2 Validation of P-RAT2 using paste mixtures

Three paste mixtures made with *w/cm* of 0.50, 0.42, and 0.35 (Mix-1, Mix-2, and Mix-3, respectively) were employed in the first part of the validation. In this part of validation, the paste mixtures were chosen to evaluate the behaviour of the *P-RAT2* on simple medium that contains only cement and water without aggregates. The paste mixtures were designed to produce a given target slump flow of 75 ± 5 mm. To secure this slump flow, Mix-2 and Mix-3 incorporated HRWRA at moderate and high dosages, respectively, while Mix-1 did not contain any HRWRA. The paste mixtures were designed with various *w/cm* in order to obtain wider range in setting and hydration properties as well as early-age compressive strength. The mix designs of the three paste mixtures are given in Table 3.4 and the fresh properties are summarized in Table 3.6.

5.2.1 Measurement of setting time

The time of setting for the paste mixtures were determined using the Vicat needle test in accordance to the ASTM C 403/ C403M. The distances of the Vicat needle from the mould base were determined with the elapsed time for the three paste mixtures are shown in Fig. 5.1. The figure shows clearly the influence of the *w/cm* on the development of the needle penetration with the elapsed time. Paste made with 0.5 *w/cm* showed delayed setting time compared to paste made with 0.35 *w/cm*. The HRWRA was added just to enhance the workability. The time of initial and final setting derived from the data presented in Fig. 5.1 are summarized in Table 5.1.

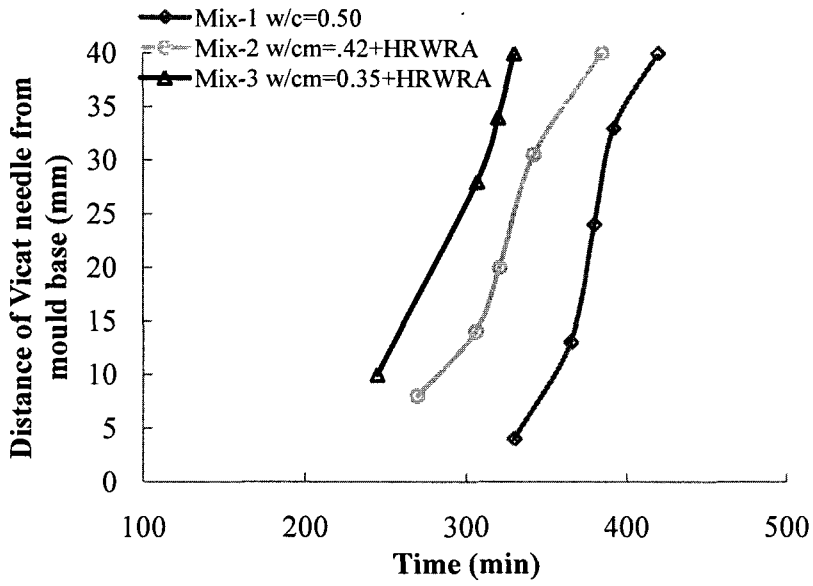

Fig. 5.1 Variations of Vicat needle penetration for paste mixtures of different *w/cm*

Table 5.1 Initial and final setting time of paste mixtures obtained using Vicat needle and the corresponding setting times and shear wave velocity obtained using

Paste mixture	*w/cm*	Vicat needle		*P-RAT2*			
		t_i (min)	t_f (min)	t_1 (min)	V_{s1} (m/s)	t_2 (min)	V_{s2} (m/s)
Mix-1	0.50	375	420	364	306	437	553
Mix-2	0.42+ HRWRA	320	385	320	318	370	548
Mix-3	0.35+ HRWRA	290	330	305	306	344	528

5.2.2 Measurement of heat of hydration

Another indicator for the hydration and setting process of cement-based materials is the development of the adiabatic heat of hydration. An example of the adiabatic heat evolutions with time for Mix-2 made with *w/cm* of 0.42 during the hydration of cement and water is shown in Fig. 5.2. The hydration processes can be divided into five stages. In Stage I, the reaction generates an explosion of heat. This stage is not clearly observed in the current curve because the monitored heat of hydration started at approximately 30 minutes after the contact of water and

cement. During Stage II, less hydration takes place and this stage is expressed as a dormant period. After critical value of calcium and hydroxide ions are reached, a rapid crystallization followed by a rapid reaction of calcium hydroxide and calcium silicate hydrate is formed (Stage III). Stage III is observed between five and seven hours from the cement and water contact. In this acceleration stage there is an onset of transformation to rigidity. In the following stages; Stage IV and Stage V, there are continuous formations of hydration products; however the rate of reaction is slowing down. From this curve, the initial set occurs somewhat after the transition from Stage II while the final set occurs just before the peak between Stage III and Stage IV, [Mindess et al., 2003] and [Neville 2002].

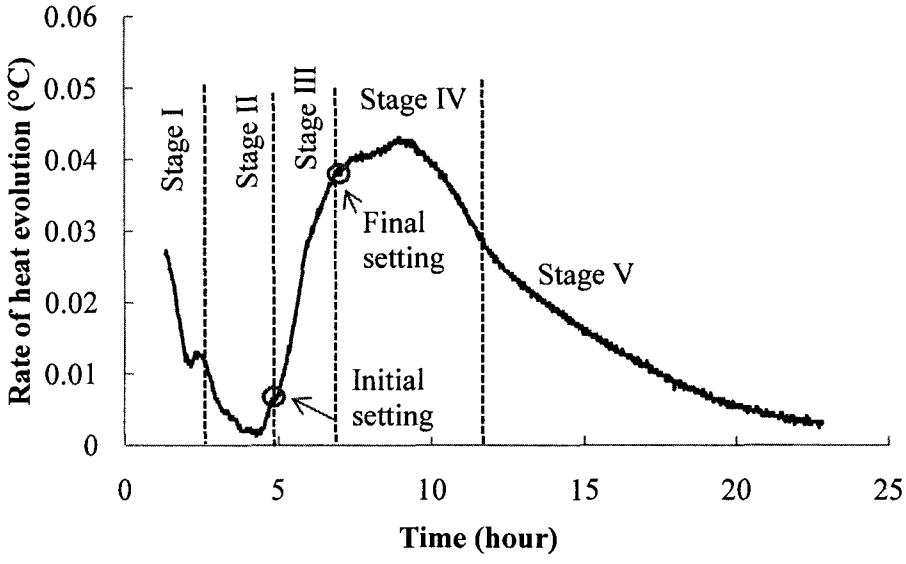

Fig. 5.2 Evolution of heat of hydration with time for Mix-2 made with *w/cm* of 0.42

Comparison between the evolution of heat of hydration with time for Mix-1, Mix-2, and Mix-3 made with *w/cm* of 0.50, 0.42, and 0.35, respectively, are shown in Fig. 5.6. Mix-1 of the 0.50 *w/cm* showed a relative delay in heat evolution compared to Mix-2 that in its turn exhibited relative delay in the heat evolution than that of Mix-3. For example, Stage IV started at approximately 6.5, 7.5, and 9 hours after the cement and water contact for Mix-3, Mix-2, and Mix-3, respectively.

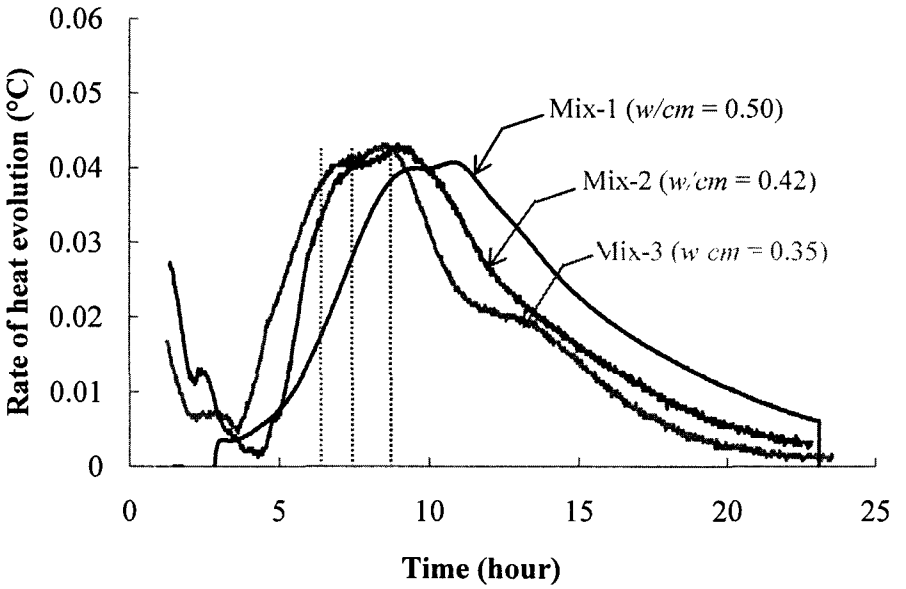

Fig. 5.3 Evolutions of heat of hydration for paste mixtures made with different *w/cm*

5.2.3 Measurement of electrical conductivity

The variations of ionic conductivity with time for Mix-2 made with *w/cm* of 0.42 (Fig. 5.4) are monitored by inserting a conductivity probe into the specimen that was used with the calorimetric test. As shown in the figure, the evolution of conductivity with time was sharply increased in the first instants following mixing of cement and water given by the rapid dissolution of alkali sulfates. These results in an increase of Na^+, K^+, and SO_4^{2-} ions and early surface hydration of the most reactive phases in the cement, generating Ca^{2+} and OH^- ions. Then, the conductivity increased slowly as the hydration reactions preceded, further increasing the concentration of Ca^+ and OH^- ions in the solution reaching a super saturation level. As the conditions for $Ca(OH)_2$ precipitation become favourable, sharp decrease in Ca^{2+} and OH^- ions concentration taken place, initiating a rapid decrease in conductivity, which signals the onset of setting [Pavate et al., 2003].

The tangents of the conductivity curve shown in Fig. 5.4, give four different distinguished times (T_1, T_2, T_3, and T_4) [Pavate et al., 2003]. The values of T_2 and T_3 correspond to the initial and final setting times from the Vicat needle test. These time are referred to be here as $t_{i,c}$ and $t_{f,c}$, for the conductivity test, respectively.

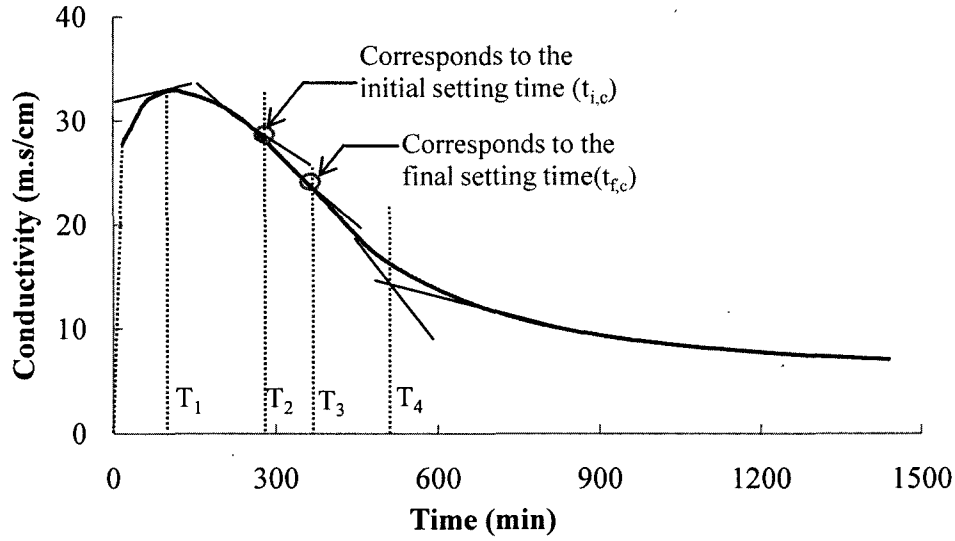

Fig. 5.4 Variation of electrical conductivity with time for Mix-2 (*w/cm* = 0.42+HRWRA): initial and final setting times are indicated

A comparison between the variations of electrical conductivity with time for Mix-1, Mix-2, and Mix-3, made with *w/cm* of 0.50, 0.42, and 0.35, respectively, are shown in Fig. 5.5. Starting from the time of 300 minutes, the conductivity was lower for Mix-3 of the *w/cm* of 0.35 and increased for the Mix-1 made with higher *w/cm* of 0.5. Generally, the resistivity is the inverse of the conductivity. Hence, the resistivity of Mix-3 (0.35 *w/cm*) was higher than the resistivity of Mix-1 (0.5 *w/cm*) as shown in Fig.5.6. Furthermore, the evolution of conductivity with time showed a faster rate of decrease for the paste mixture made with lower *w/cm* (0.35) compared to the mixture incorporated lower *w/cm* (0.35).

During the first instants following mixing of cement and water, none expected results of the conductivity was observed for these paste mixtures. The conductivity was higher for Mix-3 (0.35 *w/cm*) and decreased for the Mix-1 (0.5 *w/cm*). For example, the values of conductivity were 38, 33, and 30 m.s/cm for Mix-3, Mix-2, and Mix-1 made with *w/cm* of 0.35, 0.42, and 0.50, respectively.

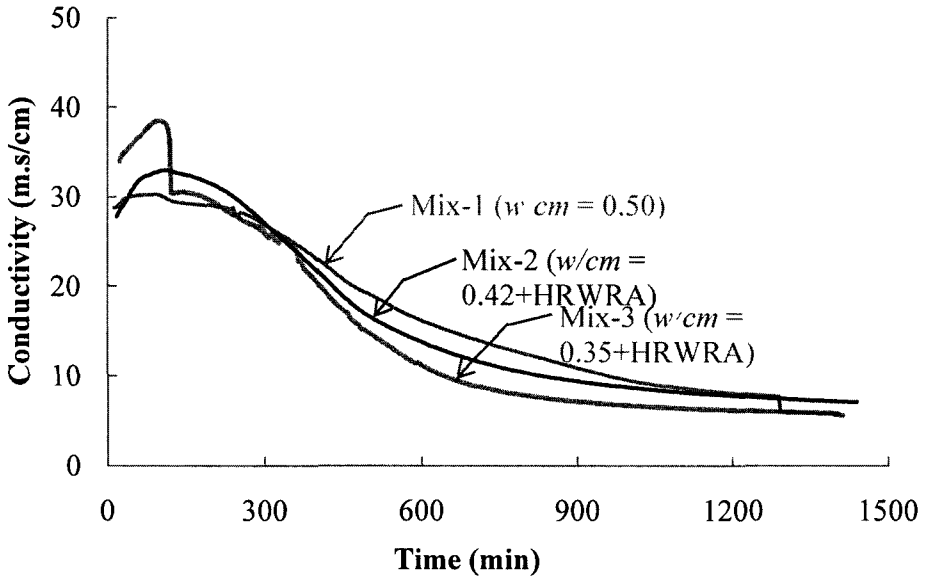

Fig. 5.5 Variations of electrical conductivity for paste mixtures made with different *w/cm* and without any additive at 24 hours

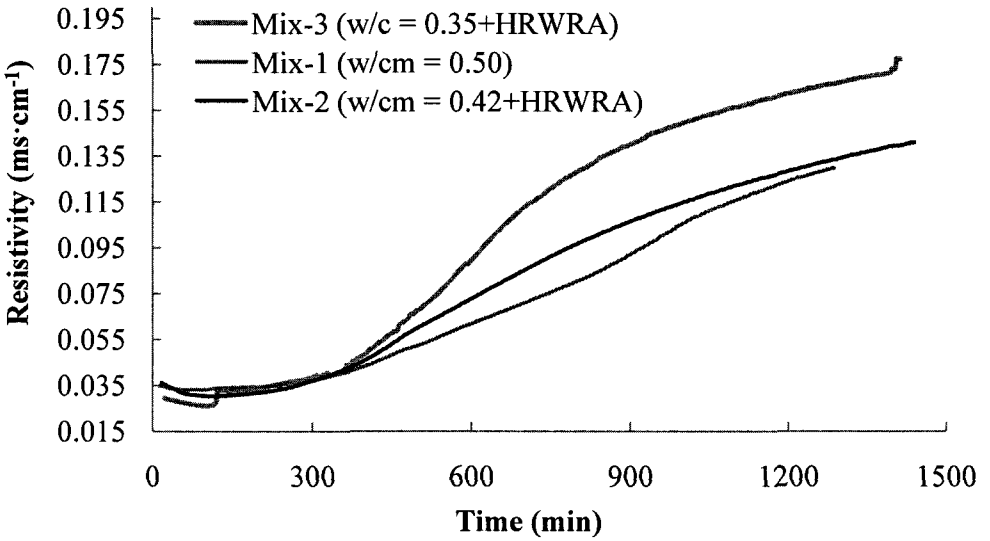

Fig. 5.6 Variations of Resistivity for paste mixtures made with different *w/cm* and without any additive at 24 hours

5.2.4 Measurement of shear wave velocity

In parallel to the tests carried out using the traditional methods (Vicat needle to monitor initial and final setting times, calorimetric to monitor heat of hydration, and electrical conductivity to

monitor change in continuity of the pore structure), the variations in the V_s with time for the paste mixtures were continuously monitored at 10 to 15-minute intervals using the *P-RAT2*. The monitoring of V_s using the *P-RAT2* was continued for a total period of 10 hours or until the time of the final set was reached.

Immediately after finishing mixing and cast the paste in the specified moulds of the *P-RAT2*, it was observed that V_s remains at a value of zero for approximately two hours before gradual increasing, elastic state. This phenomenon can be interpreted due to the absence of a continuous skeleton of solid particles that would allow the shear waves to propagate. The evolution of the V_s with the elapsed time is shown in Fig. 5.8 for the three tested paste mixtures. Mix-3 made with *w/cm* of 0.35, which exhibited the earliest initial and final setting times, showed early and sharp increase of V_s with respect to time. A maximum V_s value of 1200 m/s was determined at approximately 415 min from the time of water cement contact. On the other hand, Mix-1 made with *w/cm* of 0.5 exhibited slow rate of V_s with time. A maximum V_s value of 714 m/s was determined at approximately 470 minutes from the time of contact of cement and water.

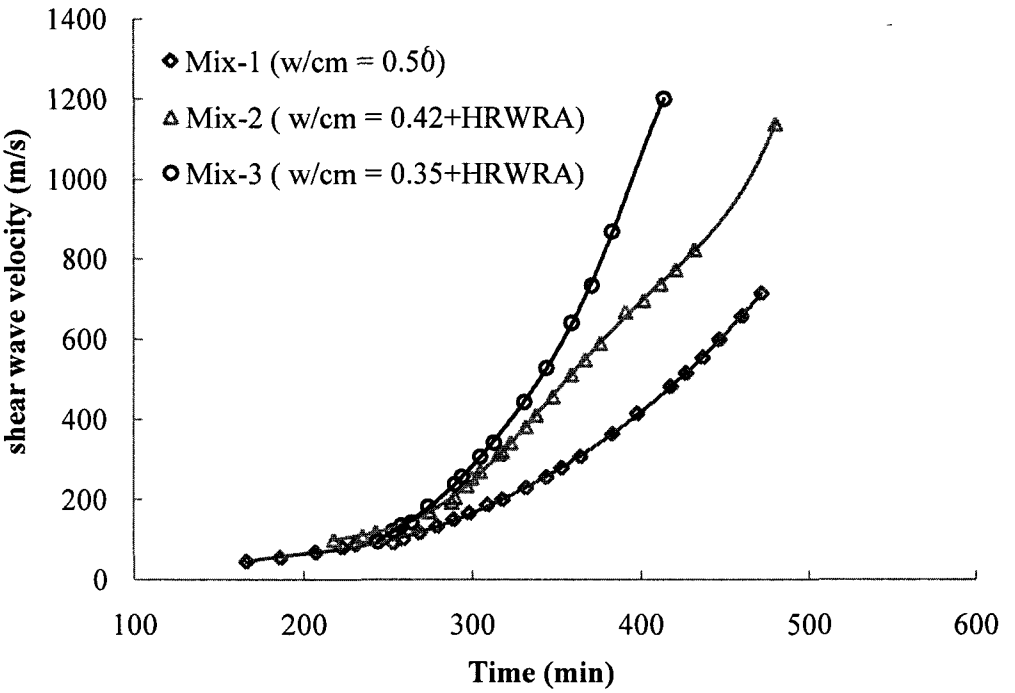

Fig. 5.7 Variations of shear wave velocity with time for paste mixtures of various *w/cm*

The "Derivatives" method was followed for estimating setting times from the evolution of V_s with time obtained using the *P-RAT2*. The "Derivatives" method defines the time corresponding to the maximum slope as the final setting time (t_2), and the time corresponding to a baseline when the curve start to increase as an initial setting time (t_1). The derivation curve of shear wave velocity is obtained from the derivation of the shear velocity with respect to time (dV_s/dt). Figure 5.8 shows the evolution of V_s and dV_s/dt with time for Mix-2 and the two values of the setting time; t_1 and t_2 obtained from the derivation curve. The t_1 and t_2 values are found to be proportioned to the initial and final setting times (t_i and t_f) determined using the penetration resistance test, respectively. For example for Mix-2, the t_i and t_f values are 320 and 385 min, respectively, while the corresponding t_1 and t_2 values are 320 and 370 min, respectively. Table 5.1 summaries the t_i and t_f values obtained using Vicat needle. The corresponding t_1 and t_2 and shear wave velocity values (V_{s1} and V_{s2}, respectively) obtained using the *P-RAT2* is also indicated in the table 5.1.

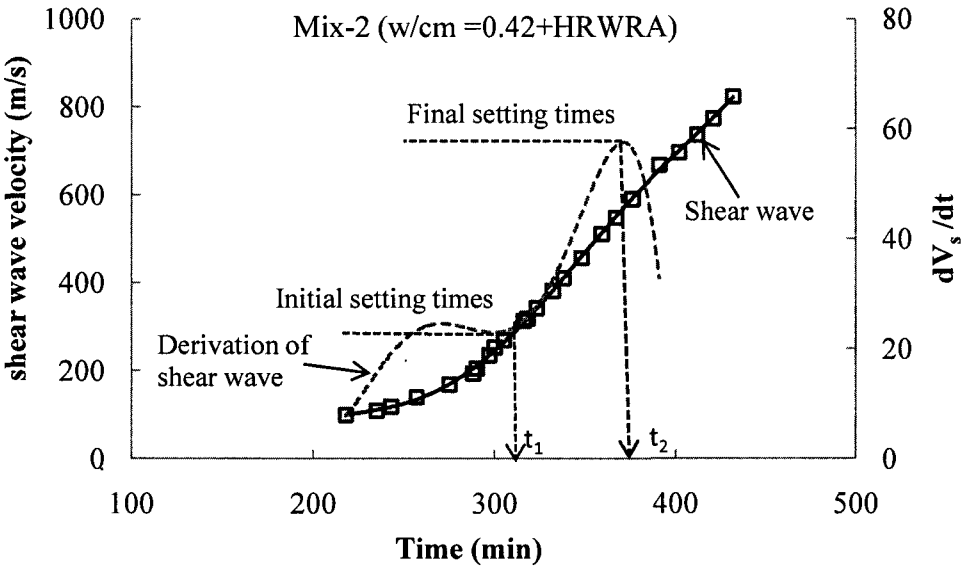

Fig. 5.8 Evolution of shear wave velocity and derivation of shear wave velocity with time for paste mixture (Mix-2 of *w/cm* = 0.42+HRWRA)

From Figs. 5.1 and 5.7, it can be observed that the variations of the V_s with elapsed time are similar to those of the penetration depth with time obtained from the Vicat needle. In fact, the

magnitude of V_s is affected by the rigidity of the medium in which the wave passes. The increase in the rigidity allows the shear wave to pass at higher speed. With the elapsed time, the physical and chemical properties of the paste changes due to the hydration processes leading to an increase in the rigidity of the inner medium that affects in its turn both the penetration resistance and V_s. This can explain the similar propagation of the penetration resistance and V_s with the time.

In addition, the evolutions of the heat of hydration and V_s with time were similar, as shown from Figs. 5.3 and 5.7, respectively. The propagation of shear wave velocity with time was proportioned to the resistivity of the materials (Figs. 5.6 and 5.7). It can be shown from Figs. 5.5 and 5.7, that the shear wave velocity is related indirectly to the conductivity. As mentioned earlier, the shear wave velocity is strongly related to the rigidity and consequently to the resistivity of the material. For example, both the V_s and resistivity were increased at higher rates for Mix-3 (*w/cm* of 0.35) and at lower rates for Mix-1 (*w/cm* of 0.5).

From the above results, the *P-RAT2* is able to reflect the effect of the different mixture proportioning on the hydration of cement-based materials. The shear wave velocity obtained using the *P-RAT2* can used to describe the hydration processes of the cement. An agreement between the *P-RAT2* and conventional test methods, Vicat needle, calometric, and conductivity tests are observed. The preliminary agreement between the *P-RAT2* measurements and these determined using conventional tests can encourage to a wider usage of the *P-RAT2* to evaluate different cement-based materials, including mortar and concrete.

5.3 Validation of *P-RAT2* using mortar mixtures

In the second part of validation, the mortar mixtures were selected to evaluate the behaviour of the *P-RAT2* on complex medium that contains sand in addition to the cement and water. In total, nine mortar mixtures proportioned with *w/cm* varied between 0.35 and 0.50 and various chemical admixtures were employed in order to obtain wider ranges in setting and hydration properties as well as the conductivity. The mixture proportions and the fresh properties for the mortar mixtures are given in Tables 3.5 and 3.6, respectively. The penetration resistance, calorimetry, and electrical conductivity tests were used as to determine the setting time, heat of hydration, and electrical conductivity, respectively, with elapsed time. the variations in the V_s with time was continuously monitored at 10-15 minutes intervals using the *P-RAT2* until 2-3 hours after the final set was reached concurrently with these previous conventional tests.

In order to investigate the effect of *w/cm*, three mortar mixtures Mix-4, Mix-10, and Mix-11 made with *w/cm* of 0.5, 0.42, and 0.35, respectively were tested. In order to investigate the effect of chemical admixtures, two schemes were followed. In the first scheme, the target slump flow values were fixed to 265 ± 5 mm. Three mortar mixtures Mix-5, Mix-6, and Mix-4 made with *w/cm* of 0.35, 0.42, and 0.5, respectively, were tested in the first phase. To secure the target slump flow, two different dosages of the HRWRA were added to Mix-5 and Mix-6. However, Mix-4 did not include any HRWRA. In the second scheme, different types of chemical admixtures were employed. Mix-6 made with 0.42 *w/cm* and contained HRWRA was set as reference for this scheme. Three other mortar mixtures of similar mix designs to Mix-6 except various chemical admixtures were prepared. Mix-7 included SAA, Mix-8 included SRA, and Mix-9 incorporated with VMA. Greater dosage of HRWRA was required with the latter mortar mixture (Mix-9) to enhance the workability.

5.3.1 Measurement of setting time

The time of setting for the mortar mixtures were determined using the penetration resistance test in accordance to ASTM C 403. The measurements of penetration resistance were performed in regular-time intervals until the specimen was completely set. The penetration resistance was calculated as the ratio between the applied force and the bearing area of the used needle. The measurements of penetration resistance are plotted against the elapsed time, as shown in Fig. 5-9 for mortar mixtures made with various *w/cm* and without any additives. These measurements are shown in Figs. 5.10 and 5.11 for mortars proportioned with different contents and types of chemical admixtures, respectively. The initial and final setting times corresponded to penetration resistances of 3.5 and 27.6 MPa, respectively. Table 5.2 summarizes the initial and final setting time obtained using the penetration resistance test.

5.3.1.1 Influence of w/cm

Mix-11, Mix-10 and Mix-4 proportioned with *w/cm* of 0.35, 0.42 and 0.5, respectively, were designed to investigate the effect of *w/cm* on the variation of penetration resistance determined using the penetration resistance test and the variation of V_s with time determined using the *P-RAT2*. The three mortar mixtures did not include any HRWRA. Fig. 5.9 shows the

influence of *w/cm*. The mortar mixture made with 0.35 *w/cm* (Mix-11) showed faster setting time compared to the mortar mixture made with *w/cm* 0.50 (Mix-4).

Table 5.2 Initial and final setting time determined using penetration resistance test and corresponding time and shear wave velocity obtained using *P-RAT2* for mortar mixtures

Mortar mixture	*w/cm*	Penetration resistant test		*P-RAT2*			
		t_i (min)	t_f (min)	t_1 (min)	V_{s1} (m/s)	t_2 (min)	V_{s2} (m/s)
Mix-4	0.50	310	365	300	305	355	590
Mix-5	0.35+ HRWRA	325	380	325	370	375	620
Mix-6	0.42+ HRWRA	315	370	315	320	370	660
Mix-7	0.42+SAA+ HRWRA	275	325	260	300	320	610
Mix-8	0.42+SRA+ HRWRA	600	675	580	300	680	610
Mix-9	0.42+VMA+ HRWRA	510	580	515	275	580	640
Mix-10	0.42	245	315	260	350	325	695
Mix-11	0.35	185	245	200	355	250	690
Mix-12	0.39	245	300	245	320	300	625

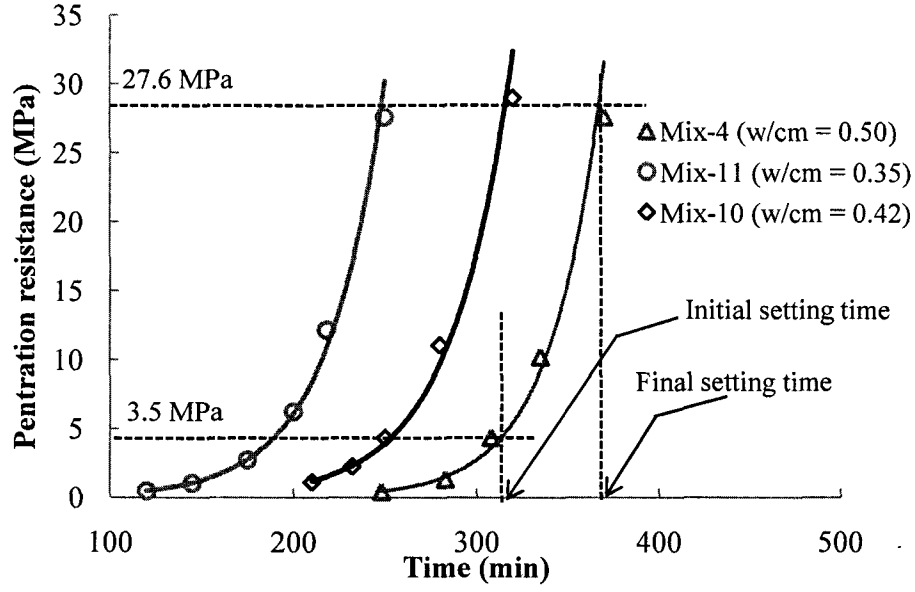

Fig. 5.9 Variations of penetration resistance with time for mortar mixtures made with different *w/cm*

5.3.1.2 Influence of chemical admixtures

The setting behaviour of cement-based materials is highly influenced by chemical admixtures. The chemical admixture introduced to change set characteristics and to validate the *P-RAT2* vs. other conventional methods. The development of the penetration resistance of the tested mortars is given in Figs. 5.10 and 5.11.

Figure 5.10 shows the influence of the HRWRA on the development of the penetration resistance with the elapsed time. Adding more HRWRA dosages in Mix-5 and Mix-6 to produce similar slump flow value of Mix-4 of 265 ± 5 mm lead to approximately initial and final setting times for the three mortars.

To evaluate the effect of HRWRA content on setting time, Mix-6 and Mix-10 made with the same *w/cm* of 0.42 are compared. Mix-6 contained the HRWRA had initial and final setting 315 and 369 min, respectively, while Mix-10 without contain HRWRA had setting times of 246 and 314 min, respectively.

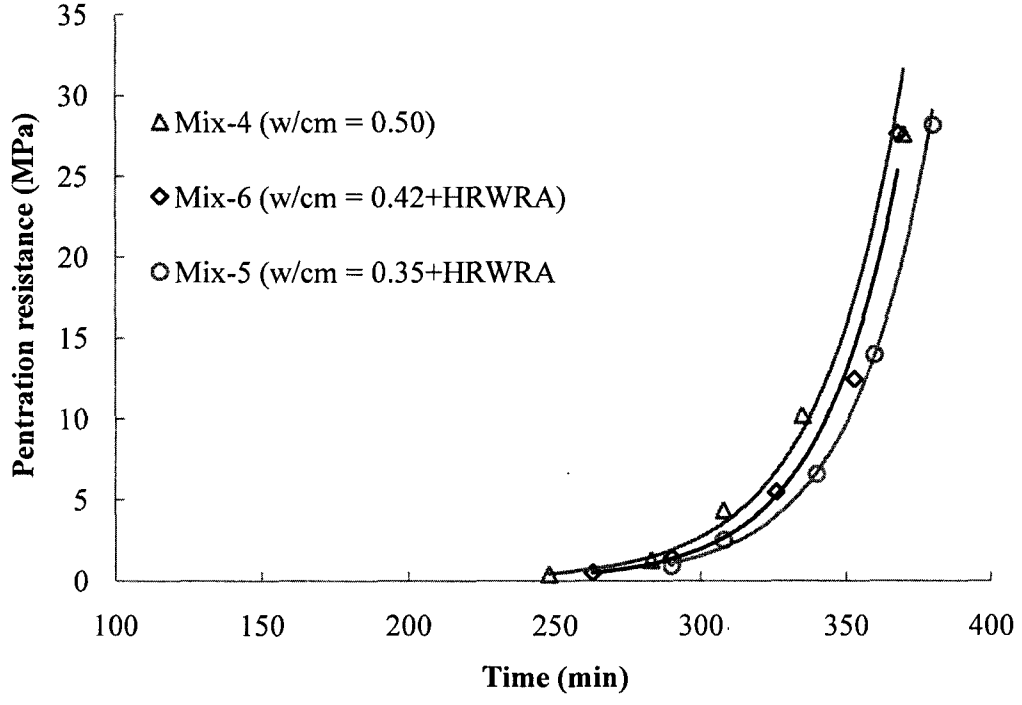

Fig. 5.10 Variations of penetration resistance with time for mortar mixtures made with different *w/cm* and HRWRA

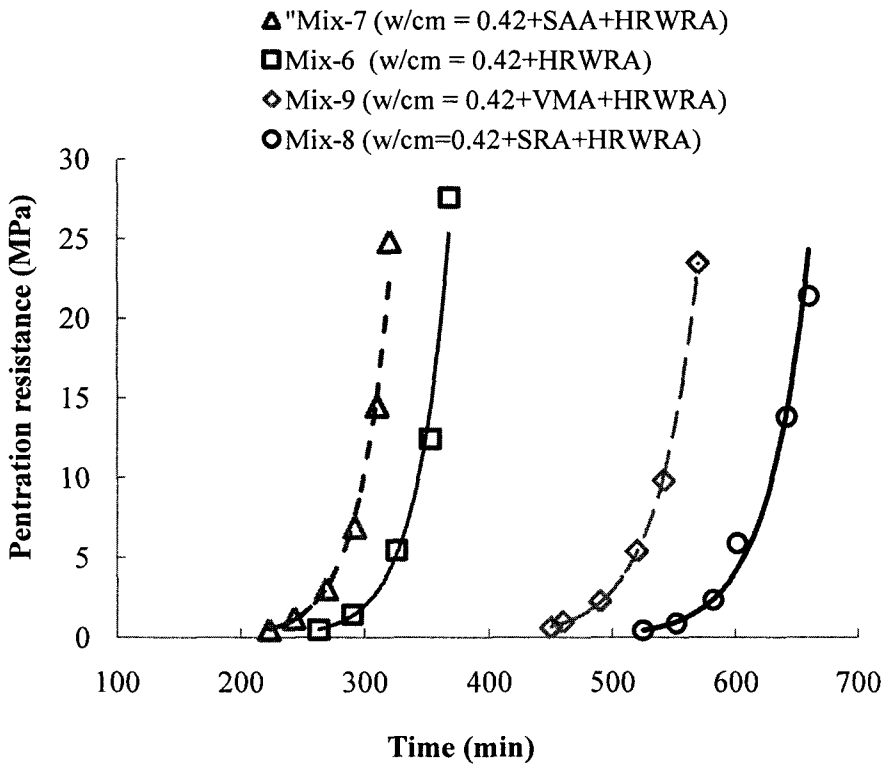

Fig. 5.11 Variations of penetration resistance with time for mortar mixtures made with fixed *w/cm* and different types of chemical admixtures

Different chemical admixtures (SAA, SRA and VMA) were added to Mix-6 that was proportioned with *w/cm* of 0.42 and HRWRA in order to produce Mix-7, Mix-8 and Mix-9, respectively. Mix-7 made with SAA showed faster setting time compared to Mix-8 with SRA, as shown in Fig. 5.11. The initial and final setting times for Mix-7 were 273 and 325 minutes, respectively. These values were 600 and 675 minutes for Mix-8, respectively. Mix-9 contained VMA showed delay in setting time compared to Mix-6. This can be related to the higher demand of HRWRA in Mix-9.

5.3.2 Measurement of heat of hydration

Another indicator for the setting process of cement-based materials is the development of the adiabatic heat of hydration. An example of the adiabatic heat evolution with time was discussed in section 5.3.2 for a paste mixture.

5.3.2.1 Influence of *w/cm*

The evolution of the heat of hydration with time for Mix-4, Mix-10, and Mix-11 made with *w/cm* of 0.50, 0.42, and 0.35, respectively, are compared in Fig. 5.12. Mix-4 showed relative delay in the heat evolution compared to that of Mix-11 which exhibited some delay in heat evolution than Mix-10. For example, the stage IV started at an earlier time after cement and water contact for Mix-11, followed by Mix-10, and then Mix-4.

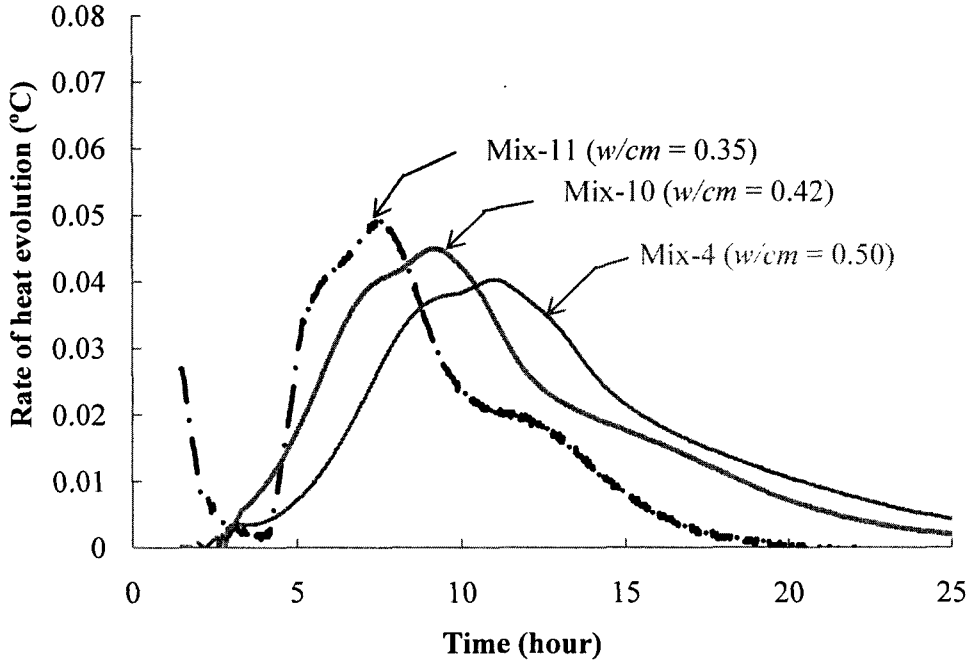

Fig. 5.12 Evolution of heat of hydration with time for mortar mixtures proportioned with various *w/cm* without any additive

5.3.2.2 Influence of chemical admixtures

As mention before hydration behaviour of cement-based materials is highly dependent on the chemical admixtures incorporated in the mixtures. The developments of the adiabatic heats of hydration are given in Figs. 5.13 and 5.14.

Figure 5.13 shows clearly the influence of the different dosages of HRWRA employed in the mixture on the development of the heat of hydration with time. Higher and medium dosages of HRWRA were added to Mix-5 and Mix-6, respectively to produce the same slump spread of

Mix-4 (265 ± 5 mm). This resulted in approximate amounts of heat of hydration for the three mortar mixtures.

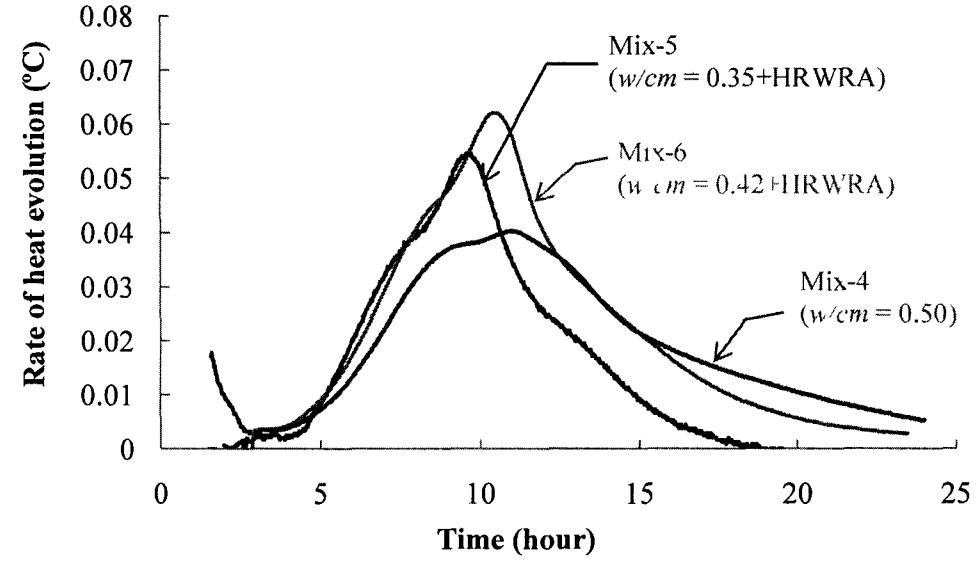

Fig. 5-13: Evolution of heat of hydration with time for mortar mixtures proportioned with various *w/cm* and different contents of HRWRA to produce fixed slump flow

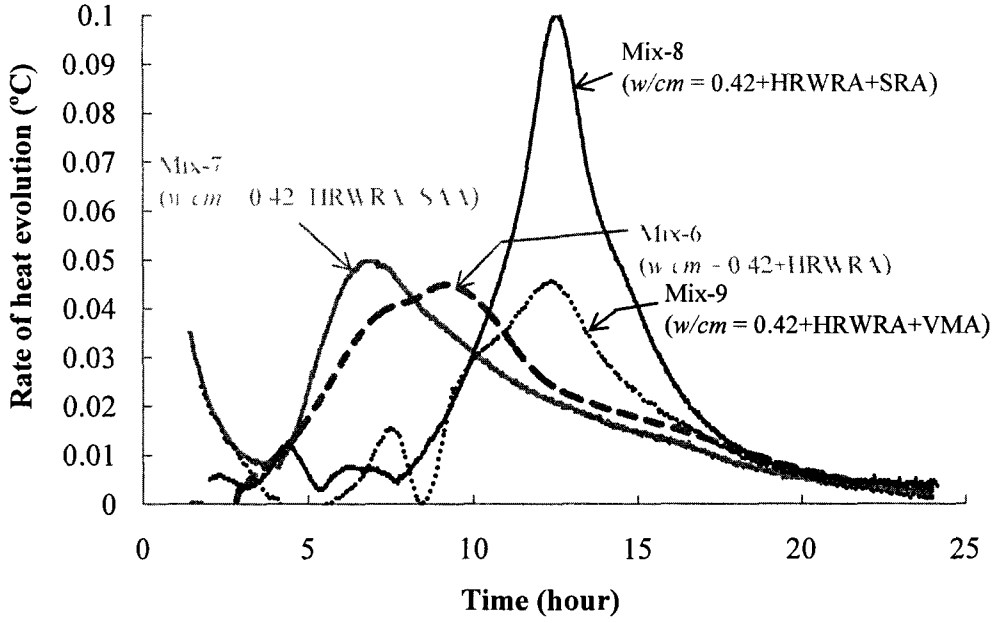

Fig. 5-14: Evolution of heat of hydration with time for mortar mixtures proportioned with *w/cm* of 0.42 and contained different types of chemical admixtures

The effects of different types of the chemical admixtures (HRWRA, SAA, SRA, and VMA) on the evolution of heat of hydration are shown in Fig. 5.14, through Mix-6, Mix-7, Mix-8, and Mix-9, respectively Mix-7 made with SAA showed an increase in the heat of hydration earlier than Mix-6 that prepared without SAA. On the other hand, Mix-9 prepared with SRA exhibited the increase in the heat of hydration at later time compared at Mix-6 that prepared without SAA.

5.3.3 Measurement of electrical conductivity

5.3.3.1 Influence of w/cm

A comparison between the variations of electrical conductivity with time for Mix-4, Mix-10, and Mix-11, made with *w/cm* of 0.50, 0.42, and 0.35, respectively, are shown in Fig. 5.15. As known, the resistivity is the inverse of the conductivity. Hence, the resistivity of Mix-11 (0.35 *w/cm*) was higher than that of Mix-4 (0.5 *w/cm*). Consequently, the conductivity was lower for Mix-11 (*w/cm* of 0.35) and increased for the Mix-4 made with higher *w/cm* of 0.5. For example at around 90 minutes, the values of conductivity were 7.23, 12.75, and 14.6 m.S/cm for Mix-11, Mix-10, and Mix-4 made with *w/cm* of 0.35, 0.42, and 0.50, respectively.

Furthermore, the evolution of conductivity with time showed a faster rate of decrease for the mortar mixture made with lower *w/cm* of 0.35 compared to the mixture incorporated higher *w/cm* of 0.50.

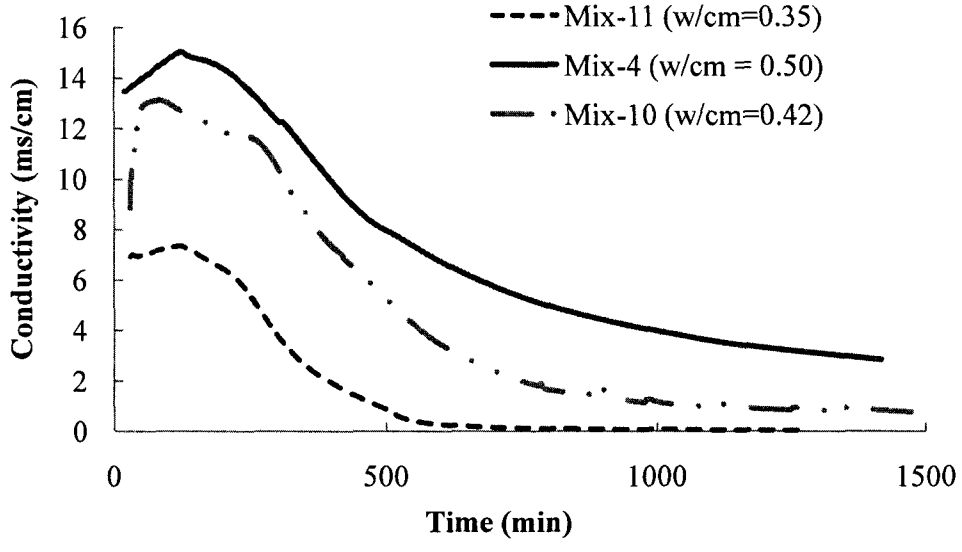

Fig. 5.15 Variations of electrical conductivity with time for mortar mixtures made with different *w/cm* and without any chemical admixtures

5.3.3.2 Influence of chemical admixture

Figure 5.16 shows clearly the influence of the different dosages of HRWRA employed in the mortar on the variations of conductivity with time. In order to see clearly this effect of HRWRA on conductivity behaviour, Mix- 6 and Mix-10 can be compared. The conductivity values at 120 minutes from the water and cement contact were 13 and 12.4 m.S/cm for Mix-6 containing HRWRA and Mix-10 without contain any HRWRA, respectively.

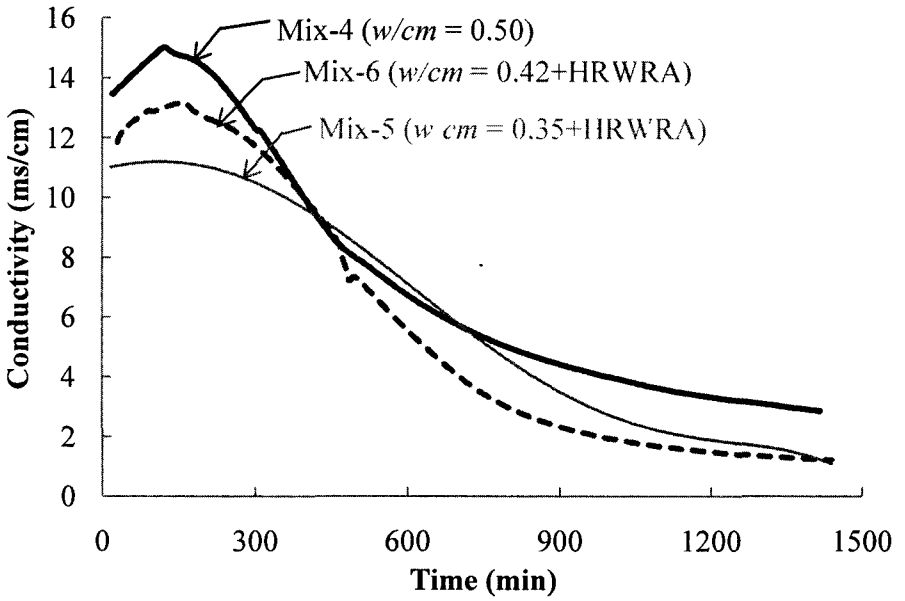

Fig. 5.16 Variations of electrical conductivity with time for mortars proportioned with different *w/cm* and with dosages of HRWRA to given constant slump flow

The effect of different type of the chemical admixtures (HRWRA, HRWRA+ SAA, and HRWRA+VMA) on the evolution of conductivity with time is shown in Fig. 5.17. Mix-7 containing (HRWRA+ SAA) exhibited less variation of conductivity with time compared to the other mixtures.

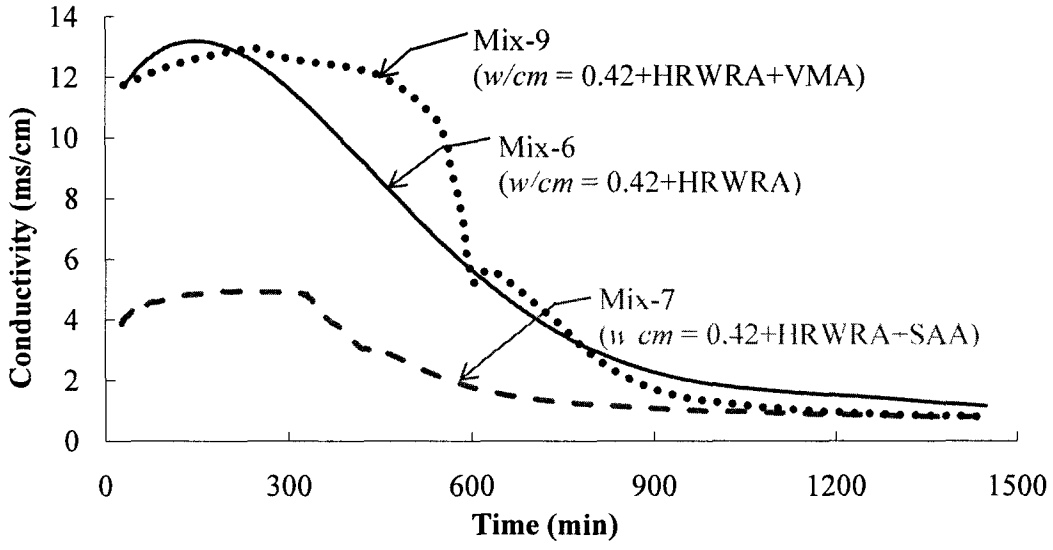

Fig. 5.17 Variations of electrical conductivity with time for mortars incorporated *w/cm* of 0.42 and various chemical admixtures

5.3.4 Measurement of shear wave velocity

5.3.4.1 Influence of w/cm

Mix-11, Mix-10 and, Mix-4 made with *w/cm* of 0.35, 0.42 and 0.5, respectively, were designed to investigate the effect of *w/cm* on the variations of V_s with time determined using the *P-RAT2* (Fig. 5.18). The three mortar mixtures did not include any HRWRA. For example the Mix-11 made with the lowest *w/cm* of 0.35 showed an early and sharp increase in the V_s with time. The V_s value of 1430 m/s was determined at approximately 400 min after the contact of cement and water. On the other hand, Mix-4 made with the highest *w/cm* of 0.50 exhibited slaw increasing rate of V_s with time. The V_s value of 815 m/s was determined at the same time of cement and water contact of 400 min.

The "Derivatives" method was also used to determine the setting times from the evolution of V_s with time obtained using the *P-RAT2* for the mortar mixture. Figure 5.19 shows the evolution of V_s and the derivation of V_s with respect to time (dV_s/dt) for Mix-10. For example, the t_i and t_f values obtained using the penetration resistance test were approximately 245 and 315 min, while the corresponding t_1 and t_2 values determined using the *P-RAT2* were 260 and 325 min, respectively. Table 5.2 summarizes t_i, t_f, t_1 and t_2 The shear wave velocity values corresponding to t_1 and t_2 (i.e., V_{s1} and V_{s2}, respectively) obtained using *P-RAT2* are also indicated in Table 5.2.

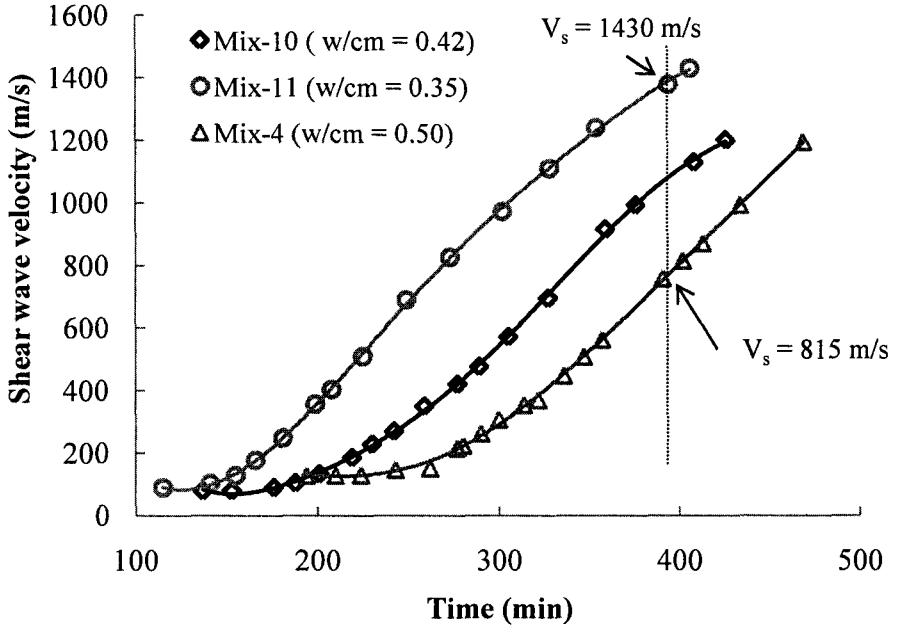

Fig. 5.18 Variations of shear wave velocity with time for mortars made with different *w/cm* and without chemical admixtures

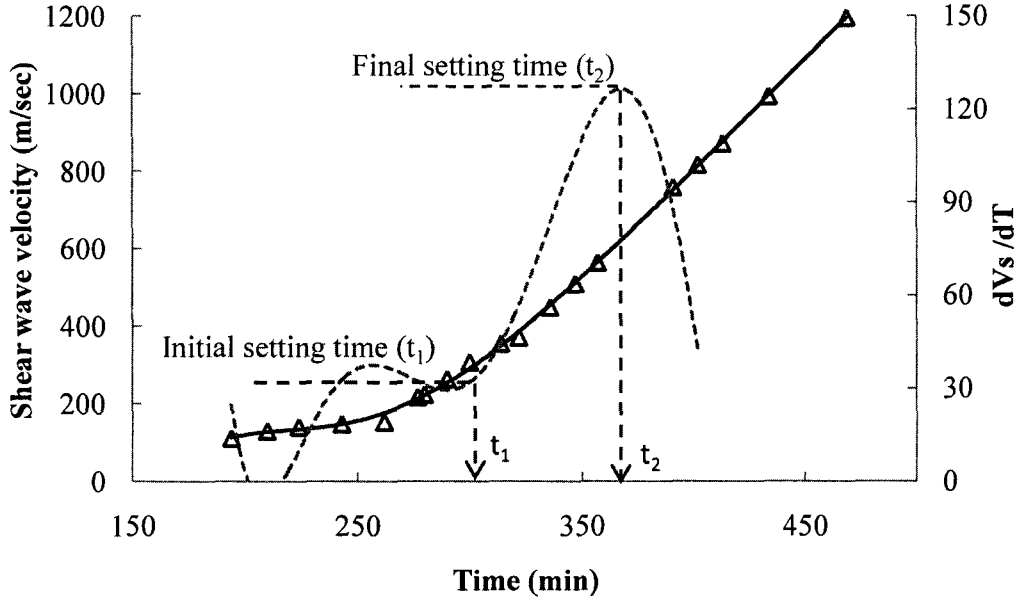

Fig. 5.19 Evolution of shear wave velocity and derivation of shear wave velocity with time for mortar mixture (Mix-10, *w/cm* = 0.42+HRWRA)

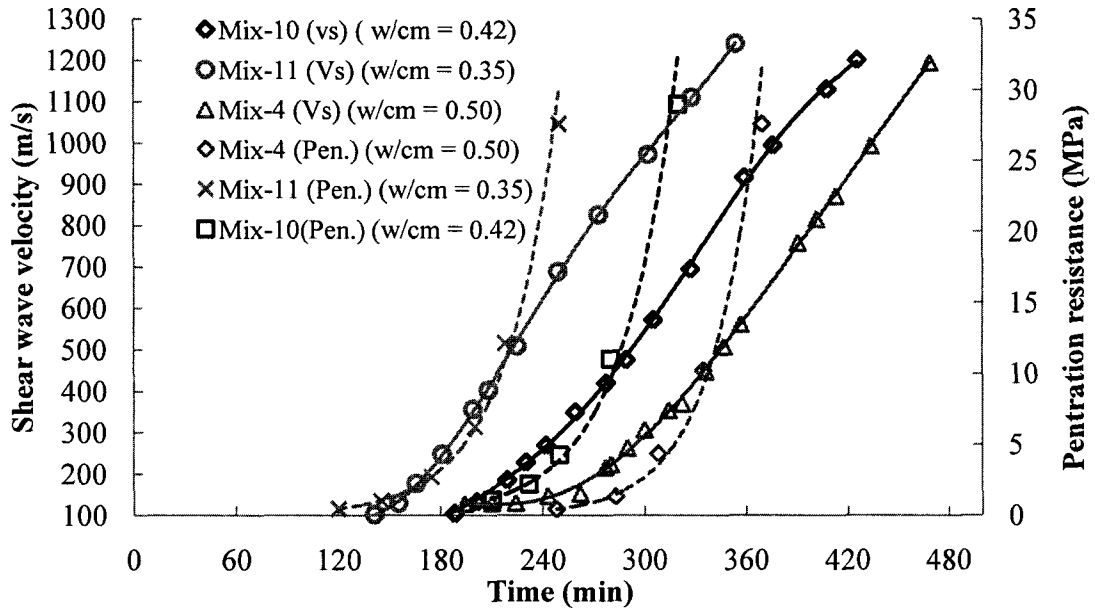

Fig. 5.20 Shear wave velocity and penetration resistance test for mortar made with different *w/cm* values

It can be clearly observed from Figs. 5.9, 5.18 and 5.20 that the variations of V_s with elapsed time are similar to the variations of the penetration resistance obtained from the penetration resistance test. At an elapsed time corresponding to the initial setting time determined from the penetration resistance test, two different changes in the variation of V_s with time can be noticed. The t_1 and t_2 determined using the *P-RAT2* were found to be proportioned to the t_i and t_f determined from the penetration resistance test, respectively. These two values correspond to two practical points; limit of handling, and beginning of mechanical strength development, respectively.

Furthermore, the evolutions of the heat of hydration and V_s with time were similar, as shown from Figs. 5.12 and 5.18, respectively. In addition, it can be shown from Figs. 5.17 and 5.18, that the shear wave velocity is related indirectly to the conductivity, as known the conductivity decrease in the beginning of strength gain. As mentioned earlier, the shear wave velocity is strongly related to the rigidity and consequently to the resistivity of the material. For example, the V_s was increased at higher rates for Mix-11 (*w/cm* of 0.35) and at lower rates for

Mix-4 (*w/cm* of 0.5). On the other hand the conductivity was lower for Mix-11 (*w/cm* of 0.35) and increased for the Mix-4 made with higher *w/cm* of 0.5.

From the above results, the agreement between the *P-RAT2* and conventional test methods, penetration resistance, calometric and conductivity tests are very important to proof the ability of *P-RAT2* to trade off the cement hydration processes. Also, it can be stated that *P-RAT2* is able to reflect the effect of different water cement ratio on the hydration processes of cement-based materials.

5.3.4.2 Influence of chemical admixture

In order to investigate the effect of chemical admixtures, two schemes were followed. In the first scheme, the target slump flow values were fixed to 265 ± 5 mm. Three mortar mixtures Mix-5, Mix-6, and Mix-4 made with *w/cm* of 0.35, 0.42, and 0.5, respectively, were tested in the first phase. In the second scheme, different types of chemical admixtures were employed. Mix-6 made with 0.42 *w/cm* and contained HRWRA was set as reference for this scheme. Three other mortar mixtures of similar mix designs to Mix-6 except various chemical admixtures were prepared. Mix-7 included SAA, Mix-8 included SRA, and Mix-9 incorporated with VMA.

The variations of V_s with elapsed time for the mortar mixtures Mix-5, Mix-6, and Mix-4 of the same workability were found approximately similar, as shown in Fig. 5.21. However, the absolute values of the Vs were different according to tested mixture and its ingredients. For example at 400 min from the water cement contact, the Vs value was approximately 1000 m/s for Mix-6 of high w/cm of 0.42 compared to 800 m/s for Mix-4 made with low w/cm of 0.50.

In addition, to see the ability of *P-RAT2* to detect the effect of HRWRA on the shear wave measurement, Mix- 6 and Mix-10 can be compared. The V_s values at 400 minutes from the water and cement contact were 950 and 1150 m/s for Mix-6 contained HRWRA and Mix-10 without HRWRA, respectively.

The effects of different types of chemical admixtures (HRWRA, HRWRA+ SAA, HRWRA+SRA, and HRWRA+VMA) through Mix-6, Mix-7, Mix-8, and Mix-9, respectively on the evolution of shear wave velocity are shown in Fig. 5.23. Mix-7 made with SAA showed early and sharp increase in the V_s with time. Maximum V_s value of 1051 m/s was determined at approximately 372 minutes after the water and cement contact. On the other hand, Mix-8 made with

SRA exhibited lower increasing rate in the V_s with the time. Maximum V_s value of 610 m/s was determined at approximately 680 minutes from the water and cement contact.

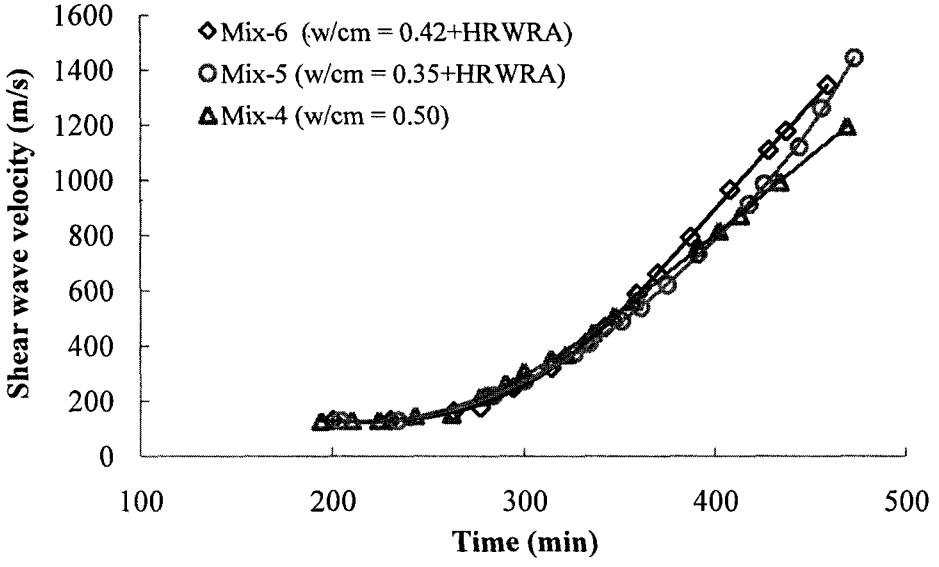

Fig. 5.21 Variations of shear wave velocity with time for mortar mixtures of different *w/cm* and HRWRA

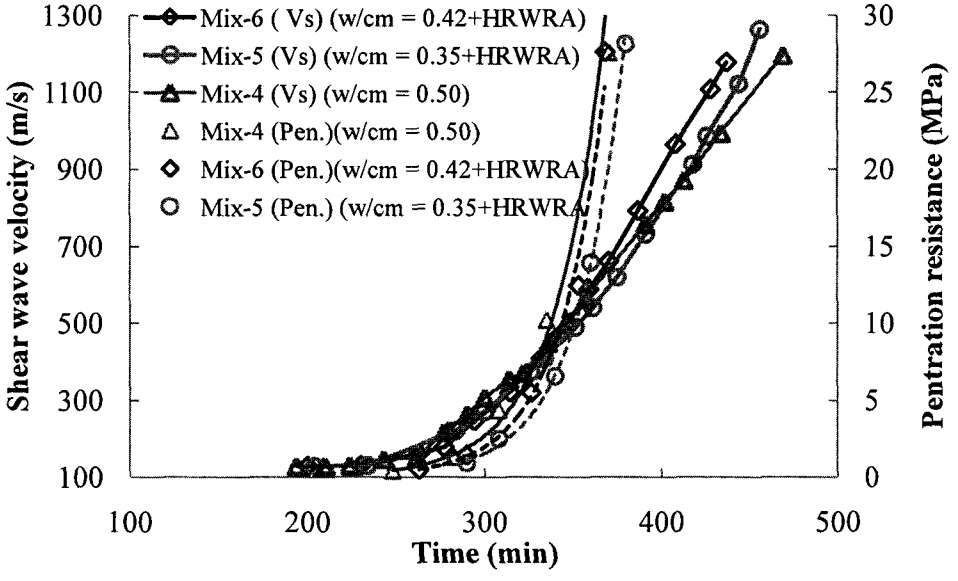

Fig. 5.22 Shear wave velocity and penetration resistance test with time for mortar mixtures of different *w/cm* and HRWRA

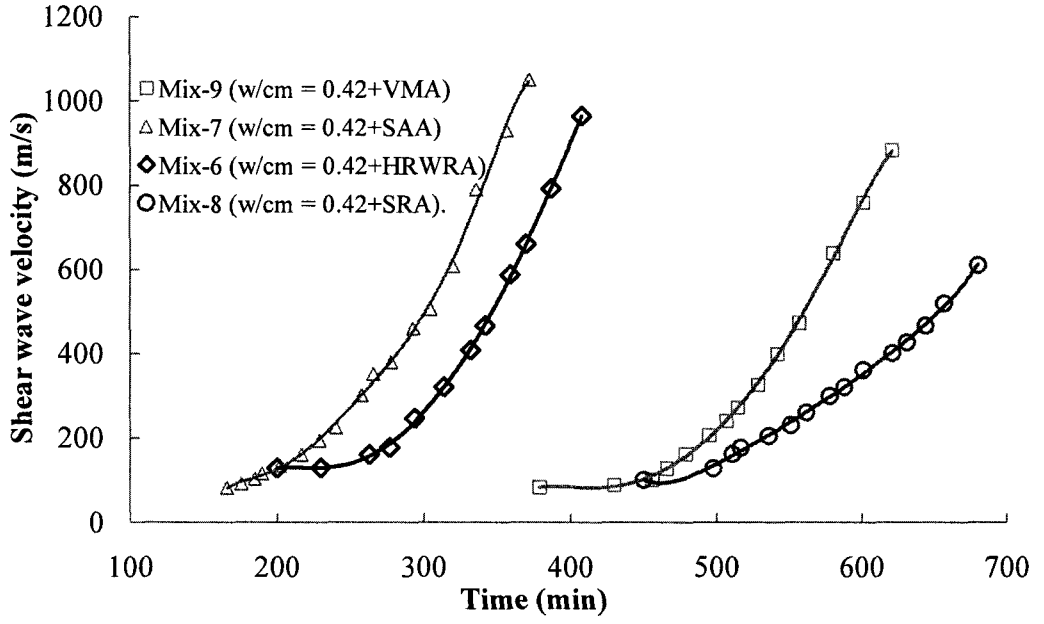

Fig. 5.23 Variations of shear wave velocity with time for mortar mixtures made with fixed *w/cm* and different types of chemical admixtures

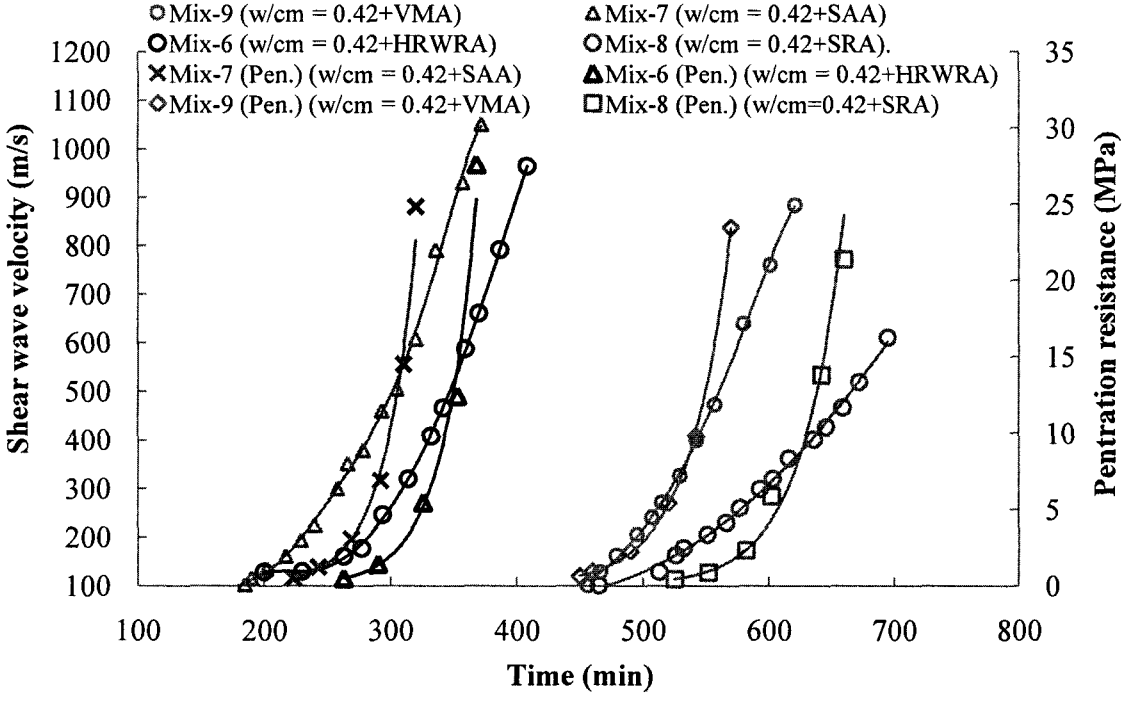

Fig. 5.24 Shear wave velocity and penetration resistance test with time for mortar made with fixed *w/cm* and different types of chemical admixtures

Based on the above results, the *P-RAT2* offers adequate estimation of the setting time of mortar mixtures. The *P-RAT2* can also be employed to differentiate between the hydration behaviour of the mortar mixtures proportioned different contents of HRWRA, and different types of chemical admixtures.

Similar trends between the variations of V_s and the evolution of heat of hydration with respect to the time are observed, as shown from Figs. 5.13 and 5.14 as well as Figs. 5.21and 5.23, respectively. The rate of kinetic heat evolution coincides with the variations of V_s. It can clearly be seen that the results of shear wave velocity obtained with *P-RAT2* method reproduce very well the characteristics of the hydration behaviour indicated by the kinetic heat of hydrations. The *P-RAT2* can also be employed to differentiate between the hydration behaviour of the mortar mixtures proportioned with different contents of HRWRA and various types of chemical admixtures.

It can be concluded from the previous results, that the shear wave velocity measured using the *P-RAT2* can indirectly proportioned to the conductivity; however it's directly proportional to the resistivity.

5.4 Validation of P-RAT2 with compressive strength

The compressive strength after 24 hours ($F_{c@24hr}$) following casting for the paste and mortar mixtures was determined in accordance to ASTM C109. Paste and mortar cubes were prepared and demolded from the moulds at 24 hours for testing.

At the same age (24 hours), the shear wave velocity (V_s) was determined by using *P-RAT2*. The shear modulus (G) was then calculated according to Eq. 8 knowing the unit weight of the tested mixture. Table 5.3 summarizes the $F_{c@24hr}$, V_s, and G values for investigated paste and mortar mixtures.

The increase in the *w/cm* from 0.35 to 0.50 in the paste mixtures (Mix-3 to Mix-1, respectively) corresponded to a decrease in the $F_{c@24hr}$ values from 38 to 17 MPa as shown in Fig. 5.25. A decrease in the V_s values from 2300 to 1380 m/s was determined form the same reduction in the *w/cm* (Fig. 5.25).

Table 5.3 Compressive strength and shear wave velocity and shear modulus for mixtures

Mixture		*w/cm*	Compressive strength, $f_{c@24hr}$ (MPa)	Shear wave velocity, V_s (m/s)	Shear modulus, G (GPa)
Paste	Mix-1	0.50	17	1380	3.77
	Mix-2	0.42 + HRWRA	26	1802	6.12
	Mix-3	0.35 + HRWRA	38	2400	10.34
Mortar	Mix-4	0.50	16.7	1350	3.65
	Mix-5	0.35 + HRWRA	35.6	1950	8.75
	Mix-6	0.42 + HRWRA	27.1	--	--
	Mix-7	0.42 + SAA+ HRWRA	29	1470	4.74
	Mix-8	0.42 + SRA+ HRWRA	24	1200	3.25
	Mix-9	0.42 + VMA+ HRWRA	26.2	1290	3.66
	Mix-10	0.42	25.4	1600	4.68
	Mix-11	0.35	34.4	1870	7.98

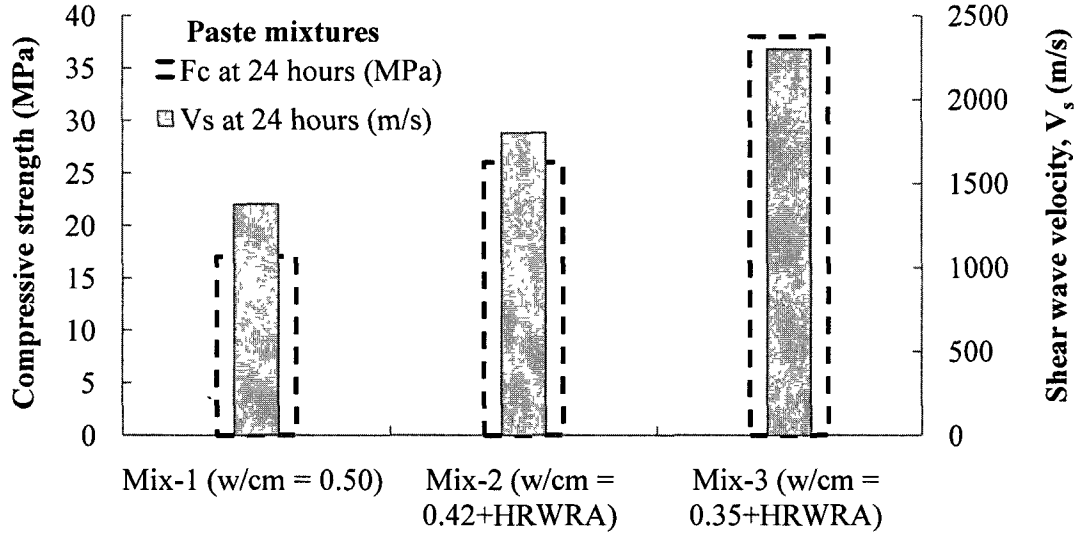

Fig. 5.25 Shear wave velocity and compressive strength values at 24 hours for paste mixtures

The compressive strength and corresponding shear wave velocity values at 24 hours for the mortar mixtures are shown in Fig. 5.26. The effect of *w/cm* can be observed by comparing results

obtained on Mix-11, Mix-10, and Mix-4. The increase in the *w/cm* from 0.35 to 0.50 in Mix-11 to Mix-4, respectively, lead to a decrease in the $F_{c@24hr}$ values from 34.4 to 16.7 MPa , and a decrease in the V_s values from 1870to 1300 m/s, respectively. Adding more HRWRA in mortar resulted in slight increase in compressive strength and shear wave velocity. For example, the $F_{c@24hr}$ values increased from 34.4 to 35 MPa and the V_s increased from 1870 to 1950 m/s for mortar mixtures incorporated *w/cm* of 0.35 and made without and with HRWRA, Mix- 11 and Mix-5, respectively. Mortar mixtures contained (SAA), Mix-7, showed an increase in $F_{c@24hr}$ and V_s values compared to Mix-6 (the reference mixture for the effect of chemical admixtures). For example, an increase of 1.9 MPa in $F_{c@24hr}$ and 28 m/s in V_s was determined between Mix-7 and Mix-6. On the other hand, the mortar mixtures contained (SRA), Mix-8, showed a decrease in the $F_{c@24hr}$ and V_s values compared at Mix-6. The mortar mixture designed with viscosity-modifying agent (VMA), Mix-9, showed slight reduction in the $F_{c@24hr}$ and V_s values compared to Mix-6.

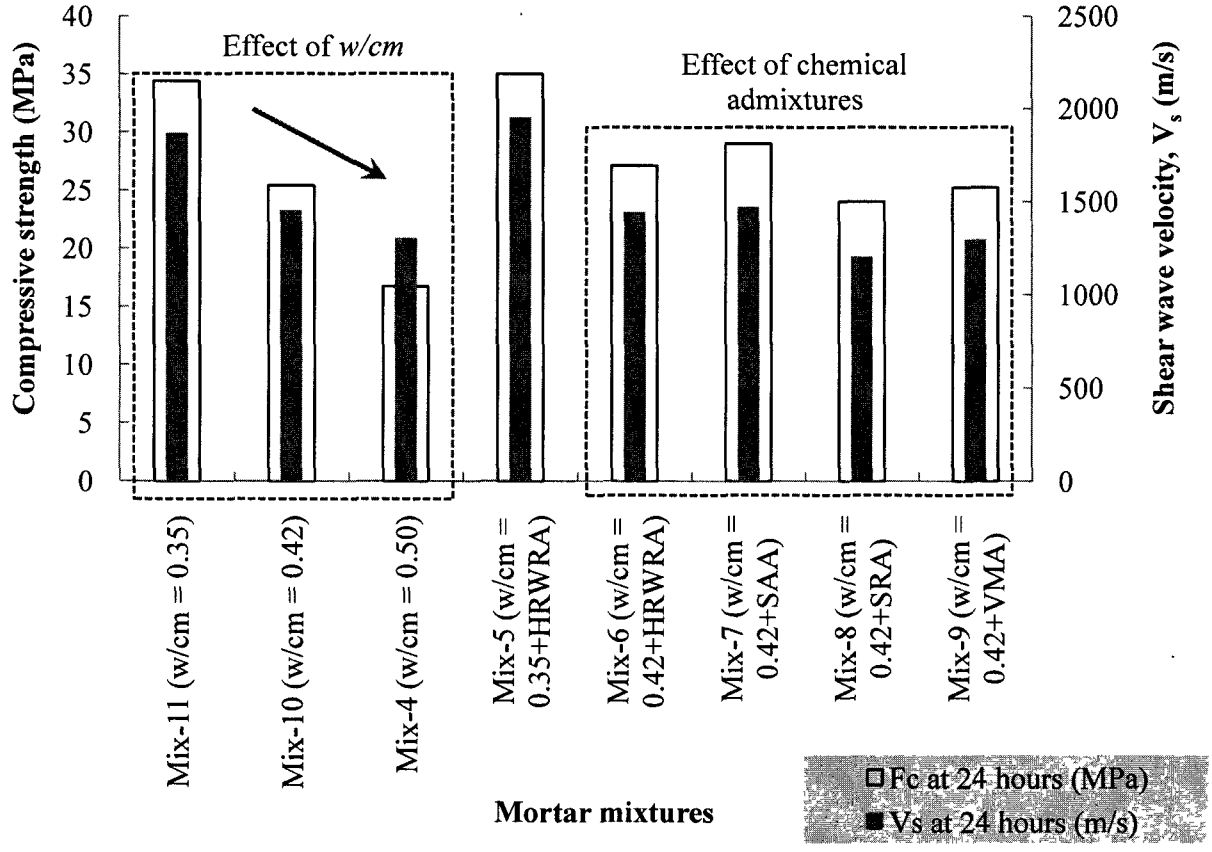

Fig. 5.26 Shear wave velocity and compressive strength (24 hours)) for mortar

From the data presented above for $F_{c@24hr}$ against V_s, there are comparable relationships between V_s determined using the *P-RAT2* against $F_{c@24hr}$.Since the shear modulus (G) is proportional to the shear wave velocity (V_s) by the unit weight of the tested mixture, similar relationships between (G) and $F_{c@24hr}$ were observed. The relationships of both V_s and G as function of the $F_{c@24hr}$ are presented in the next chapter.

5.5 Summary and conclusions

A number of series of validation was performed on cement paste and mortar mixtures proportioned with various water-to-cement ratios (w/cm) as well as chemical admixtures. The w/cm ratio ranged between (0.35 and 0.50). The investigated chemical admixtures comprise of high-range water-reducing agent, viscosity-modifying agent, set-accelerating agent, and set-retarding agent. The presented validations examine the ability of P-RAT2 to monitor the hydration of the cement-based materials. The hydration is characterized by setting time, heat of hydration, electrical conductivity, and compressive strength at 24 hours. Based on the results presented in Chapter 5, the following conclusions can be summarized, as follow:

- The *P-RAT2* offers adequate estimation of the initial and final setting for the paste and mortar mixtures. The initial and final time of setting can be determined from the derivation of shear wave velocity vs. time curve.
- The results of shear wave velocity obtained using *P-RAT2* reproduce similar characteristics of the hydration behaviour indicated by the kinetic heat of hydrations.
- The *P-RAT2* can be employed to differentiate between the hydration behaviour of the mortar mixtures proportioned with different contents of HRWRA and various types of chemical admixtures.
- The shear wave velocity measured using the *P-RAT2* can indirectly proportioned to the conductivity; however it is directly proportioned to the resistivity.

CHAPTER 6
CORRELATIONS AND MODELING

6.1 Introduction

This chapter presents correlations among the time of setting obtained using the conventional test methods (penetration resistance, calorimetry and conductivity) and the compressive strength. On the other hand, the results of the conventional test methods are correlated to the physical properties obtained using the *P-RAT2*, including shear wave velocity, setting time, and shear modulus.

6.2 Mutual Correlations between conventional tests

6.2.1 Relationships between time of setting from penetration test, calorimetry and conductivity tests

For the three paste mixtures, the initial and final setting time values determined using Vicat needle test versus those determined using the calorimetry are shown in Fig. 6.1. The setting times determined using the penetration resistance test for the investigated mortar mixture are plotted against the setting times determined using the calorimetry and conductivity tests in Figs. 6.2 and 6.3, respectively. From Fig. 6.2, the calorimetry test resulted higher setting times compared to the penetration resistance test. The relationship becomes almost 1:1 between the setting times determined using the conductivity and penetration resistance tests as shown in Fig. 6.3. The setting times from the conductivity test are shown as function of the setting times determined using the calorimetry test in Fig. 6.4 for the mortar mixtures. The latter relationship indicates that the setting time values determined using the calorimetry test is higher by 35% than those determined using the conductivity test.

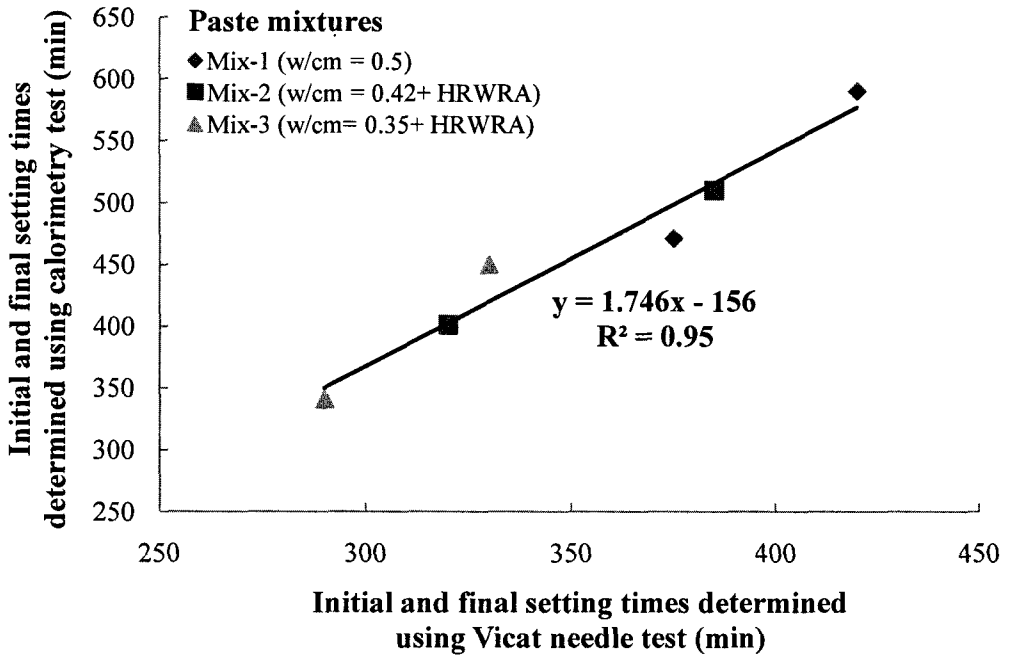

Fig. 6.1 Initial and final setting times determined using Vicat Needle test vs. calorimetry test for paste mixtures

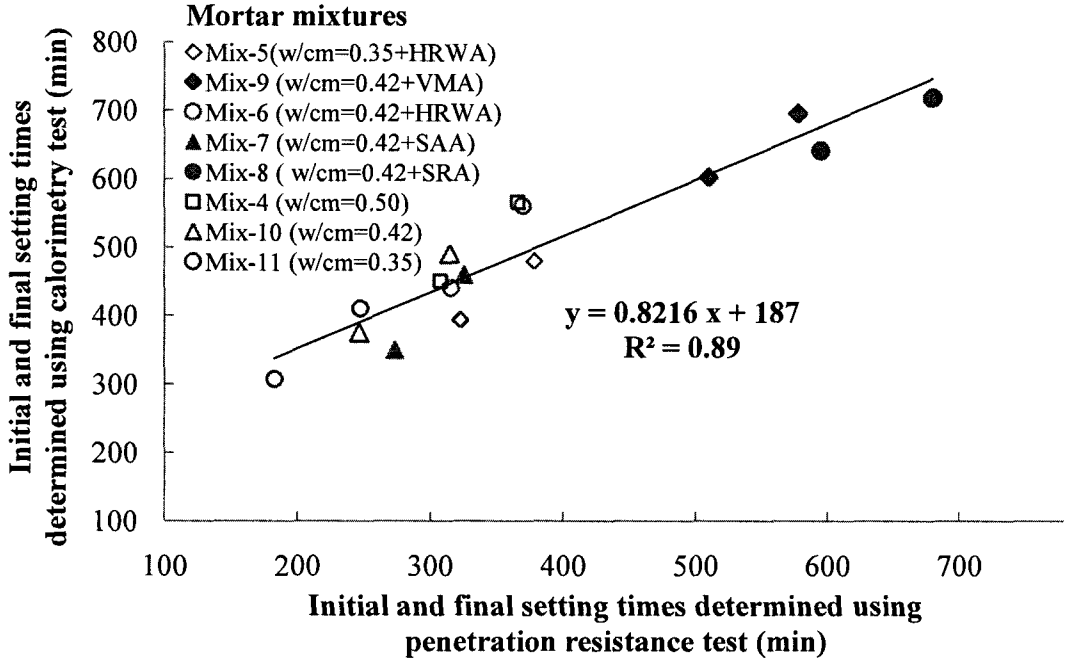

Fig. 6.2 Initial and final setting times determined using penetration resistance test vs. calorimetry test for mortar mixtures

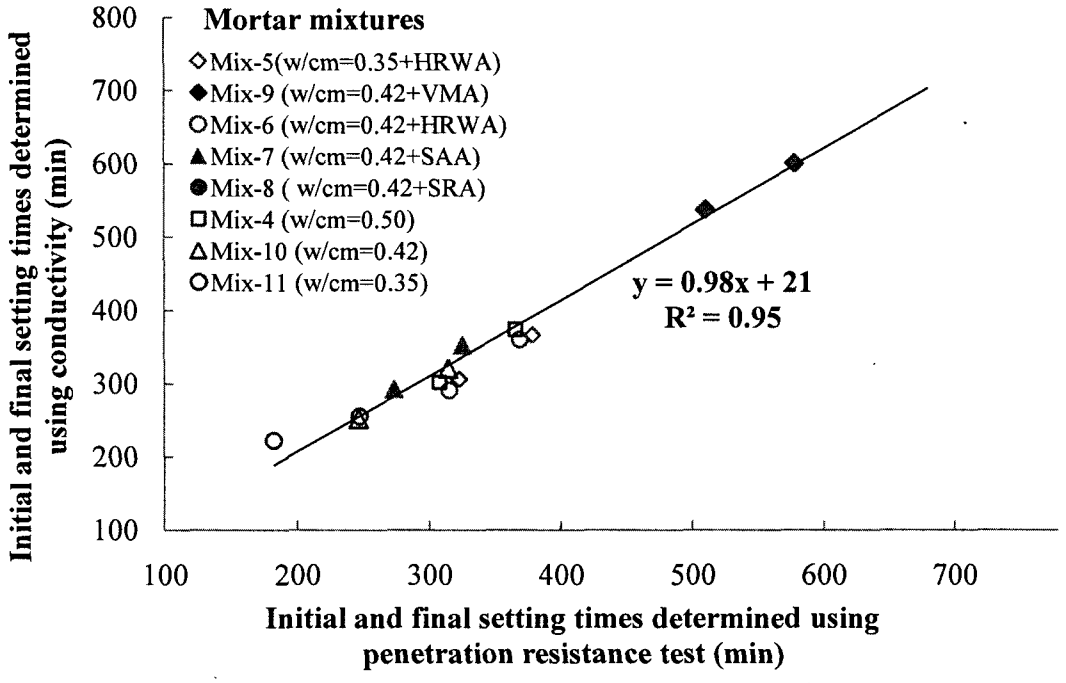

Fig. 6.3 Initial and final setting times determined using penetration resistance test vs. conductivity test for mortar mixtures

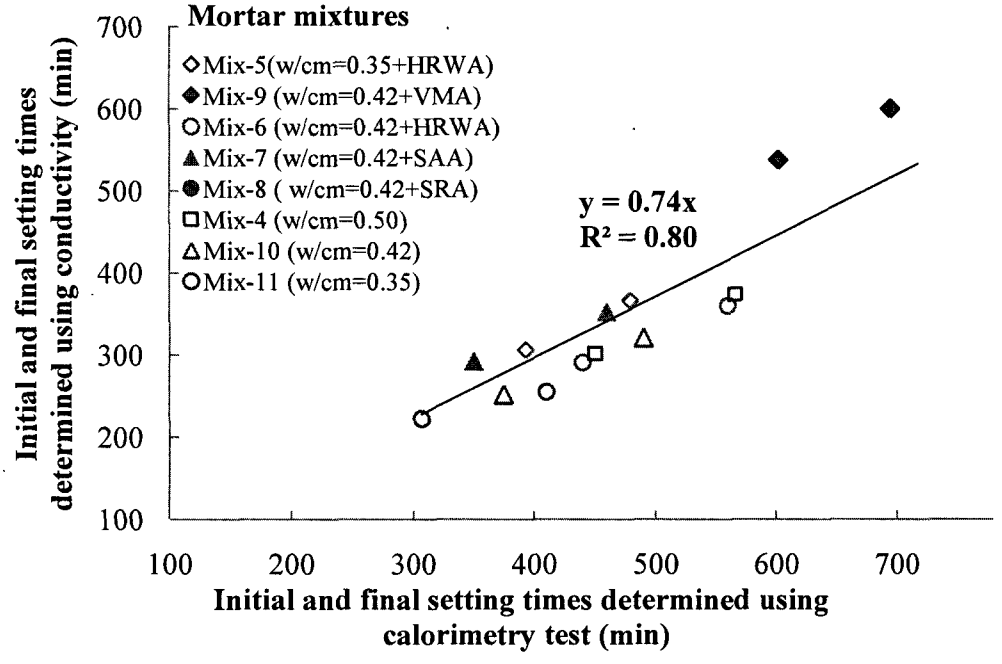

Fig. 6.4 Initial and final setting times determined using calorimetry test vs. conductivity test for mortar mixtures

6.2.2 Correlations between resistivity and rate of increase in compressive strength

The inverse of the drop in the conductivity is referred to as the drop in resistivity ($1/\Delta y$). The difference between the time at which the maximum conductivity occurs and the 24 hours ($t_{24hr} - t_{max}$) was used to calculate the drop in resistivity, as follows:

$$Rate\ of\ drop\ in\ resistivity = \frac{(1/\Delta y)}{(t_{24hr} - t_{max})} \quad (ms \cdot cm^{-1}/hr) \tag{6.1}$$

A direct relationship between the rate of increase in the compressive strength $f_c'/(t_{24hr} - t_{max})$ and rate of drop in resistivity can be obtained as shown in Fig. 6.5. This indicates that increasing the rigidity of the mixtures provides an augmentation in both the compressive strength and resistivity.

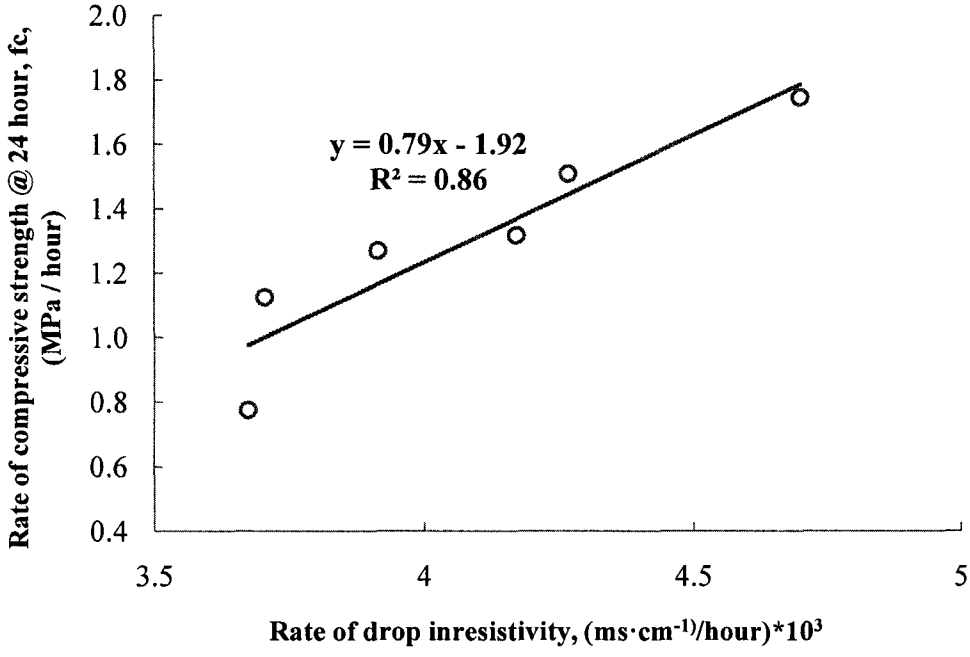

Fig. 6.5 Correlation between rate of compressive strength and rate of electrical resistivity for mortar mixtures

6.3 Correlations between *P-RAT2* and results of conventional tests

6.3.1 Setting time from penetration resistance, calorimetry and conductivity test vs. setting time from *P-RAT2*

For the three paste mixture the relationship between the setting times determined using Vicat needle (t_i and t_f) versus that determined using the *P-RAT2* (t_1 and t_2) is shown in Fig. 6.6. The obtained correlation has R^2 value of 0.90. In addition, and for the same three paste mixtures, the relationship of the setting time (t_i and t_f) determined using the calorimetry test for three paste mixtures against the setting time (t_1 and t_2) determined using the *P-RAT2* was with R^2 of 094, as shown in Fig. 6.7. Each paste is characterized by two distinguished points for the initial and final setting times, as shown in Figs. 6.6 and 6.7.

On the other hand, the setting times (t_1 and t_2) determined using the *P-RAT2* test for the investigated mortar mixtures are plotted against the setting times determined using the penetration resistance, calorimetry and conductivity tests in Figs. 6.8, 6.9, and 6.10, respectively. The relationship becomes almost 1:1 with R^2 of 1.0 between the setting times determined using the penetration resistance and *P-RAT2* tests as shown in Fig. 6.8. From Fig. 6.9, the calorimetry test resulted in higher setting times compared at the *P-RAT2* test. In addition, the relationship established between the setting times determined using the conductivity and *P-RAT2* tests is shown in Fig. 6.10 with R^2 of 0.94. Each mortar had two points for the initial and final setting times, as shown in Figs. 6.8, 6.9, and 6.10.

The excellent relationship indicates the ability of the *P-RAT2* to interact with conventional methods. As will as the capability of the *P-RAT2* to predict initial and final setting times similar to those obtained using Vicat needle, penetration resistance, calorimetry and conductivity test.

6.3.2 Correlation between shear wave velocity and measurements of penetration resistance test

Relationship between penetration resistance and shear wave velocity values determined at different elapsed times using the nine mortar mixtures is indicated in Fig. 6.11. The relationship has high coefficient of correlation (R^2) of 0.96. This relationship is beneficial in correlating the development of the penetration resistance at any given time to the corresponding shear wave at that time. Since the shear wave velocity was determined on continuous bases, this relationship can provide continuous prediction for the development of the penetration resistance with time.

The value of the shear velocity that was found to correlate to the time of initial and final set was 320 & 675 m/s, respectively.

6.3.3 Correlation between shear wave velocity and conductivity test

The obtained Vs data were analyzed in regard electrical conductivity (expressed as 100 × conductivity/ V_s) for the three paste mixtures showed high R^2 value of 0.99, as shown in Fig. 6.12 [Karray 2009]. Similar relationship using the nine mortar mixtures is shown in Fig. 6.13, R^2 value is 0.93. The two correlations indicate that the increase in the conductivity produce a reduction in the V_s. It is worth to not that these relationships are valid for the range of the tested mixtures and time of testing.

6.3.4 Correlation between shear wave velocity and resistivity

The resistivity equals to the inverse of the conductivity. Direct relationships between shear wave velocity (V_s) and electrical resistivity are shown in Fig.6.14 for the three paste mixtures (R^2 = 0.92) and in Fig. 6.15 for the six mortar mixtures (R^2 = 0.90). These relationships indicate that the increase in the resistivity reflects an increase in Vs, which in its turn is strongly affected by the development of the rigidity of the materials. It is worth to not that these relationships are valid for the range of the tested mixtures and time of testing.

6.3.5 Correlation between shear wave characteristics and compressive strength test

The compressive strength values at 24 hours ($F_{c@24\ hr}$), are correlated, in Figs. 6.16 and 6.17 to both the shear wave velocity (V_s) and shear modulus (G) obtained using the *P-RAT2* at the same age, respectively. Higher values for V_s and G can be observed at higher $F_{c@24\ hr}$ values, which reflect changes in the mixture microstructure at early age. For example in the case of paste mixtures, the increase for the $F_{c@24\ hr}$ values from 17 to 38 MPa corresponded to increase in the V_s values from 1380 to 2400 m/s, and also lead to an increase in the G values from 3.77 to 10.34 GPa, respectively. As well as, the increase in the $F_{c@24\ hr}$ values from 17 to 30 MPa, lead to an approximate increase in the V_s values from 1250 to 1600 m/s, and also lead to an increase in the G values from 3.5 to 5.6 GPa, respectively. The paste mixtures demonstrated higher values of $F_{c@24\ hr}$, V_s, and G compared to the mortar mixtures. This can be referred to the higher porosity level of the latter mixtures.

6.3.6 Correlation between shear wave velocity and compressive strength (rate of strength)

The inverse of the drop in the conductivity is referred to as the drop in resistivity ($1/\Delta y$). The difference between the time at which the maximum conductivity occurs and the 24 hours ($t_{24hr} - t_{max}$) was used to calculate the drop in resistivity (Eq. 6.1).

A direct relationship between the rate of increase in the shear wave velocity, V_s / ($t_{24\ hr} - t_{max}$) and rate of rate in resistivity can be obtained as shown in Fig. 6.18. This indicates that increasing the rigidity of the mixtures provides an augmentation in both the shear wave velocity and resistivity

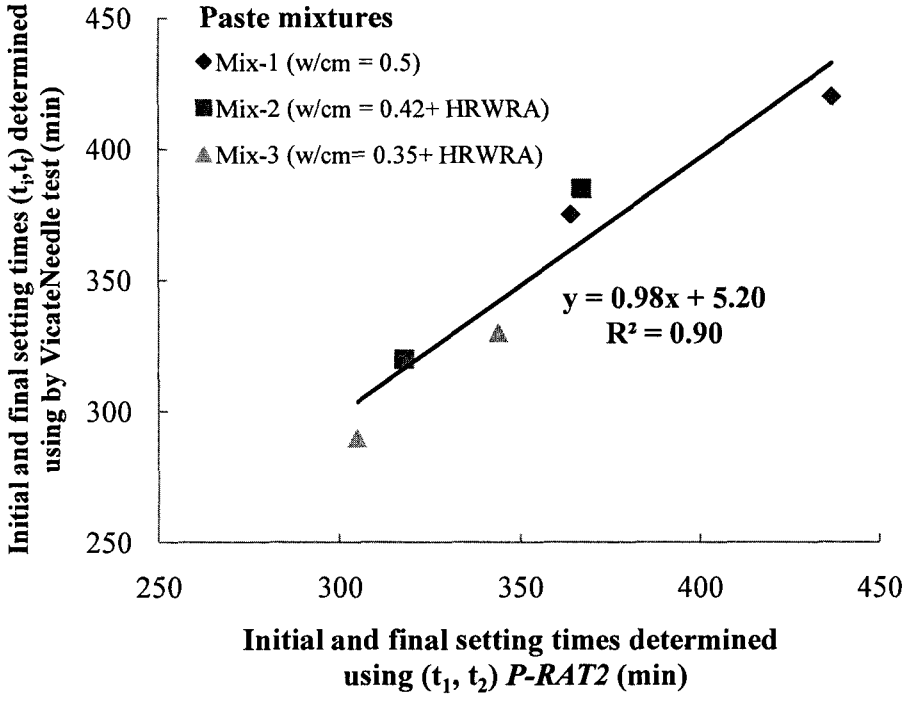

Fig. 6.6 Correlation between initial and final setting times determined using the Vicat needle test and the *P-RAT2* for paste mixtures

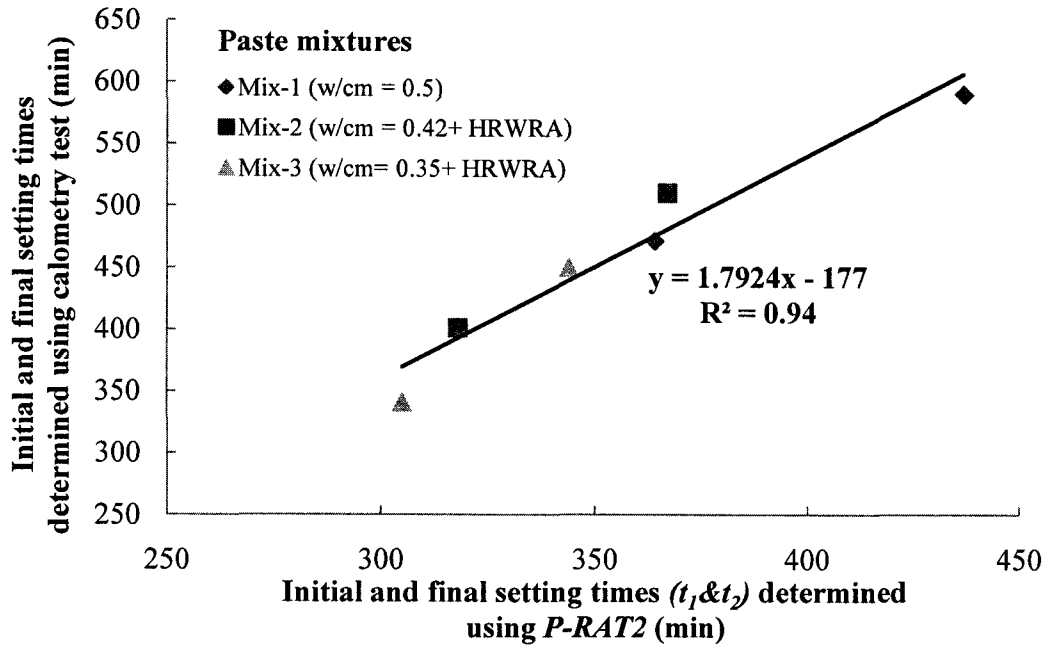

Fig. 6.7 Correlation between initial and final setting times determined using the calometric test and the *P-RAT2* for paste mixtures

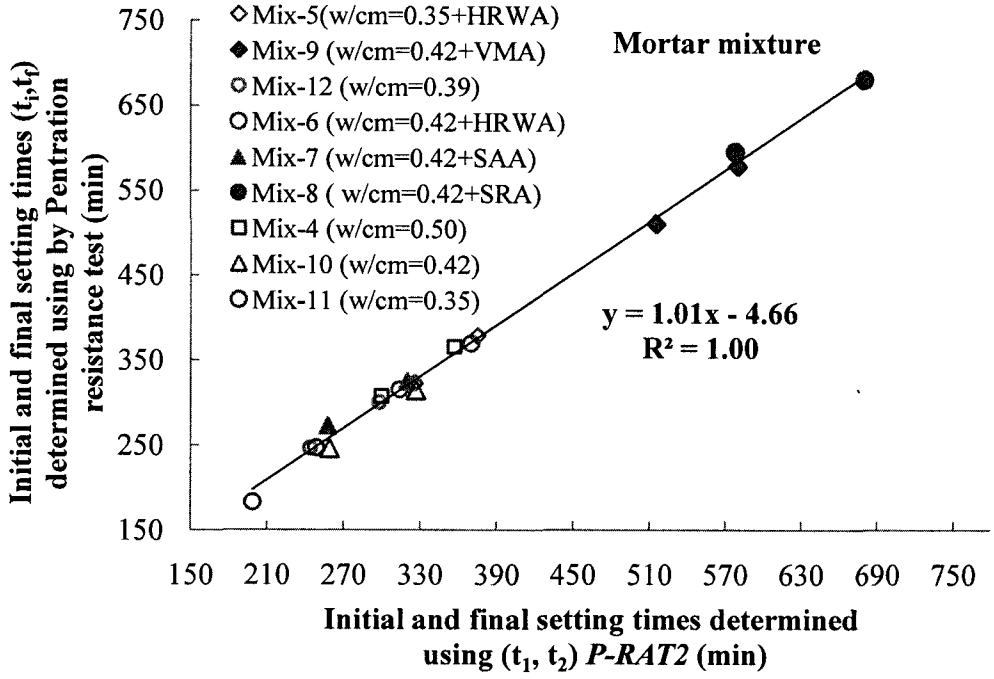

Fig. 6.8 Correlation between initial and final setting times determined using the penetration resistance test and the *P-RAT2* for mortar mixtures

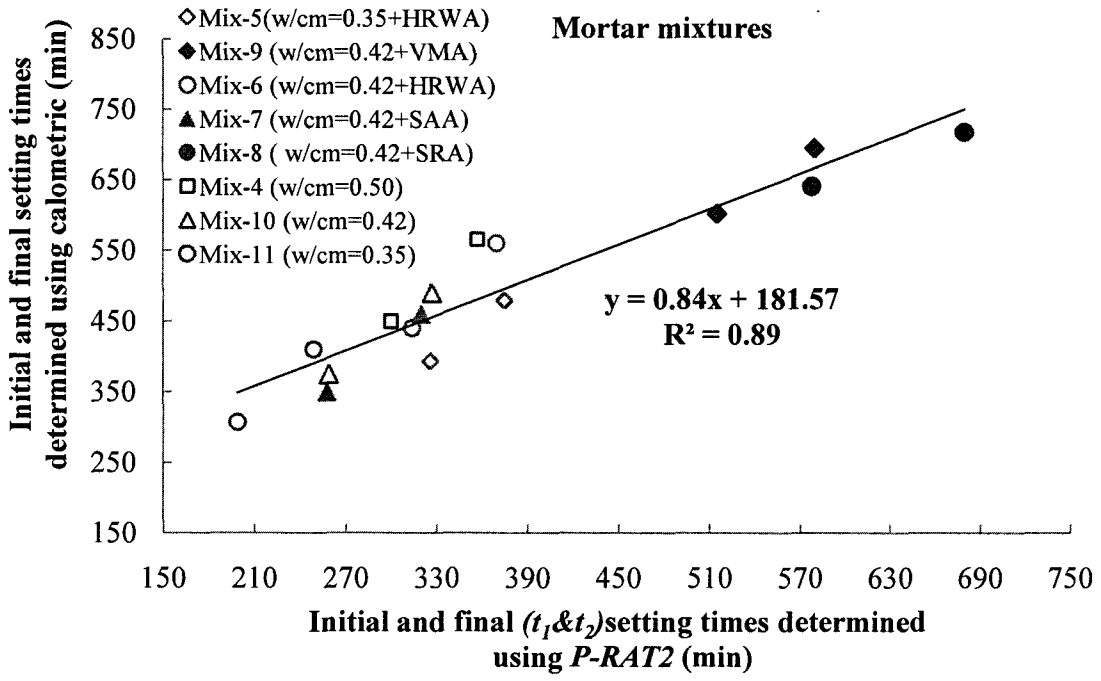

Fig. 6.9 Correlation between initial and final setting times determined using calorimetry test and the *P-RAT2* for mortar mixtures

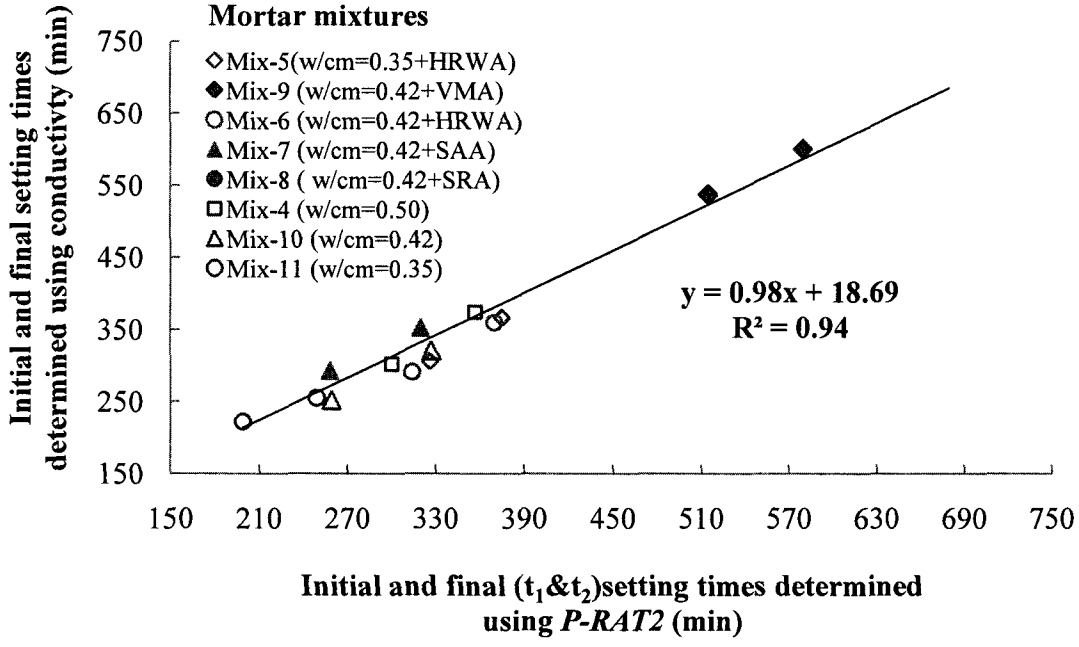

Fig. 6.10 Correlation between initial and final setting times determined using conductivity test and the *P-RAT2* for mortar mixtures

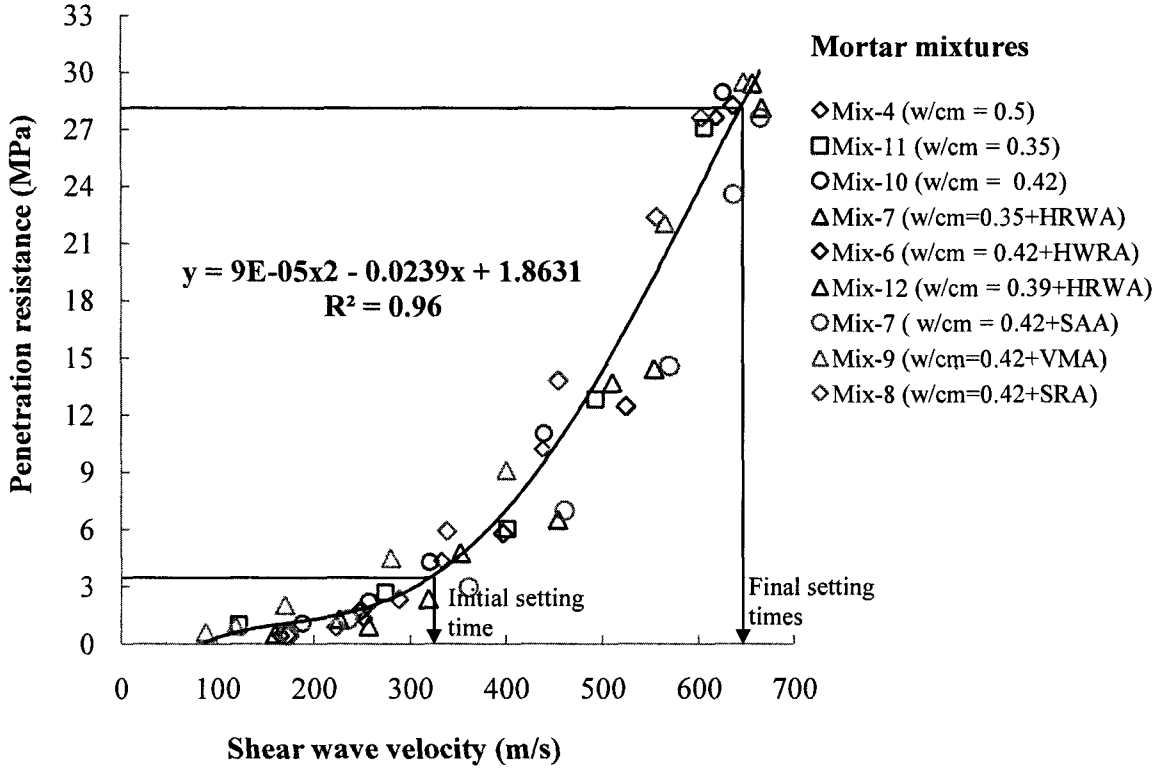

Fig. 6.11 Relationship between penetration resistance and shear wave velocity of mortars made with different elapsed times

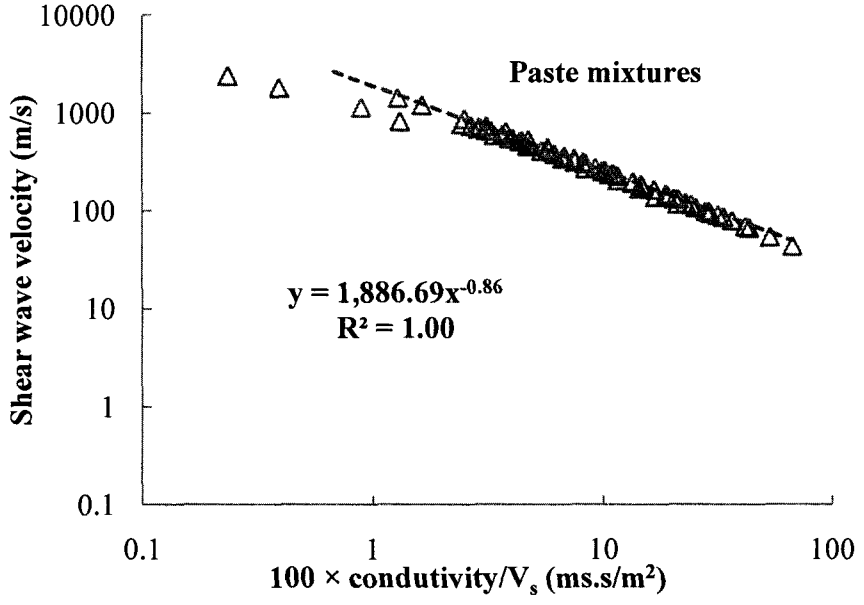

Fig. 6.12 Relationship between shear wave velocity and electrical conductivity for paste mixtures

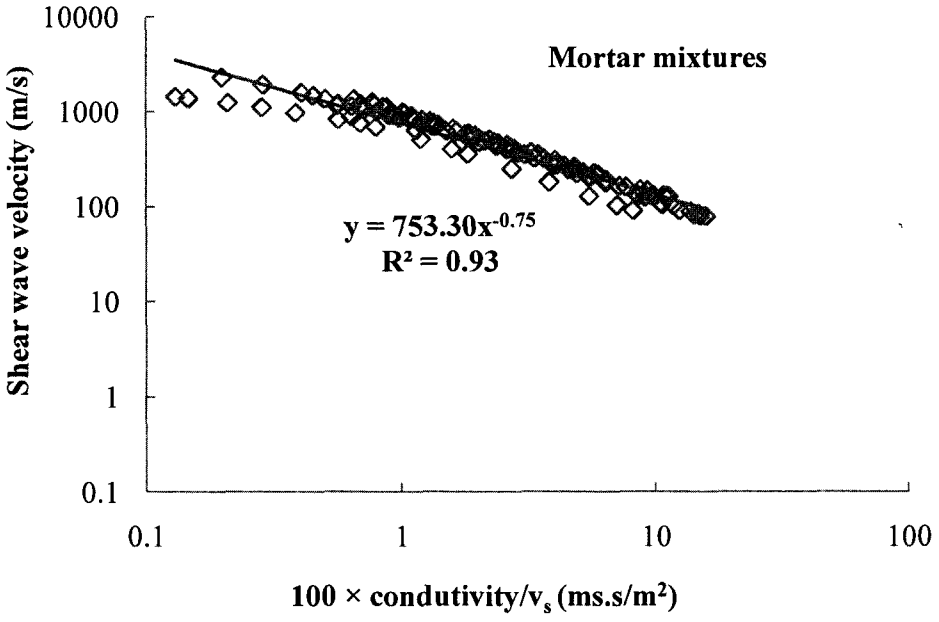

Fig. 6.13 Correlation between shear wave velocity and electrical conductivity for the mortar mixtures

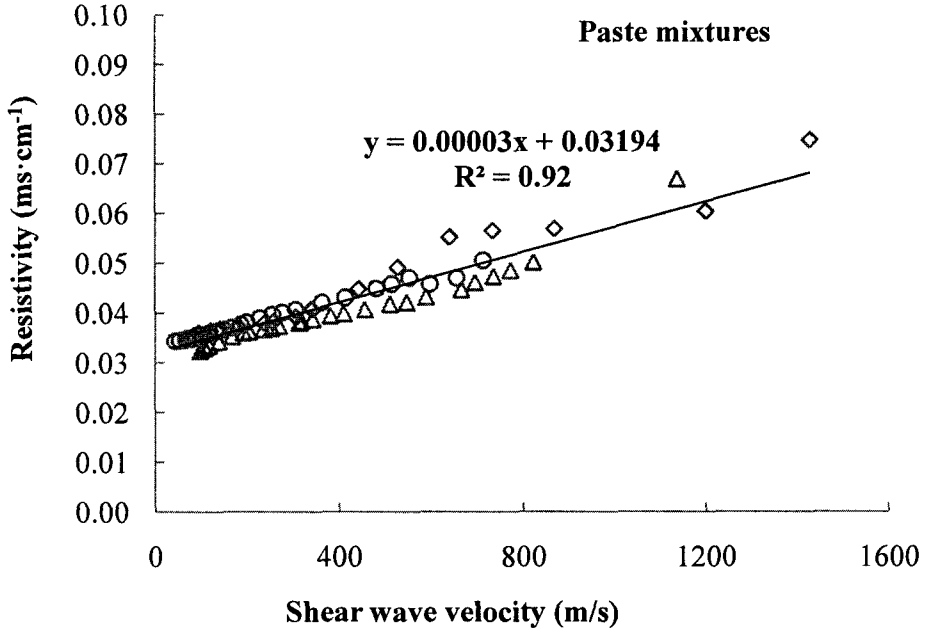

Fig. 6.14 Relationship between resistivity and shear wave velocity for paste mixtures

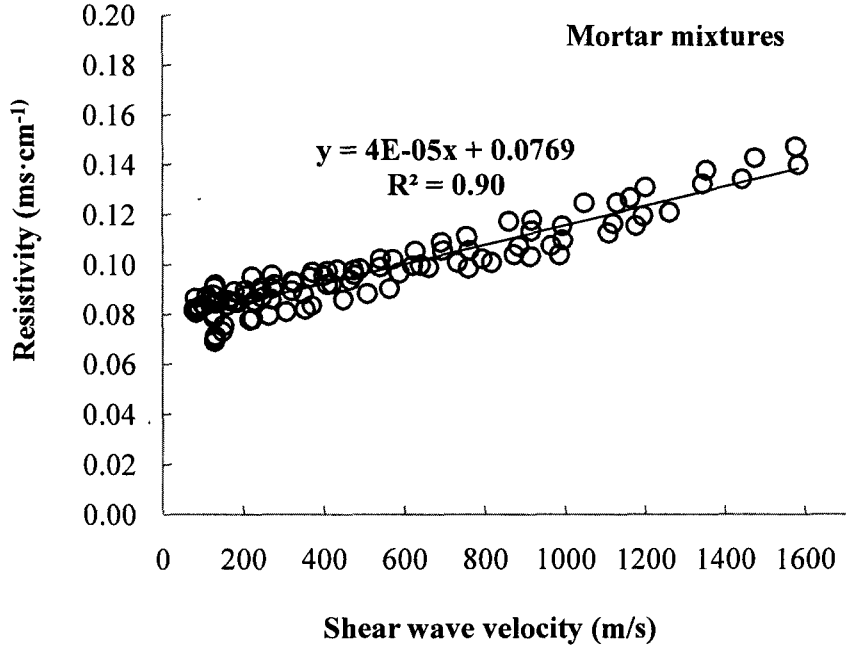

Fig. 6.15 Correlation between resistivity and shear wave velocity for the mortar mixtures

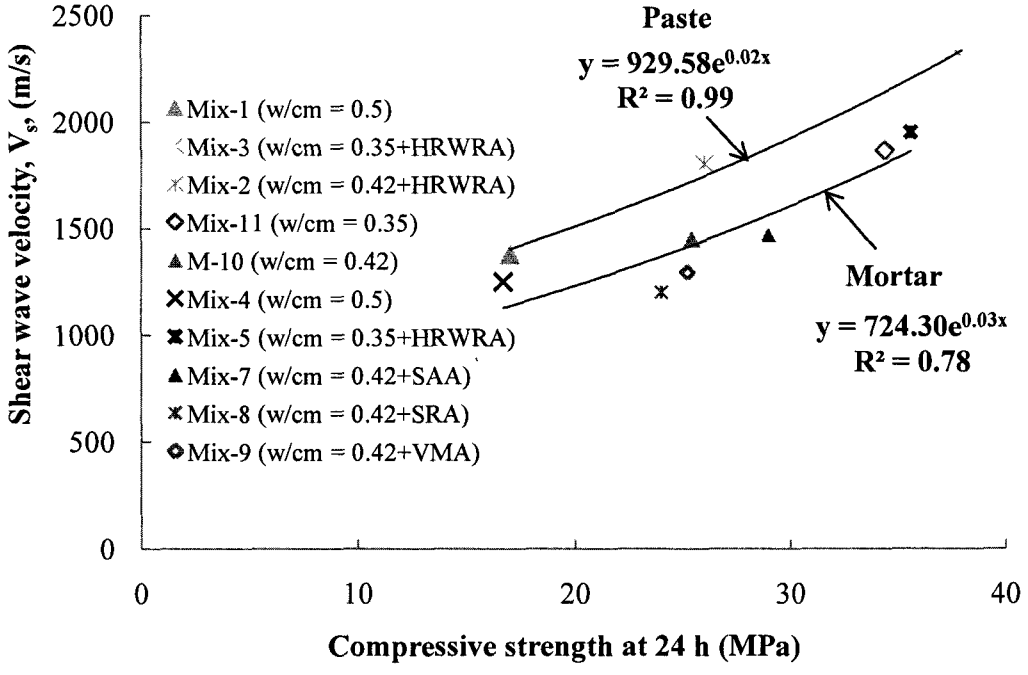

Fig. 6.16 Relationship between shear wave velocity obtained using *P-RAT2* and compressive strength for the paste and mortar mixtures at age of 24 hours

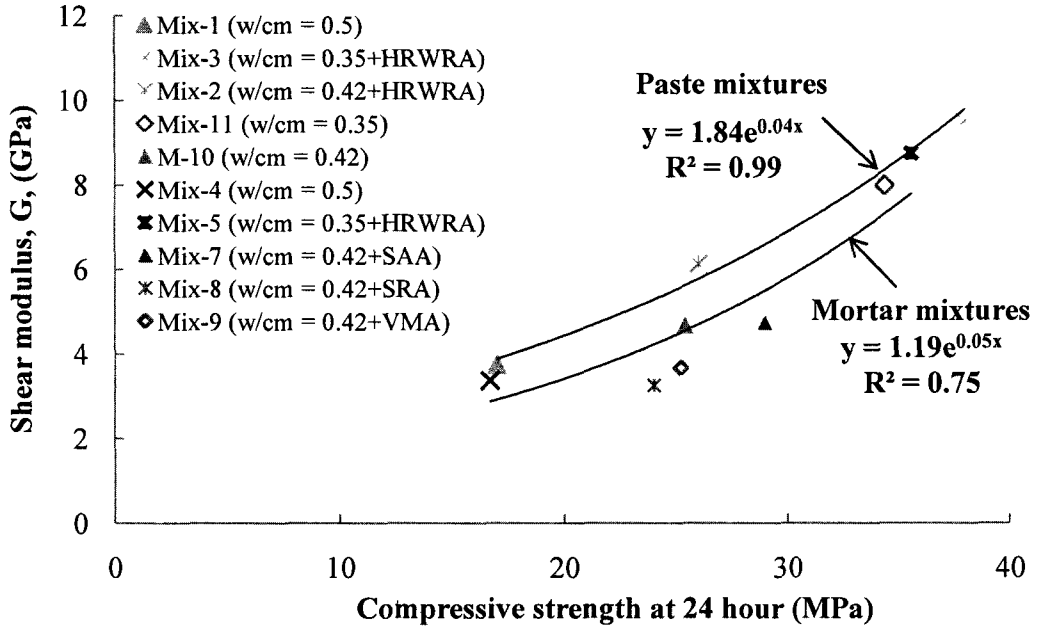

Fig. 6.17 Relationship between shear modulus obtained using *P-RAT2* and compressive strength for pastes and mortars mixtures at age of 24 hours

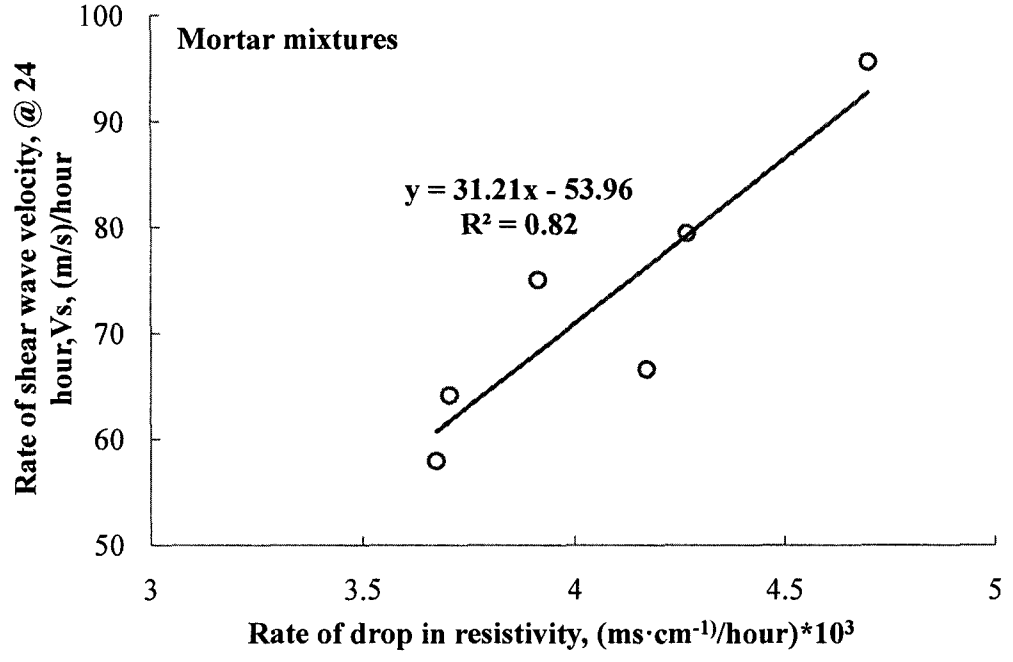

Fig. 6.18 Correlation between rate of shear wave velocity and rate of resistivity for the mortar mixtures

6.4 Analytical model for w/cm determination as function of shear wave velocity and time of measurement

Based on the experimental results for mortar mixtures tested, three analytical models were derived to estimate the *w/cm* in mortar mixture by measuring the shear wave velocity (V_s) and the time corresponding to the elapsed time after cement water contact (t) at the measurement, as shown in Eqs. (6.2), (6.3) and (6.4).

In total, 51 data points were employed to establish these models. The analytical model in Eq. (6.2) incorporated two constants, where the model of Eqs. (6.3) and (6.4). were derived using three and four constants, respectively. The larger numbers of constants produce more precision in the prediction; however, the model becomes more complex. The model of Eq. (6.4) resulted in R^2 between the measured and predicted values of the *w/cm* of an order of 0.96 compared to 0.93 and 0.88 for the models given in Eqs. (6.3) and (6.2), respectively, as indicated in Figs. 6.21, 6.20 and 6.19, respectively.

$$w/cm = \frac{\text{time}}{396 + 0.529935\,V_s} \tag{6.2}$$

$$w/cm = \frac{t}{870} - \frac{V_s}{4110} + 0.23187 \tag{6.3}$$

$$w/cm = \frac{433 + t}{745.25 + \left(\frac{V_s}{128.8}\right)^2} - \frac{Ln\,(V_s)}{11.9} \tag{6.4}$$

where; *w/cm* is the water-to-cementitious ratio, *t* is the elapsed time of measurement (in minutes) after water and cement contact, and V_s is the shear wave velocity in (m/s).

The models of Eqs. (6.2), (6.3) and (6.4) are only valid for the testing ranges; time is around 10 hr. The testing ranges should be extended in the future work by testing mortar specimens of different *w/cm* tested for V_s over large period of time.

The model given by Eq. (6.3) is a linear and simple model with adequate R^2 value and is recommended. The model in Eq. (6.3) can be re-written to determine the values of V_s by knowing the *w/cm* and the time of measurement, as follows:

$$V_s = 4.72\,t - 4110\,w/cm + 953 \tag{6.5}$$

Based on the model of Eq. (6.3), a chart diagram presented in Fig. 6.22 was constructed to provide the value of the *w/cm* at a specific time and corresponding shear wave velocity.

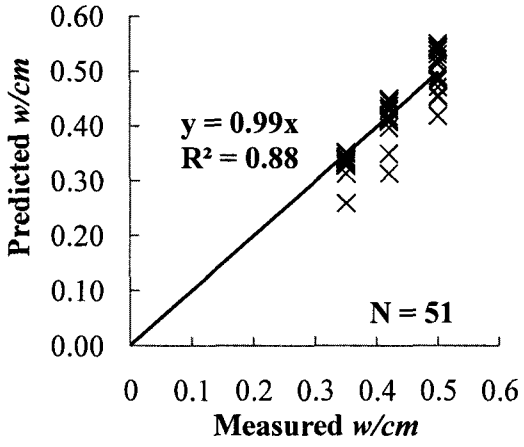

Fig. 6.19 Relationship between predicted and measured *w/cm* using Eq. (6.2)

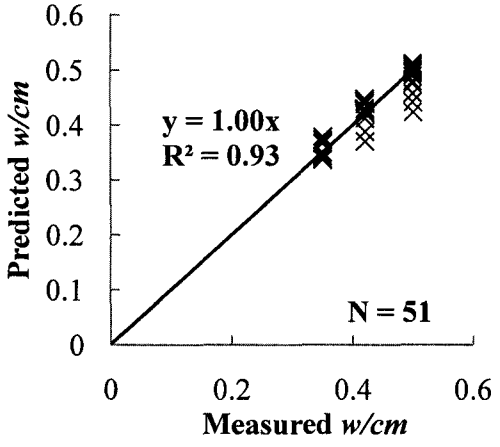

Fig. 6.20 Relationship between predicted and measured *w/cm* using Eq. (6.3)

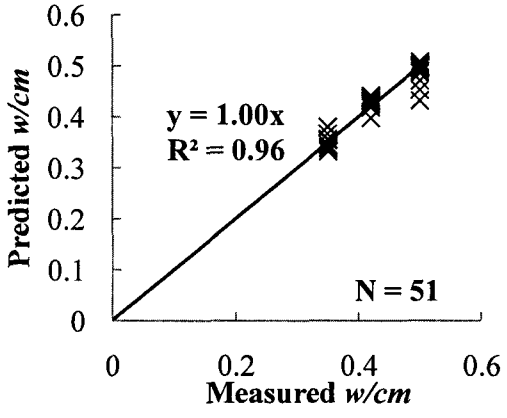

Fig. 6.21 Relationship between predicted and measured *w/cm* using Eq. (6.4)

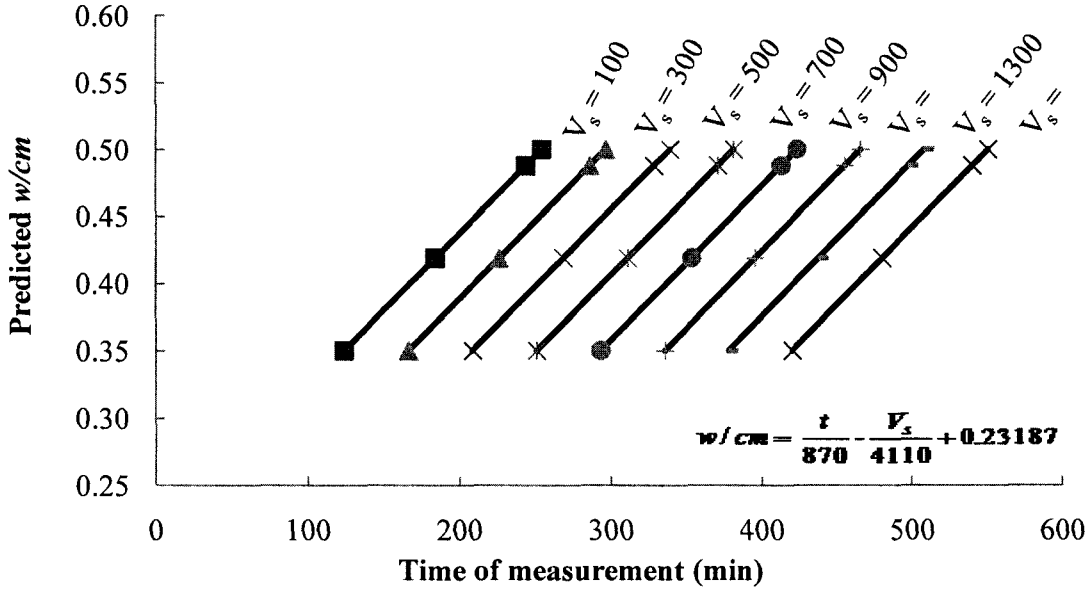

Fig. 6.22 Predicted *w/cm* corresponding to given shear wave velocity (V_s) determined at certain elapsed time using Eq. (6.3).

6.5 Conclusions

Based on the results presented in Chapter 6, the following conclusions can be drawn:

- The initial and final setting time measured by Vicat needle, penetration resistance, calorimetry and conductivity tests are correlated to the initial and final setting time obtained using the *P-RAT2*. Furthermore, the initial and final setting times of the mortar mixtures obtained using the *P-RAT2* are always observed around shear wave velocity values of 320 and 675 m/s, respectively.
- At any given time from the cement and water contact, the conductivity and resistivity have a linear relationship with the shear wave velocity with R^2 values greater than 0.9. It is very important to note that these relationships are valid for the range of the tested mixtures and time of testing.
- Higher values of shear wave velocity and shear modulus obtained using *P-RAT2* can be observed at higher compressive strength values at 24 hours values, which reflect changes in the mixture microstructure at early age.
- Analytical models are derived to estimate the *w/cm* of mortar mixture by measuring the shear wave velocity and the corresponding time from the water-cement contact.

CHAPTER 7
SUMMARY, CONCLUSIONS AND FUTURE WORK

7.1 Introduction

The global idea of this research is to adapt the *P-RAT2* to evaluate properties of cement-based materials at early age. The research aimed at determining how the variation of shear wave velocity can be related to hydration of cement based-materials using the *P-RAT2*. Validations of the *P-RAT2* with four conventional test setups, penetration resistance, calormitry, electrical conductivity, and compressive strength were conducted. The validation aimed at monitoring the hydration process of cement-based materials, and the compressive strength at 24 hr. The main idea of the validation was to obtain accurate measurements. A brief summary of the finding main conclusions and recommendation for future work are presented in this chapter.

7.2 Summary

The main findings of this research can be summarized as follow:

- The penetration resistance test according to (ASTM C403) has been used to determine the setting time. It gives reliable results but has some disadvantage including the accuracy, which it depends largely on the skill and experience of the test operator [Mehta 1993]. In addition, this method does not lead to a continuous monitoring of setting time as function of age.
- The shear-wave velocity (V_s) and compresion wave (V_p) are fundamental parameters that correlate well to cement-based materials properties. Hence, there is an increasing interest in using these wave velocities to characterize cement-based materials properties at early ages (setting time, hydration, compressive, etc). Currently there are two standardized methods that can characterize the properties of early age cement-based materials, ultrasonic pulse velocity and maturity method. The ultrasonic pulse velocity has been applied to monitor the setting time, compressive strength, uniformity, and elastic moduli of cementitious materials. The testing procedure is simple and the equipment is easy to use in the situ as well as in the laboratory. The test methods has few disadvantages; difficulty penetrating the using waves in the large specimens due to the high attenuation of concrete,

and the speed of sound is dependent on many factors in concrete, which effects the velocity of the wave [Borgerson, 2007]. The maturity method has achieved moderate success for monitoring the strength gain development. The method relates early-age strength to a chemical reaction, its temperature over time. The large variation in the environmental condition can cause inaccurate estimation of strength [Voigt, 2004]. Ultrasonic shear wave reflection a method has shown it can be effectively monitor the development hydration cement-based materials at early-age. While this approach has proven to be successful, it only gives information at or near the surface of the concrete, and properties of concrete will often vary with depth [Borgerson, 2007]. Ultrasonic guided wave, this approach has proven to be successful to evaluate hydration of early age properties, unfortunately little research connected and also there is no application on the field at the current time. Ultrasonic guided wave, this approach has proven to be successful, unfortunately little research connected and also there is no application on the field. at the current time.

- A new piezoelectric pulse testing device Piezoelectric Ring Actuators technique (*P-RAT*) was initially developed at the University of Sherbrook as a non-destructive test (NDT) for soil. This technique is considered a completely new, versatile, advanced and accurate. The development of the new technique *P-RAT* was done on two main bases: the first was the development of piezoelectric ring actuators set-up by team work, El-Dean [2007] for granular soil and Ethier [2009] for clay. The second is the development of the interpretation method used in the results analysis by Karray [personal communication, 2008]. The setup is composed of two main units; emitter and receiver, and is capable of measuring shear wave velocity in specimens. With this technique, many problems of pulse tests, which make interpretation of results difficult and ambiguous, were solved in soil. The *P-RAT* overcomes wave reflections at boundaries (end-caps and sides), sample disturbance, weak shear coupling between soil and device (interaction) as well as the fixation problems, low resonant frequency and limited input voltage of the existing device.
- The *P-RAT* was exploited forward to measure the hydration properties of cement- based material. To adapt this test method trial tests was conducted to investigate the possibility of employing the original setup used for soil *P-RAT* to determine setting and hardening properties of cement-based material. Based on the results of the primary test, two modifications were conducted. The resultant version of *P-RAT* after the modification was

referred to be as *P-RAT2*. Calibration of the *P-RAT2* with water specimen was undertaken using the compression wave velocity. One paste mixture was tested three times to determine the experimental error of the *P-RAT2*.

- A number of series of validation was performed on cement paste and mortar mixtures proportioned with various water cement ratios (w/cm) as well as chemical admixtures. The w/cm ratio ranged 'between' (0.35 to 0.50). The chemical admixtures comprise of (high-range water-reducing agent, viscosity-modifying agent, set-accelerating agent, and set-retarding agent). The presented validations examine the ability of a *P-RAT2* to monitor the hydration of the cement-based materials. The hydration is characterized by setting time to monitor initial and final setting respectively, calorimetric to monitor heat of hydration, electrical conductivity to monitor change in continuity of the pore structure and compressive strength at 24 hours. The results obtained using the *P-RAT2* was correlated to those obtained using the traditional physical and strength measurement.

7.3 Conclusions

In this section the conclusions that can be drawn from the conducted experimental analysis is presented. The conclusions are summarized into several groups according to the nature of the findings.

P-RAT2:

Based on the results of the primary test, two modifications were conducted to the previous version of the test setup used in the soil applications to fit and obtain adequate resonant frequency with cement-based materials. The modifications included the design of the container and the dimensions of the rings. The resultant version of *P-RAT* after the modification was referred to be as *P-RAT2*. Sealed trapezoidal mould was selected for the new setup that matches with the characteristics of the cement-based materials. A resonant frequency of 30 kHz was approved success with the new version of setup that is matching with fresh characteristics of the cement-based materials. Schematic for *P-RAT2* and data acquisition system is shown in Fig. 7.1. The new version of the *P-RAT2* was calibrated by generating a compression wave velocity through a water sample that showed a 99.33% accuracy of the measurements. The repeatability carried out on the *PAR-T2* showed a relative error less than 9%.

Setting process:

The *P-RAT2* method can be used to evaluate qualitatively and quantitatively the setting behaviour of the cement-based materials. The initial and final setting time can be determined from the derivation of shear wave velocity vs. time curve. The initial and final setting time was measured by Vicat needle, penetration resistance, calorimetry and conductivity tests are correlated to the initial and final setting time obtained from *P-RAT2*. Furthermore, the initial and final setting times of the mortar mixtures are always observed around shear wave velocity values of 320 and 675 m/s, respectively.

Conductivity:

The shear wave velocity determined on paste and mortar mixtures proportioned with different *w/cm* and containing various dosages and types of chemical admixtures have indirect and direct relationships with the conductivity and resistivity results, respectively. The relationships indicated higher R^2 values greater than 0.9. It is very important to note that these relationships are valid for the range of the tested mixtures and time of testing.

Compressive Strength:

The shear wave velocity and shear modulus were found to be in close relationships with the compressive strength of the paste and mortar mixtures at 24 hours. The relationships between the shear wave and compressive strength showed higher values for the paste mixtures compared to the mortar mixtures. This can reflect the ability of the shear wave velocity to differentiate between the paste and mortar mixtures that varied in the porosity. Higher values of shear wave velocity and shear modulus obtained using P-RAT2 can be observed at higher compressive strength values at 24 hours values, which reflect changes in the mixture microstructure at early age.

Analytical models:

Analytical models are derived to estimate the *w/cm* of mortar mixture by measuring the shear wave velocity and the corresponding time from the water-cement contact.

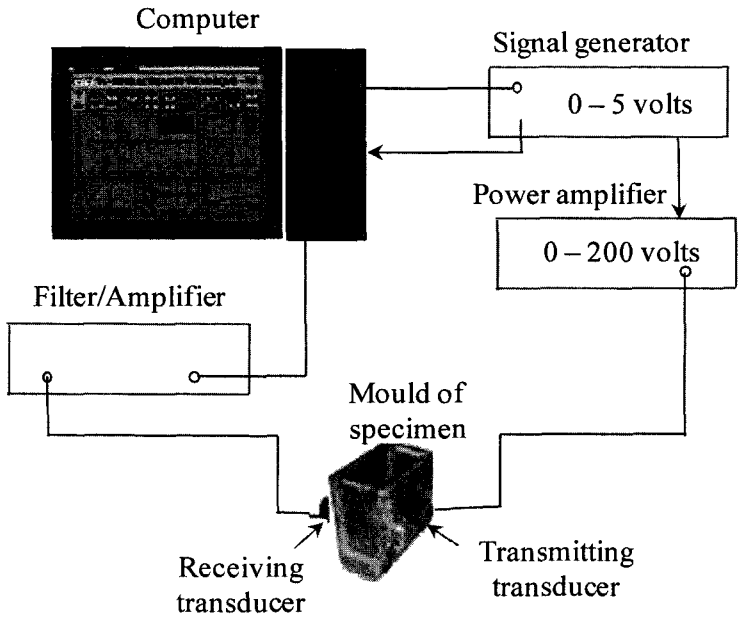

Fig. 7.1 Schematic of an experimental apparatus for *P-RAT2* used for cement hydration monitoring and data acquisition system

7.4 Future research

After the approval of the P-RAT2 in cement paste and mortar mixtures to predict the hydration properties at early age, other areas should be investigated on the future including:

- Monitoring of shear wave velocity using *P-RAT2* for cement-based materials continuously during 24 hours.
- An important aspect would be to investigate the ability of *P-RAT2* to detect the effect of mineral admixtures, such as silica fume or fly ash, on the hydration properties for cement-based materials.
- The tests conducted in this thesis have been in a controlled laboratory environment. It would be worthwhile how different condition, temperature and humidity) would affect the established correlations.
- Effect of air void on shear wave velocity measurements.
- Investigation early hydration in microstructure by *P-RAT2*.
- Figure 7.2 represents the capable of *P-RAT2* to measure shear and compression wave velocity accurately. It is important to extend the work to evaluate the Poisson's ratio and

young's modulus for cement-based materials. In addition compression these results with ultrasonic pulse velocity methods.

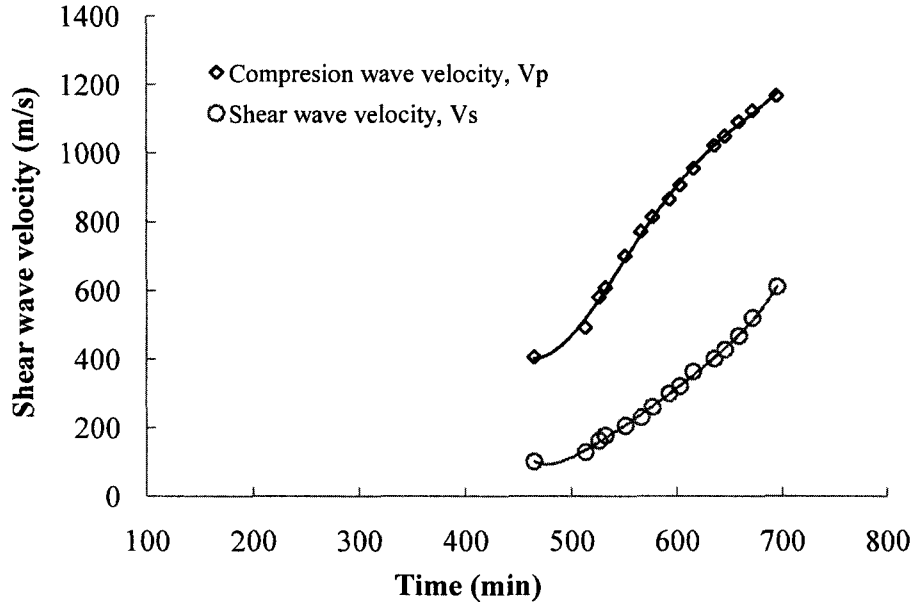

Fig. 7.2 Shear wave velocity (V_s) and compression wave velocity (V_p) determined by *P-RAT2*

- It is significant to accomplish *P-RAT2* in the field measurement.
- It is important to apply the current methodology to other concrete mixtures including high performance concrete in the next stage of the research. Full factorial design as shown in next table can be proposed. The main tested parameters are the slump flow, water-to-cement ratio (*w/cm*), volume of paste (V_{paste}), and fresh concrete temperature (T). 16 mixtures for the matrix and other five mixtures as central points to test the errors will be tested. The tested parameters will include the following items:

1. Fresh concrete properties including (slump flow, air content, unit weight, fresh temperature, Segregation index, stability index, ...);
2. Form work pressure
3. Evolution of shear wave velocity for long term (can be extend to 1 year);
4. Development of penetration resistance until hardening;
5. Evolution of heat of hydration;

6. Evolution of micro structure for cement:
7. Change of concrete temperature with time;
8. Conductivity and resistivity for long term (can be extend to 1 year);
9. Mechanical properties including (compressive strength) at different ages (1 day, 7 days, 28 days, 3 months, 6 months, 9 months, 12 months); and
10. Durability including the permeability change, porosity, thermal change, sulfate expansion change).

This experimental plan is useful in proposing statistical models that enables the determination of the effect of each parameter of the mix design parameter as well as the combinations between these parameters on the tested response (the target property). This plan gives results on a wide range of each tested parameter and also reduces the number of the tested mixtures.

Based on the experimental results provided from this investigation and in addition to the statistical models provided from the factorial design, analytical models can be derived to predict different properties of the concrete determined either by using the traditional test methods and or the *P-RAT2* method. Example for the expected models is the extension for the model established in Eqs. 17, 18, 19 to predict the *w/cm*.

Table 7.1 Factorial plan to study the effect of mix design and fresh temperatures

	Mixture	Coded values				Absolute values			
		ϕ	*w/cm*	V_{paste}	T	ϕ (mm)	*w/cm*	V_{paste} (l/m^3)	T (°C)
Main matrix	Mix-1	-1	-1	-1	-1	560	0.34	300	12
	Mix-2	-1	-1	-1	1	560	0.34	300	32
	Mix-3	-1	-1	1	-1	560	0.34	400	12
	Mix-4	-1	-1	1	1	560	0.34	400	32
	Mix-5	-1	1	-1	-1	560	0.44	300	12
	Mix-6	-1	1	-1	1	560	0.44	300	32
	Mix-7	-1	1	1	-1	560	0.44	400	12
	Mix-8	-1	1	1	1	560	0.44	400	32
	Mix-9	1	-1	-1	-1	720	0.34	300	12
	Mix-10	1	-1	-1	1	720	0.34	300	32
	Mix-11	1	-1	1	-1	720	0.34	400	12
	Mix-12	1	-1	1	1	720	0.34	400	32
	Mix-13	1	1	-1	-1	720	0.44	300	12
	Mix-14	1	1	-1	1	720	0.44	300	32
	Mix-15	1	1	1	-1	720	0.44	400	12
	Mix-16	1	1	1	1	720	0.44	400	32
Central points	Mix-17	0	0	0	0	640	0.39	350	22
	Mix-18	0	0	0	0	640	0.39	350	22
	Mix-19	0	0	0	0	640	0.39	350	22
	Mix-20	0	0	0	0	640	0.39	350	22
	Mix-21	0	0	0	0	640	0.39	350	22

Appendix A: CHAPTER 4

ADAPTION OF PIEZOELECTRIC RING ACTUATOR TECHNIQUE FOR USAGE WITH CEMENT-BASED MATERIALS

Table A.1 Standard Piezo Cylinders manufactured by APC International Ltd and constructed from Type II ceramic material (See properties in Table A.3).

APCI Catalog No.	Dimensions (mm)			Capacitance at 1kHz (pF)	Resonance Freq. (kHz)		Coupling Coef. K_{31}
	OD	ID	length		length	thickness	
42-1000	6.35 ± 0.15	4.9 ± 0.15	6.35 ± 0.15	2500	260	2760	0.35
42-1006	10.0 ± 0.15	8.0 ± 0.15	10.0 ± 0.15	4500	165	2000	0.35
42-1011	15.5 ± 0.15	11.2 ± 0.15	18.0 ± 0.15	5500	92	930	0.35
42-1021	19.0 ± 0.15	16.0 ± 0.20	20.0 ± 0.15	11,600	83	1330	0.35
42-1031	22.0 ± 0.15	16.0 ± 0.20	20.0 ± 0.15	6300	82	670	0.35
42-1041	30.0 ± 0.20	26.0 ± 0.20	20.0 ± 0.15	14,000	83	1000	0.35
42-1051	38.0 ± 0.20	34.0 ± 0.20	25.0 ± 0.15	22,500	66	1000	0.35
42-1060	44.0 ± 0.25	38.0 ± 0.25	30.0 ± 0.15	20,500	55	670	0.35
42-1081	68.0 ± 0.35	60.0 ± 0.30	25.0 ± 0.15	20,000	66	500	0.35
42-1091	85.0 ± 0.35	77.0 ± 0.30	30.0 ± 0.15	30,400	55	500	0.35

Table A.2 Type II Material Properties*

Material	Type II
K	1800
DF	0.02
Tc [C]	300
k31	> .35
d33 [pC/N]	350
d31 [pC/N]	175
D [g/cc]	7.50
Qm	85
Ag [um]	6 - 12

*Nominal values

Table A.3 Physical and Piezoelectric Properties of APCI Materials

	Material:	842	844	851	854	881
Relative Dielectric Constant	K^T	1375	1500	1950	3400	1030
Dielectric Dissipation Factor (Dielectric Loss (%)*	tan δ	0.45	0.4	1.5	1.7	0.4
Curie Point (°C)**	T_c	325	320	360	180	310
Electromechanical Coupling Factor	k_p	0.65	0.68	0.71	0.77	0.58
	k_t	0.48	0.48	0.51	0.52	0.46
Piezoelectric Charge Constant (10^{-12} C/N or 10^{-12} m/V)	d_{33}	300	300	400	650	260
Piezoelectric Voltage Constant (10^{-3} Vm/N or 10^{-3} m^2/C)	g_{33}	26.3	24.5	24.8	20.9	26.7
Young's Modulus (10^{10} N/m^2)	Y^E_{11}	8	7.6	6.3	5.9	9
	Y^E_{33}	6.8	6.3	5.4	5.1	7.2
Frequency Constants (Hz•m or m/s)	N_T (thickness)	2050	2050	2040	2040	2050
	N_P (planar)	2230	2250	2080	1980	2300
Density (g/cm^3)	ρ	7.6	7.7	7.6	7.6	7.6
Mechanical Quality Factor	Q_m	600	1500	80	65	1000

REFERENCES

A. G. A. Saul, (1951). "Principles underlying the steam curing of concrete at atmospheric," Magazine of Concrete Research, Vol.2, No. 6, pp.127-140,.

A.Boumiz, C.Vernet, and F. C. Tenoudje," Mechanical properties of cement pastes and mortar at early age :evolution with time and degree of hydration," Advanced Cement Based Materials, vol.3, No.3-4, PP.94-106,1996

ARROYO, M., MUIR WOOD, D., GREENING, P.D., MEDINA, L., RIO, J. (2006) Effects of sample size on bender-based axial G_0 measurements, Geotechnical testing journal, vol. 56, no.1, p. 39-52.

ARULNATHAN, R., BOULANGER, R.W., RIEMER, M.F. (1998) Analysis of benderelement tests, ASTM Geotechnical testing journal, vol. 21, no. 2, p. 120-131.

ASTM C1074 (1998). Standard Practice for Estimating Concrete Strength by the Maturity Method. American Society for Testing and Materials (ASTM International).

ASTM C109 (2002). Standard Test Method for Compressive Strength of Hydraulic Cement Mortars (Using 2-in. or [50-mm] Cube Specimens). American Society for Testing and Materials (ASTM International).

ASTM C403 (1999). Standard Test Method for Time of Setting of Concrete Mixtures by Penetration Resistance. American Society for Testing and Materials (ASTM International).

ASTM C597 (2002). Standard test method for pulse velocity through concrete. American Society for Testing and Materials (ASTM International).

ASTM Proceedings, vol. 51, pp. 1166–1183.

BRIGNOLI, E.G.M., GOTTI, M., STOKOE II, K.H. (1996) Measurement of shear waves in laboratory specimens by means of piezoelectric transducers, ASTM Geotechnical testing journal, vol. 19, no. 4, p. 384-397.

Carino, N. J. (1984). The maturity method: Theory and application. Cement, Concrete, and Aggregates, vol. 6, no. 2, pp. 61–73.

Carino, N. J. (2004a). Stress wave propagation methods. In Malhotra, V. M., N. J. Carino (Eds.), Handbook on non-destructive testing of concrete, CRC Press, Boca Raton; London.2nd ed., pp. 14.1–14.34.

Carino, N. J. (2004b). The maturity method. In Malhotra, V. M., N. J. Carino (Eds.),Handbook on non-destructive testing of concrete, CRC Press, Boca Raton; London. 2nd ed., pp. 5.1–5.47.

Cheesman, W. J. (1949). Dynamic testing of concrete with the soniscope apparatus. Proceedings of the Highway Research Board, vol. 29, pp. 176–183.

Domone, P. L., H. Thurairatnam (1990). The relationship between early age property measurements on cement pastes. In Banfill, P. F. G. (Ed.), Rheology of Fresh Cement and

Concrete: Proceedings of the International Conference organized by the British Society of Rheology. E. & F.N. Spon, London; New York, pp. 181–191.

Elvery, R. H., L. A. M. Ibrahim (1976). Ultrasonic assessment of concrete strength at early ages. Magazine of Concrete Research, vol. 28, no. 97, pp. 181–190.

Gamal El Dean, D. (2007) Development of a new piezoelectric pulse testing device and soil characterization using shear waves, PhD thesis, faculty of engineering, department of civil engineering, University of Sherbrook pp,282 .

Gartner E.M., Young J.F., Damidot D.A., Jawed I., "Hydration of Portland cement", in Structure and Performance of Cements (Ed. Bensted & Barnes) Spoon Press, London, 2002.

Gartner et al., 2002] Schematic representation of heat evolution during hydration of cement and water

Grosse, C. U., H. W. Reinhardt, R. Beutel (2004). Impact-echo measurements on fresh and hardening concrete. In Kovler, K., J. Marchand, S. Mindess, J. Weiss (Eds.), Proceedings of the International RILEM Symposium on Concrete Science and Engineering: A Tribute to Arnon Bentur. RILEM Publications s.a.r.l., Bagneux, France, RILEM Proceedings PRO 36, pp. 95–104.

Hills, (1998), Non-destructive Test Methods for Evaluating of concret in Strucure, ACI 228.2R-98.

ISMAIL, M.A., RAMMAH, K.I. (2006) A New Setup for Measuring G_0 during Laboratory Compaction, ASTM Geotechnical testing journal, vol. 29, no. 4, p. 280-288.

Jacob L.Borgerson, (2007). Monitoring early age cementitious materials using ultrasonic guided waves, PhD thesis, University of Illinois at Urbana-Champaign.

Jones, R. (1949). A non-destructive method of testing concrete during hardening,Concrete and Constructional Engineering, vol. 44, no. 4, pp. 127–128.

Jones, R. (1949). A non-destructive method of testing concrete during hardening. Concreteand Constructional Engineering, vol. 44, no. 4, pp. 127–128.

Karray from personal communication, 2008

Khayat, T., Trimbak, P., Assaad, J., and Jolicoeur, C., "Phenomenological Analysis of Variations in Electrical Conductivity to Assess Stability of Fresh Mortar Systems," ACI materials Journal, Vol. 100, No. 4, 2003, pp. 302-310.

Kruml, F. (1990). Setting process of concrete. In Wierig, H. J. (Ed.), Properties of fresh concrete: Proceedings of the colloquium organized on behalf of the Coordinating Committee for Concrete Technology of RILEM. Chapman and Hall, London; New York, pp. 10–16.

Lasi˘c, D. D., J. Stepi˘snik (1984). An investigation of the osmotic model of cement curing by ultrasonics. Cement and Concrete Research, vol. 14, no. 3, pp. 345–348.

Lasic, D. D., J. Stepi˘snik (1984). An investigation of the osmotic model of cement curing by ultrasonic, Cement and Concrete Research, vol. 14, no. 3, pp. 345–348.

Lee, H. K., K. M. Lee, Y. H. Kim, H. Yim, D. B. Bae (2004). Ultrasonic in-situ monitoring ofsetting process of high-performance concrete, Cement and Concrete Research, vol. 34, no. 4,pp. 631–640.

Lee, H. K., K. M. Lee, Y. H. Kim, H. Yim, D. B. Bae (2004). Ultrasonic in-situ monitoring of setting process of high-performance concrete. Cement and Concrete Research, vol. 34, no. 4, pp. 631–640.

Lings and Greening (2001)

LINGS, M.L., GREENING, P.D. (2001), A novel bender/extender element for soil testing, Geotechnical, vol. 51, no. 8, p. 713-717.

Mehta PK, Monteiro JM (1993) Concrete: structure, properties, and materials, 2nd ed. Prentice-Hall, New Jersey

Mehta, P.K., Monteiro, J.M., Concrete: Structure, Properties, and Materials, 3nd ed., Prentice-Hall, New Jersey, 2006.

Mindess S., Young J. F., Darwin D., "Concrete", 2nd Ed., Prentice Hall, New Jersey, 2003.

Mindess, and Young, (1981). Progress of setting and hardening of concrete [Mindess, S., and J. F. young, concrete, p. 401, 1981]

Neisecke, J. (1974). Ein dreiparametriges, komplexes Ultraschall-Pr¨ufverfahren f¨ur die zerst¨orungsfreie Materialpr¨ufung im Bauwesen (A three parameter, complex ultrasonic test method for non-destructive testing of materials in civil engineering). PhD thesis, Technische Universit¨at Braunschweig, Braunschweig.

Neville A.M., "Properties of concrete", 4th Ed., Prentice Hall, London, 2000.

Ozt¨urk, T., J. R. Rapoport, J. S. Popovics, S. P. Shah (1999). Monitoring the setting andhardening of cement-based materials with ultrasound, Concrete Science and Engineering,vol. 1, no. 2, pp. 83–91.

Ozt¨urk, T., O. Kroggel, P. Gr¨ubl (2004). The influence of temperature on the hydration process of concrete evaluated through ultrasound technique. In Proceedings of the International RILEM Symposium: Advances in Concrete through Science and Engineering. On CD-RO

P.F. Hansen and E.J Pedersen, "Maturity Computre for controlled curing and hardening of concrete" Nordisck Betong, Vol. 1, pp.21-24, 1977.

Pavate, T. V.; Khayat, K. H.; and Jolicoeur, C., "In-Situ Conductivity Method for Monitoring Segregation, Bleeding, and Strength Development in Cement-Based Materials," Sixth CANMET/ACI International Conference on Superplasticizers and Other Chemical Admixtures in Concrete, SP-195, V. M. Malhotra, ed., American Concrete Institute, Farmington Hills, Mich., 2000, pp. 535-547.

Pessiki, S. P., N. J. Carino (1988). Setting time and strength concrete using the impact-echo method, ACI Materials Journal, vol. 85, no. 5, pp. 389–399.

Pessiki, S. P., N. J. Carino (1988). Setting time and strength to concrete using the impact-echo method. ACI Materials Journal, vol. 85, no. 5, pp. 389–399.

Pimenov, V. V., R. D. Barkan, V. B. Grapp (1972). Ultraschall zur Kontrolle der Herstellungstechnologie des Betons (Use of ultrasound for the control of concrete production technology).Bauplanung–Bautechnik, vol. 26, no. 8, pp. 378–380. (in German).

Popovics, S. (1971). Physical aspects of the setting of Portland cement concrete. Journal of Materials, vol. 6, no. 1, pp. 150–162.

Popovics, S., J. S. Popovics (1998). Ultrasonic testing to determine water-cement ratio for freshly mixed concrete. Cement, Concrete and Aggregates, vol. 20, no. 2, pp. 262–268.

Popovics, S., R. Silva-Rodrigez, J. S. Popovics, V. Martucci (1994). Behavior of ultrasonic pulses in fresh concrete. In Stevens, D. J., M. A. Issa (Eds.), New experimental techniques for evaluating concrete material and structural performance, ACI Special Publication SP- 143, American Concrete Institute, Detroit. pp. 207–225.

Radji, F. F., W. V. Douglas (1994). Heat signature testing of concrete, In Scandella, R. J. (Ed.), Structural Materials Technology: An NDT Conference. CRC Press.

Rapoport, J. R., J. S. Popovics, K. V. Subramaniam, S. P. Shah (2000). Using ultrasound to monitor stiffening process of concrete with admixtures, ACI Materials Journal, vol. 97, no. 6, pp. 675–683.

Reinhardt, H. W., C. U. Grosse (2004). Continuous monitoring of setting and hardening of mortar and concrete. Construction and Building Materials, vol. 18, no. 3, pp. 145–154.

Reinhardt, H. W., C. U. Grosse, A. T. Herb (2000). Ultrasonic monitoring of setting and hardening of cement mortar – A new device. Materials and Structures, vol. 33, no. 233, pp.581–583.

S.H.Pu, F.Celgla, M. Drozdz, M.J. S. Lowe, P. Cawley, and N. R. Buenfeld. 'Mointoring the setting and early hardening of concrete using an ultersonic waveguided,' Insight, Vol. 46, No. 6, pp. 350-354, 2004

Sandberg et al, [2007] Monitoring and Evaluation of Cement Hydration by Semi-Adiabatic field calorimetry, personal communications.

Sansalone, M, and Streett,W.B., Nondistuctive Testing of concrete and Masonry, Bullbrier Press, Jersey Shore, Pa, 1997

SANTAMARINA, J.C., KLEIN, K.A., FAM, M.A. (2001) Soils and Waves, Chichester, John Wiley & Sons Ltd, 488 p.

Schreiber, E., Anderson, O. L., Soga, N., (1973), Elastic Constants and their Measurement, McGraw-Hill Inc, 196 pp.

Shah, S. P., K. V. Subramaniam, J. S. Popovics (2000). Use of nondestructive ultrasonic techniques for material assessment and in-service monitoring of concrete structures. Online Journal NDT.net, vol. 5, no. 2. URL http://www.ndt.net.

Standard test method for time of setting of concrete mixtures by penetration resistance, ASTM C 403, Annual Books of ASTM Standards ASTM, Philadelphia, USA (1985) 273–276.

Stepi˘snik, J., M. Luka˘c, I. Kocuvan (1981). Measurement of cement hydration by ultrasonic. American Ceramic Society Bulletin, vol. 60, no. 4, pp. 481–483.

Stepisnik, J., M. Luka˘c, I. Kocuvan (1981). Measurement of cement hydration by ultrasonics, American Ceramic Society Bulletin, vol. 60, no. 4, pp. 481–483.

Struble, L., Kim, T.Y., and Zhang, H., (2001), Setting of cement and concrete, Cement, Concrete, and Aggregates, vol. 23, no. 2, pp. 88-93.

Timoshenko, S.P. and Goodier, J.N., Theory of elasticity, 3 rd ed., McGraw- Hill, New York, 1970

Viktorov, I., Rayleigh and Lamb waves, translated by W.P Mason, Plenum Pressé New York, 1967].

Voigt, T., (2004). The application of an ultrasonic shear wave reflection method for non-destructive testing of cement-based materials at early ages, report, the Center for Advanced Cement-Based Materials at Northwestern University, Illinois, USA.

Voigt, T., G. Ye, Z. Sun, S. P. Shah, K. van Breugel (2004). Early age microstructure of Portland cement mortar investigated by ultrasonic shear waves and numerical simulation. Cement and Concrete Research.

Voigt, T., S. P. Shah (2002-2003). Nondestructive testing of early age concrete. Cementing the Future, Newsletter of the Center for Advanced Cement-Based Materials, vol. 14, no. 1, pp. 4–5. URL, http://acbm.northwestern.edu/cfpub.html.

Voigt, T., S. P. Shah (2003). Nondestructive monitoring of setting and hardening of Portland cement mortar with sonic methods. In Proceedings of the Sixth International Symposium on Non-Destructive Testing in Civil Engineering (NDT-CE 2003).

Voigt, T., S. P. Shah (2004). Properties of early age Portland cement mortar monitored with shear wave reflection method. ACI Materials Journal, vol. 101, no. 6, pp. 473–482.

Voigt, T., Y. Akkaya, S. P. Shah (2002). Determination of early age concrete strength by a reflective ultrasonic technique. In K¨onig, G., F. Dehn, T. Faust (Eds.), Proceedings of the Sixth International Symposium on Utilization of High Strength/High Performance Concrete. vol. 2, pp. 1489–1501.

Voigt, T., Y. Akkaya, S. P. Shah (2003). Determination of early age mortar and concrete strength by ultrasonic wave reflections. Journal of Materials in Civil Engineering, vol. 15, no. 3, pp. 247–254.

Whitehurst, E. A. (1951). Use of the soniscope for measuring setting time of concrete. ASTM Proceedings, vol. 51, pp. 1166–1183.

Yannic Ethier. (2009) La mesure en Laboratoirede la vitesse de propagation des ondes de cisaillement, PhD thesis, faculty of engineering, department of civil engineering, University of Sherbrooke.